University of Groningen

Overview of the MOSAiC expedition

Fong, Allison; Hoppe, Clara; Aberle, Nicole; Ashjian, Carin J.; Assmy, Philipp; Bai, Youcheng; Bakker, Dorothee C.E.; Bozzato, Deborah; Stefels, Jacqueline; van Leeuwe, Maria

DOI:
[10.31223/x5p091](10.31223/x5p091)

IMPORTANT NOTE: You are advised to consult the publisher's version (publisher's PDF) if you wish to cite from it. Please check the document version below.

Document Version
Early version, also known as pre-print

Publication date:
2023

[Link to publication in University of Groningen/UMCG research database](#)

1 **Overview of the MOSAiC expedition: Ecosystem**

2

3 Allison A. Fong, Clara J. M. Hoppe*, Nicole Aberle, Carin J. Ashjian, Philipp Assmy,
4 Youcheng Bai, Dorothee C. E. Bakker, John Paul Balmonte, Kevin R. Barry, Stefan
5 Bertilsson, William Boulton, Jeff Bowman, Deborah Bozzato, Gunnar Bratbak, Moritz
6 Buck, Robert G. Campbell, Giulia Castellani, Emelia J. Chamberlain, Jianfang Chen,
7 Melissa Chierici, Astrid Cornils, Jessie M. Creamean, Ellen Damm, Klaus Dethloff,
8 Elise S. Droste, Oliver Ebenhöh, Sarah Lena Eggers, Anja Engel, Hauke Flores,
9 Agneta Fransson, Stefan Frickenhaus, Jessie Gardner, Cecilia E. Gelfman, Mats A.
10 Granskog, Martin Graeve, Charlotte Havermans, Céline Heuzé, Nicole Hildebrandt,
11 Thomas C. J. Hill, Mario Hoppema, Antonia Immerz, Haiyan Jin, Boris Koch, Xianyu
12 Kong, Alexandra Kraberg, Musheng Lan, Benjamin A. Lange, Aud Larsen, Benoit
13 Lebreton, Eva Leu, Brice Loose, Wieslaw Maslowski, Camille Mavis, Katja Metfies,
14 Thomas Mock, Oliver Müller, Marcel Nicolaus, Barbara Niehoff, Daiki Nomura, Eva-
15 Maria Nöthig, Marc Oggier, Ellen Oldenburg, Lasse Mork Olsen, Ilka Peeken, Donald
16 K. Perovich, Ovidiu Popa, Benjamin Rabe, Jian Ren, Markus Rex, Anette Rinke,
17 Sebastian Rokitta, Björn Rost, Serdar Sakinan, Evgenii Salganik, Fokje L.
18 Schaafsma, Hendrik Schäfer, Katrin Schmidt, Katyanne M. Shoemaker, Matthew D.
19 Shupe, Pauline Snoeijs-Leijonmalm, Jacqueline Stefels, Anders Svenson, Ran Tao,
20 Sinhué Torres-Valdés, Anders Torstensson, Andrew Toseland Adam Ulfsbo, Maria
21 A. Van Leeuwe, Martina Vortkamp, Alison L. Webb, Rolf R. Gradinger

22

23 *see Author Information table for author affiliations, ORCID IDs etc.*

24

25

26

27 * corresponding author (email: Clara.Hoppe@awi.de)

28

29

Full Name	Email	ORCID	Affiliation
Fong, Allison A.	allison.fong@awi.de	0000-0002-3779-9624	Alfred-Wegener-Institute - Helmholtzzentrum für Polar- und Meeresforschung
Hoppe, Clara Jule Marie	choppe@awi.de	0000-0002-2509-0546	Alfred-Wegener-Institute - Helmholtzzentrum für Polar- und Meeresforschung
Aberle, Nicole	nicole.aberle-malzahn@ntnu.no	0000-0003-3254-5710	Department of Biology, Norwegian University of Science and Technology (NTNU), Trondheim, Norway
Ashjian, Carin J.	cashjian@whoi.edu	0000-0002-7894-1519	Woods Hole Oceanographic Institution, USA
Assmy, Philipp	philipp.assmy@npolar.no	0000-0002-8241-7541	Norwegian Polar Institute, Fram Centre, Tromsø, Norway
Bai, Youcheng	ycbai@sio.org.cn	0000-0003-1116-7319	Key Laboratory of Marine Ecosystem Dynamics, Second Institute of Oceanography, Ministry of Natural Resources, Hangzhou, China
Bakker, Dorothee C. E.	d.bakker@uea.ac.uk	0000-0001-9234-5337	Centre for Ocean and Atmospheric Sciences, University of East Anglia, Norwich, UK
Balmonte, John Paul	jpb422@lehigh.edu	0000-0001-5571-4893	Stockholm University, Department of Ecology, Environment and Plant Sciences, Stockholm, Sweden
Barry, Kevin R.	kevin.barry@colostate.edu	0000-0002-1896-1921	Department of Atmospheric Science, Colorado State University
Bertilsson, Stefan	stefan.bertilsson@slu.se	0000-0002-4265-1835	Swedish University of Agricultural Sciences, Department of Aquatic Sciences and Assessment, Uppsala, Sweden
Boulton, William	W.Boulton@uea.ac.uk	0000-0002-8258-4673	School of Computing Sciences, University of East Anglia, Norwich, United Kingdom
Bowman, Jeff	jsbowman@ucsd.edu	0000-0002-8811-6280	Scripps Institution of Oceanography, University of California San Diego, USA
Bozzato, Deborah	d.bozzato@rug.nl	0000-0002-6004-1096	Groningen Institute for Evolutionary Life Sciences, University of Groningen, Groningen, The Netherlands
Bratbak, Gunnar	gunnar.bratbak@uib.no	0000-0001-8388-4945	University of Bergen, Department of Biological Sciences, Bergen, Norway
Buck, Moritz	moritz.buck@slu.se	0000-0001-6632-5324	Swedish University of Agricultural Sciences, Department of Aquatic Sciences and Assessment, Uppsala, Sweden
Campbell, Robert G.	rgcampbell@uri.edu	0000-0002-3710-9750	University of Rhode Island, Graduate School of Oceanography, USA
Castellani, Giulia	giulia.castellani@awi.de	0000-0001-6151-015X	Alfred-Wegener-Institute - Helmholtzzentrum für Polar- und Meeresforschung
Chamberlain, Emelia J.	echamber@ucsd.edu	0000-0003-2218-3488	Scripps Institution of Oceanography, University of California San Diego, USA
Chen, Jianfang	jfchen@sio.org.cn	0000-0002-6521-0266	Key Laboratory of Marine Ecosystem Dynamics, Second Institute of Oceanography, Ministry of Natural Resources, Hangzhou, China
Chierici,Melissa	melissa.chierici@hi.no	0000-0003-0222-2101	Institute of Marine Research, Tromsø, Norway
Cornils, Astrid	astrid.cornils@awi.de	0000-0003-4536-9015	Alfred-Wegener-Institut Helmholtz-Zentrum für Polar- und Meeresforschung
Creamean, Jessie M.	jessie.creamean@colostate.edu	0000-0003-3819-5600	Department of Atmospheric Science, Colorado State University
Damm, Ellen	ellen.damm@awi.de	0000-0002-1487-1283	Alfred-Wegener-Institut Helmholtz-Zentrum für Polar- und Meeresforschung
Dethloff, Klaus	Klaus.Dethloff@awi.de	0000-0003-4162-148X	Alfred-Wegener-Institut Helmholtz-Zentrum für Polar- und Meeresforschung
Droste, Elise S.	elise.droste@awi.de	0000-0002-3467-0083	Centre for Ocean and Atmospheric Sciences, School of Environmental Sciences, University of East Anglia, Norwich, UK
Ebenhöh, Oliver	oliver.ebenhoeh@hhu.de	0000-0002-7229-7398	Institute of Quantitative and Theoretical Biology, Heinrich-Heine University Düsseldorf, Düsseldorf, Germany
Eggers, Sarah Lena	lena.eggers@awi.de	0000-0001-6094-3201	Stockholm University, Department of Ecology, Environment and Plant Sciences, Stockholm, Sweden
Engel, Anja	aengel@geomar.de	0000-0002-1042-1955	GEOMAR Helmholtz Centre for Ocean Research, Kiel, Germany
Flores, Hauke	hauke.flores@awi.de	0000-0003-1617-5449	Alfred-Wegener-Institute - Helmholtzzentrum für Polar- und Meeresforschung
Fransson, Agneta	agneta.fransson@npolar.no	0000-0003-1403-2110	Norwegian Polar Institute, Fram Centre, Tromsø, Norway
Frickenhaus, Stephan	Stephan.Frickenhaus@awi.de	0000-0002-0356-9791	Alfred-Wegener-Institut Helmholtz-Zentrum für Polar- und Meeresforschung
Gardner, Jessie	jessiegardner001@gmail.com	0000-0003-1730-023X	UiT The Arctic University of Norway
Gelfman, Cecilia E.	cgelfman@uri.edu	0000-0002-3523-5702	University of Rhode Island, Graduate School of Oceanography, USA
Granskog, Mats A.	mats.granskog@npolar.no	0000-0002-5035-4347	Norwegian Polar Institute, Fram Centre, Tromsø, Norway
Graeve, Martin	martin.graeve@awi.de	0000-0002-2294-1915	Alfred-Wegener-Institute - Helmholtzzentrum für Polar- und Meeresforschung
Havermans, Charlotte	Charlotte.Havermans@awi.de	0000-0002-1126-4074	Alfred-Wegener-Institute - Helmholtzzentrum für Polar- und Meeresforschung
Heuzé, Céline	celine.heuze@gu.se	0000-0002-8850-5868	Department of Earth Sciences, University of Gothenburg, Gothenburg, Sweden
Hildebrandt, Nicole	Nicole.Hildebrandt@awi.de	0000-0003-0555-3096	Alfred-Wegener-Institute - Helmholtzzentrum für Polar- und Meeresforschung
Hill, Thomas C. J.	thomas.hill@colostate.edu	0000-0002-5293-3959	Department of Atmospheric Science, Colorado State University

Hoppema, Mario	Mario.Hoppema@awi.de	0000-0002-2326-619X	Alfred-Wegener-Institut Helmholtz-Zentrum für Polar- und Meeresforschung, Bremerhaven
Immerz, Antonia	antonia.immerz@gmx.de	0000-0002-9859-3558	Alfred-Wegener-Institute - Helmholtzzentrum für Polar- und Meeresforschung
Jin, Haiyan	jinhaiyan@sio.org.cn	0000-0002-4965-2830	Key Laboratory of Marine Ecosystem Dynamics, Second Institute of Oceanography, Ministry of Natural Resources, Hangzhou, China
Koch, Boris	boris.koch@awi.de	0000-0002-8453-731X	Alfred-Wegener-Institute - Helmholtzzentrum für Polar- und Meeresforschung
Kong, Xianyu	xianyu.kong@awi.de	0000-0002-7366-5180	Alfred-Wegener-Institute - Helmholtzzentrum für Polar- und Meeresforschung
Kraberg, Alexandra	Alexandra.Kraberg@awi.de	0000-0003-2571-2074	Alfred-Wegener-Institute - Helmholtzzentrum für Polar- und Meeresforschung
Lan, Musheng	lanmusheng@pric.org.cn		Polar Research Institute of China, Shanghai
Lange, Benjamin A.	blange.sea.ice@gmail.com	0000-0003-4534-8978	Norwegian Polar Institute, Fram Centre, Tromsø, Norway
Larsen, Aud	aula@norceresearch.no	0000-0001-6927-5537	Environment and Climate Division, NORCE Norwegian Research Centre, 5008 Bergen, Norway
Lebreton, Benoit	benoit.lebreton@univ-lr.fr	0000-0001-8802-2287	Joint Research Unit Littoral, Environment and Societies (CNRS - University of La Rochelle)
Leu, Eva	eva.leu@akvaplan.niva.no	0000-0002-5328-3396	Akvaplan-niva, Tromsø, Norway
Loose, Brice	bloose@uri.edu	0000-0002-3002-4113	University of Rhode Island, Graduate School of Oceanography, USA
Maslowski, Wieslaw	maslowsk@nps.edu	0000-0002-5790-9229	Naval Postgrduate School
Mavis, Camille	camille.mavis@colostate.edu		Department of Atmospheric Science, Colorado State University
Metfies, Katja	Katja.Metfies@awi.de	0000-0003-3073-8033	Alfred-Wegener-Institute - Helmholtzzentrum für Polar- und Meeresforschung
Mock, Thomas	T.Mock@uea.ac.uk	0000-0001-9604-0362	School of Environmental Sciences, University of East Anglia, Norwich, United Kingdom
Müller, Oliver	oliver.muller@uib.no	0000-0001-5405-052X	University of Bergen, Department of Biological Sciences, Bergen, Norway
Nicolaus, Marcel	marcel.nicolaus@awi.de	0000-0003-0903-1746	Alfred-Wegener-Institut Helmholtz-Zentrum für Polar- und Meeresforschung
Niehoff, Barbara	barbara.niehoff@awi.de	0000-0002-7483-9373	Alfred-Wegener-Institut Helmholz center for Polar and Marine Research
Nomura, Daiki	daiki.nomura@fish.hokudai.ac.jp	0000-0003-3047-4023	Hokkaido Univeristy, Hakodate, Japan
Nöthig, Eva-Maria	eva-maria.noethig@awi.de	0000-0002-7527-7827	Alfred-Wegener-Institut Helmholtz-Zentrum für Polar- und Meeresforschung, Bremerhaven
Marc Oggier	moggier@alaska.edu	0000-0003-4679-1103	International Arctic Research Center, University of Alaska Fairbanks
Oldenburg, Ellen	ellen.oldenburg@hhu.de	0000-0002-0993-9247	Institute of Quantitative and Theoretical Biology, Heinrich-Heine University Düsseldorf, Düsseldorf, Germany
Olsen, Lasse Mork	lasse@aqua-kompetanse.no	0000-0003-1328-2687	University of Bergen, Department of Bioscience, Bergen, Norway
Peeken, Ilka	ilka.peeken@awi.de	0000-0003-1531-1664	Alfred-Wegener-Institute - Helmholtzzentrum für Polar- und Meeresforschung
Perovich, Donald K.	donald.k.perovich@dartmouth.ed	0000-0002-0576-0864	Dartmouth College, Hanover, NH, USA
Popa, Ovidiu	ovidiu.popa@hhu.de	0000-0003-4470-0378	Institute of Quantitative and Theoretical Biology, Heinrich-Heine University Düsseldorf, Düsseldorf, Germany
Rabe, Benjamin	benjamin.rabe@awi.de	0000-0001-5794-9856	Alfred-Wegener-Institut Helmholtz-Zentrum für Polar- und Meeresforschung
Ren, Jian	jian.ren@sio.org.cn	0000-0002-1889-5661	Key Laboratory of Marine Ecosystem Dynamics, Second Institute of Oceanography, Ministry of Natural Resources, Hangzhou, China
Rex, Markus	markus.rex@awi.de	0000-0001-7847-8221	Alfred-Wegener-Institut, Helmholtz-Zentrum für Polar- und Meeresforschung, Potsdam, Germany & University of Potsdam, Potsdam, Germany
Rinke, Anette	annette.rinke@awi.de	0000-0002-6685-9219	Alfred-Wegener-Institut, Helmholtz-Zentrum für Polar- und Meeresforschung, Potsdam, Germany
Rokitta, Sebastian	sebastian.rokitta@awi.de	0000-0002-7540-9033	Alfred-Wegener-Institute - Helmholtzzentrum für Polar- und Meeresforschung
Rost, Björn	bjoern.rost@awi.de	0000-0001-5452-5505	Alfred-Wegener-Institute - Helmholtzzentrum für Polar- und Meeresforschung
Sakinan, Serdar	serdar.sakinan@wur.nl	0000-0002-5651-2836	Wageningen Marine Research, IJmuiden, The Netherlands
Salganik, Evgenii	evgenii.salganik@npolar.no	0000-0001-8383-7815	Norwegian Polar Institute, Fram Centre, Tromsø, Norway
Schaafsma, Fokje L.	fokje.schaafsma@wur.nl	0000-0002-8945-2868	Wageningen Marine Research, Ankerpark 27, 1781 AG Den Helder, The Netherlands
Schäfer, H.	H.Schaefer@warwick.ac.uk	0000-0001-8450-7893	University of Warwick, School of Life Sciences
Schmidt, Katrin	katrin7schmidt@gmail.com	0000-0002-6488-623X	University of Plymouth, School of Geography, Earth and Environmental Sciences
Shoemaker, Katyanne M.	katyanne.shoemaker@noaa.gov	0000-0002-5129-2387	University of Rhode Island, Graduate School of Oceanography, USA

Shupe, Matthew D.	matthew.shupe@noaa.gov	0000-0002-0973-9982	Cooperative Institute for Research in Environmental Sciences, University of Colorado Boulder & NOAA Physical Sciences Laboratory, Boulder, CO; USA
Snoeijs-Leijonmalm, Pauline	pauline.snoeijs-leijonmalm@su.se	0000-0002-4544-2668	Stockholm University, Department of Ecology, Environment and Plant Sciences, Stockholm, Sweden
Stefels, J	j.stefels@rug.nl	0000-0001-9491-1611	University of Groningen, Groningen Institute of Evolutionary Life Sciences (GELifeS), Groningen, the Netherlands
Svenson, Anders	anders.svenson@slu.se		Swedish University of Agricultural Sciences, Lysekil, Sweden
Tao, Ran	ran.tao@awi.de	0000-0002-6690-9212	Alfred-Wegener-Institute - Helmholtzzentrum für Polar- und Meeresforschung
Torres-Valdés, Sinhué	sinhue.torres-valdes@awi.de	0000-0003-2749-4170	Alfred-Wegener-Institute - Helmholtzzentrum für Polar- und Meeresforschung
Torstensson, Anders	torstensson.anders@gmail.com	0000-0002-8283-656X	Stockholm University, Department of Ecology, Environment and Plant Sciences, Stockholm, Sweden
Toseland, Andrew	A.Toseland@uea.ac.uk	0000-0002-6513-956X	School of Environmental Sciences, University of East Anglia, Norwich, United Kingdom
Ulfsbo, Adam	adam.ulfsbo@gu.se	0000-0001-7550-7381	Department of Marine Sciences, University of Gothenburg, Gothenburg, Sweden
Van Leeuwe, Maria A.	m.a.van.leeuwe@rug.nl	0000-0002-9572-4700	University of Groningen, Groningen Institute of Evolutionary Life Sciences (GELifeS), Groningen, the Netherlands
Vortkamp, Martina	Martina.Vortkamp@awi.de		Alfred-Wegener-Institute - Helmholtzzentrum für Polar- und Meeresforschung
Webb, Alison Louise	alison.webb@york.ac.uk	0000-0003-1762-2060	University of Warwick, School of Life Sciences
Gradinger, Rolf R.	rolf.gradinger@uit.no	0000-0001-6035-3957	UiT The Arctic University of Norway

ABSTRACT

An international and interdisciplinary sea ice drift expedition, the 'The Multidisciplinary drifting Observatory for the Study of Arctic Climate' (MOSAiC), was conducted from October 2019 to September 2020. The aim of MOSAiC was to study the interconnected physical, chemical and biological characteristics and processes from the atmosphere to the deep sea of the central Arctic system. The ecosystem team addressed current knowledge gaps and explored unknown biological properties over a complete seasonal cycle focusing on three major research areas: biodiversity, biogeochemical cycles and linkages to the environment. In addition to the coverage of core properties along a complete seasonal cycle, dedicated projects covered specific processes and habitats, or organisms on higher taxonomic or temporal resolution. A wide range of sampling approaches from sampling, sea ice coring, lead sampling to CTD rosette-based water sampling, plankton nets, ROVs and acoustic buoys was applied to address the science objectives. Further, a wide range of process-related measurements to address e.g. productivity patterns, seasonal migrations and diversity shifts were conducted both in situ and onboard *RV Polarstern*. This paper provides a detailed overview of the sampling approaches used to address the three main science objectives. It highlights the core sampling program and provides examples of two habitat- or process-specific projects. First results presented include high biological activities in winter time and the discovery of biological hotspots in underexplored habitats. The unique interconnectivity of the coordinated sampling efforts also revealed insights into cross-disciplinary interactions like the impact of biota on Arctic cloud formation. This overview further presents both lessons learned from conducting such a demanding field campaign and an outlook on spin-off projects to be conducted over the next years.

1. INTRODUCTION

1.1. Motivation

The Multidisciplinary drifting Observatory for the Study of Arctic Climate (MOSAiC) expedition provides unique scientific opportunities to fundamentally understand the interlinked physical, chemical, and biological systems in the central Arctic Ocean. The science program was shaped over nearly a decade and provides a foundation to create new and important knowledge regarding the functioning of the Arctic ecosystem within the context of the coupled Arctic climate system. Five closely cooperating science teams were formed to develop and execute the integrated science plan, focusing on atmosphere, sea ice, ocean, ecosystem and biogeochemistry. This paper provides an overview of the multiple facets of ecosystem-related research to highlight the interlinked research activities at multiple trophic levels in relation to the environment. Within the MOSAiC ecosystem team (termed *ECO team* in the following), a total of 25 institutions across 15 nations contributed to generating the field observations and measurements as part of the research program. Similar overviews are available for other MOSAiC research topics, currently for sea ice physics, physical oceanography, and various aspects of the atmosphere (Nicolaus et al., 2022b; Rabe et al., 2022; Shupe et al., 2022), while an overview on biogeochemical research not covered in this article is forthcoming.

The integrated ecological observations and knowledge generated by the ECO team was specifically aimed at understanding seasonally-resolved processes on different scales. These are critical for future predictions related to climate change impacts on the Arctic system, including alterations to ecosystem structure and functioning (Intergovernmental Panel on Climate Change (IPCC), 2023). While the research is ongoing, new projects are emerging based on insights, data and collaborations.

Section 1 of this paper outlines the main ecological research objectives addressed via the MOSAiC ecosystem research, followed in the second section by a more detailed description of the scientific approaches and methods being used. The coordinated ecological research also included biogeochemical variables (e.g. macronutrient concentrations, seawater and ice carbonate chemistry, dissolved organic carbon) due to their close links to ecosystem processes. Example data sets provided in section 3 demonstrate what to expect in the forthcoming peer-reviewed publications. Lastly, section 4 provides insights into "lessons learned" and challenges when planning such a yearlong expedition and point towards some of the expected impacts that could arise from the compiled knowledge over the years to come.

1.2.   The Central Arctic Ecosystem and its links to the environment

The Arctic Ocean harbors unique and diverse biological communities in all available habitats: sea ice, snow, seawater, atmosphere, and sediments. Although the Arctic Ocean was once considered a relatively species-poor region with limited biological activity, research in recent decades has revised this paradigm (Bluhm et al., 2011). For example, it is now known that there is high biodiversity in all habitats and high biological activity year-round, including in the winter season (Berge et al., 2015; Hobbs et al., 2020). Furthermore, the Arctic ecosystem is not easily generalized due to the particularly high spatio-temporal variability in biological, chemical, and physical processes (Bluhm et al., 2015). Arctic marine ecosystems have regionally varying complex community structures and activity patterns, largely driven by differences in abiotic factors like water temperature, depth, salinity, light, inorganic nutrients, and sea ice properties (Balmonte et al., 2018; Bluhm et al., 2018, 2015; Clement Kinney et al., 2023; Ershova et al., 2021; Polyakov et al., 2020). Other efforts to explore ecosystem-level research in the central Arctic include SHEBA (e.g., Ashjian et al., 2003; Sherr et al., 2003), the Circumpolar Flaw Lead study (Barber et al., 2015), N-ICE2015 (Assmy et al., 2017; Granskog et al., 2018), the Synoptic Arctic Survey (Snoeijs-Leijonmalm et al., 2022), Tara Arctic (Ibarbalz et al., 2023; Royo-Llonch et al., 2021), and the Russian ice drift studies (Melnikov, 1980). Yet, despite these valuable efforts, the seasonal cycle in the central Arctic remains understudied because the region is difficult to access in winter with thick and extensive sea ice cover and harsh conditions for work in the field. Remote sensing of biological properties is also limited by the ice-covered, seasonally dark and often cloud-covered Arctic (Babin et al., 2015). New comprehensive time series data are further needed to construct numerical models and test mechanistic hypotheses within the context of Earth System Models (e.g., CMIP5 and CMIP6 for the IPCC AR5 and 6, respectively; IPCC, 2023). Representations of the marine ecosystem are lacking or less advanced than other components of the Earth system within large-scale models. Therefore, MOSAiC research is a critically needed evaluation of the current state of the Arctic marine ecosystem, required to adjust our understanding to new ecosystem components, and improve our understanding of basic biological processes to enhance predictions of future system status.

The central deep Arctic Ocean is divided into four abyssal plains separated by the Lomonosov, Gakkel, and Alpha ridges. Even so, the upper water column (~ 1000 m) is contiguous with two major ice drift and ocean circulation patterns: the Transpolar Drift (TPD) System and the Beaufort Gyre. The MOSAiC field campaign was established on a sea-ice floe at the Siberian edge of the Amundsen Basin (Figure 1), close to the origin of the TPD. During the campaign, the floe drifted in the TPD across the central Arctic towards Fram Strait. Details regarding the sea ice conditions during MOSAiC are provided by Krumpen et al. (2020) and Nicolaus et al. (2022b). The hydrography in the central Arctic Ocean is characterized by a strong, permanent vertical salinity gradient (halocline). The upper surface mixed layer in the Amundsen Basin is characterized by low salinity and largely cold waters, being affected by river discharge, ice melt / freeze processes and Pacific inflow inside the

139 TPD (Rabe et al., 2022; Rudels and Carmack, 2022; Schulz et al., 2023a). South of
140 the Amundsen Basin, as separated by the Gakkel ridge, surface waters of the
141 Nansen Basin (Figure 1) are less influenced by the TPD. Here surface waters carry a
142 stronger signal of Atlantic sourced water masses (Schulz et al., 2023b). Below the
143 surface mixed layer lay warmer and more saline waters of Atlantic origin. The core of
144 the Atlantic Water is warmest and saltiest north of Svalbard and close to the Barents-
145 Kara Sea slope. In addition, modelling studies suggest that Atlantic water can advect
146 biomass from phytoplankton blooms developed in open waters upstream under the
147 sea ice into the eastern Arctic (In addition, modelling studies suggest that Atlantic
148 water can advect biomass from phytoplankton blooms developed in open waters
149 upstream under the sea ice into the eastern Arctic (Clement Kinney et al., 2023). It is
150 modified once it enters the basins and circulates around the Arctic, mainly along the
151 shelf slopes as a deep circulation loop (Rudels and Carmack, 2022), and over time,
152 becomes colder, fresher, and is subducted deeper in the water column. The
153 influence of these major water sources (i.e. TPD- vs Atlantic-influenced) on the
154 central Arctic Ocean depends on circulation dynamics, which control the proportion,
155 layering, and mixing of different source waters and their respective nutrient
156 inventories. In surface waters of the central Arctic, nutrient concentrations are
157 variable, but low relative to the Arctic shelf regions and deeper water masses (Bluhm
158 et al., 2015; Randelhoff et al., 2020).
159   The strong vertical gradients in nutrient concentrations, and factors such as
160 irradiance and other ocean physico-chemical parameters, structure the pelagic
161 realm. Highly diverse communities of phytoplankton and sea ice algae (Poulin et al.,
162 2011) contribute to the primary production in the central Arctic (Gosselin et al., 1997;
163 Wiedmann et al., 2020). Both ice and pelagic algae have developed several
164 successful strategies to overcome months without sufficient light for photosynthesis
165 (Johnsen et al., 2020) and rapidly utilize the light returning after the Polar night
166 (Hoppe, 2022; Kvernvik et al., 2018). Still, the overwintering strategies and modes of
167 nutrition of several key groups and species remain poorly understood. Also, lower
168 trophic herbivores and omnivores, like sea ice meiofauna (Ehrlich et al., 2020;
169 Patrohay et al., 2022) or pelagic zooplankton (Ershova et al., 2021; Hop et al., 2021),
170 have evolved life cycles and physiological adaptations that allow them to survive and
171 successfully compete under these extreme conditions in the ice-covered central
172 Arctic Ocean. The microbial network, involving diverse bacterial and archaeal
173 communities (Boetius et al., 2015), drives the remineralization of organic matter in
174 ice and water (Balmonte et al., 2018; Laurion et al., 1995; Wietz et al., 2021), which
175 is a key process for supplying nutrients for algal growth. However, heterotrophic
176 bacteria and algae can also compete for inorganic nitrogen resources (Fouilland et
177 al., 2007).
178   Sea ice provides a unique habitat for diverse biota ranging from viruses to
179 marine mammals and birds. It sustains its own food web driven by the productivity of
180 sea ice algae, which has been reported to contribute up to 55% of total primary
181 production in ice covered areas (Gosselin et al., 1997; Wiedmann et al., 2020). This
182 production is channeled through ice-associated herbivores including copepods and

amphipods, and fish (specifically Arctic/polar cod, *Boreogadus saida*). In fact, trophic marker studies have demonstrated that a substantial part of the organic matter from sea ice algae culminates in apex species like ringed and bearded seals, or Arctic birds (e.g. Carlyle et al., 2022; Kohlbach et al., 2016; Kunisch et al., 2021). Diversity in sea ice systems is high, including viruses, bacteria, over 1000 species of unicellular algae and protozoa (Poulin et al., 2011), and about 100 associated metazoan taxa living in the ice brine channel system or the bottom of the ice (Bluhm et al., 2018 and references within). Summer melt ponds and low-salinity meltwater accumulated in leads and under the ice are examples of unique habitats that can form, disappear, and be replenished again multiple times over relatively short time scales during parts of a seasonal cycle (Smith et al., 2023). Similarly, also under ice productivity can be high in ice covered regions: a recent high resolution biophysical modeling study has found that 63% of the total primary production in the central Arctic occurs in waters with ≥50% sea ice cover, and 41% of the total primary production in areas with ≥85% cover (Clement Kinney et al., 2020). While considerable information exists for some regions, seasons, and taxa, the majority of biological components in the ice and ocean have not been identified and quantified through a complete annual cycle, particularly in the high Arctic. Filling this knowledge gap by investigating the full range of trophic components from bacteria to metazoans and exploring their unknown connections has been an ambitious and challenging goal of MOSAiC ecosystem research.

The activities of and interactions between different taxonomic, functional, and trophic groups change in space and time. In the Arctic, the strong seasonality and high interannual variability in environmental conditions such as temperature, nutrient availability, and irradiance drive the ecosystem state, phenology, and functions (Ardyna and Arrigo, 2020; Kosobokova and Hirche, 2000; Leu et al., 2015). Climate change has already substantially altered the Arctic marine system through increased fractions of first-year ice, stronger and warmer inflow from the Atlantic and Pacific Oceans, freshening of the surface waters, later sea ice formation and earlier onset of melt (Ingvaldsen et al., 2021; Polyakov et al., 2020) with associated biological system responses. For instance, under-ice phytoplankton blooms, algal infiltration communities at the snow-ice interface, and shifts in biodiversity due to borealization are increasingly observed (Ardyna et al., 2020; Fernández-Méndez et al., 2018; Ingvaldsen et al., 2021). Different sensitivities to climate change drivers by various ecosystem components may cause mismatches between trophic levels, such as algae blooms occurring earlier than the zooplankton life stages depending on them as food (Søreide et al., 2010). Also, the shift from a dominance of a multi-year ice (MYI) or second-year ice (SYI) to a first-year ice (FYI) regime will likely impact sea ice biota; however, evidence for change is patchy due to the limited availability of sufficiently long time-series data (Campbell et al., 2022). Comparisons between FYI and MYI diversity of sea ice protists indicate substantially lower (by 39%) diversity in FYI compared to MYI (Hop et al., 2020). The diversity and presence of sea ice meiofauna taxa has also decreased, including the nearly complete absence of flatworms and nematodes in recent studies (Ehrlich et al., 2020). MYI might also act

as a seed bank for sea ice algae and fauna for adjacent newly forming and growing FYI (Olsen et al., 2017). Sea ice biogeochemical cycles could be impacted, as FYI is typically saltier, with higher brine volume fractions creating more habitable space, and permeability resulting in higher fluxes within the ice, and increased nutrient supply (Tedesco et al., 2019). Beyond these structural and functional changes in the sea ice ecosystem itself, an alteration of the relative contribution of sea ice algae versus phytoplankton to overall annual primary production also has consequences for other ecosystem components, including through the often tight sympagic-pelagic and sympagic-benthic coupling processes (Rybakova et al., 2019; Wang et al., 2015; Wiedmann et al., 2020).

Biological processes in ice and seawater are not only relevant for the marine ecosystem, but impact the entire Arctic System. These processes are linked to physical processes in the atmosphere, ice, and ocean through various coupled processes and feedback mechanisms (Figure 2). Whereas the strong interdependence between the seasonally changing sea ice properties and ocean-atmosphere physics is widely recognized (Shupe et al., 2022), the tightly coupled interaction between the sea ice and the biology and chemistry of the ocean underneath is not well understood and, as a consequence, often neglected in numerical models. Biological activity affects the cycling and transformation of inorganic molecules and organic matter, and exerts strong controls on the cycling of climate-active gases such as carbon dioxide (CO_2), methane (CH_4), nitrous oxide (N_2O), and dimethyl sulfide (DMS) in the ocean and ice, as well as across the atmosphere-ice-ocean interfaces (Falkowski et al., 1998). For example, CO_2 concentrations are controlled by a range of chemical and biological processes including organic production, remineralization, gas exchange, and inorganic calcium carbonate precipitation within sea ice and dissolution in sea ice meltwater (Angelopoulos et al., 2022; Fransson et al., 2011; Miller et al., 2011; Nomura et al., 2018; Rysgaard et al., 2012, 2007) leading to seasonally varying air-sea-ice CO_2 exchange (e.g., Fransson et al., 2013; Mo et al., 2022). Seasonal sea ice melt decreases the partial pressure of CO_2 (pCO_2) of the stratified Arctic surface waters through dilution, ikaite dissolution, and supporting phytoplankton blooms near the surface (Fransson et al., 2017). In recent years, enhanced sea ice melt has exposed these low pCO_2 surface waters to high atmospheric pCO_2 levels, thereby promoting CO_2 uptake from the atmosphere (Qi et al., 2022). Over longer periods of time, the enhanced CO_2 uptake decreases the surface waters' pH buffering capacity and promoting vulnerability to ocean acidification (Qi et al., 2022). At the same time, the associated decreased buffer capacity for CO_2 promotes ocean acidification. Storm events in different seasons can impact air-sea CO_2 exchange by altering the surface layer pCO_2 through wind-induced mixing with subsurface water and by creating leads where direct air-sea gas exchange can occur (Fransson et al., 2017). For sea ice itself, rising temperatures and younger sea ice promote an increase in the brine volume fraction, which in turn enhances the transfer of gases and substances across gas-water interfaces within sea ice and between the sea ice and atmosphere (Nomura et al., 2018).

Marine biological processes can impact climate relevant processes through linkages beyond production cycles of climate-relevant gases. Biogenic compounds that become aerosol particles can become airborne through the air-water interfaces of the Arctic and serve as cloud condensation nuclei (CCN) and ice nucleating particles (INPs) in the atmosphere, affecting clouds and the radiative balance of the system (Creamean et al., 2022). This, in turn, may feedback on productivity through modulation of the light available to fuel primary production (Kauko et al., 2017). High standing stocks of organisms in the sea ice and water column also change the energy budget and heat uptake of these components as they increase the absorption of shortwave radiation, thereby affecting the freeze and melt cycles of their own habitat (Taskjelle et al., 2017; Zeebe et al., 1996). Also, sea ice microstructural properties relevant for gas exchange can be modified through ice algal production of extracellular polymeric substances (Krembs et al., 2011).

1.3.   The mission of MOSAiC ecosystem studies

The MOSAiC sampling program used existing knowledge on ecosystem-relevant processes and components to fill major gaps in current knowledge and explore so far unknown links. The integrated MOSAiC ecosystem research program combined year-round consistent measurements of specific core properties (Table 1) with embedded individual research projects (supplementary Table S1) and opportunistic sampling. The core program included an extensive suite of biological and chemical components sampled from the water column, and undeformed level FYI and SYI. The aim of the core measurement program was to provide a consistent and continuous backbone of key measurements over the drift period, which would allow to link different integrative and complementary process studies. The project-specific measurements either provided higher temporal or spatial resolution beyond the weekly sampling program, or focused on processes or habitats that were not part of the core parameter time-series. Our investigations relied on a combination of traditional tools and more recently developed technologies and cross-cutting approaches. This combined approach facilitated linkages to previous studies, while providing new knowledge into the seasonality of high Arctic biological and biogeochemical processes at unprecedented temporal resolution. The work of the ECO team is focused on three fundamental and essential research questions: 1) Which species are present in the Arctic Ocean (WHO, i.e. Biodiversity)? 2) How do fluxes of energy and matter flow through food webs and habitats (HOW, i.e. Ecosystem functioning)? And 3) Why do physical and chemical parameters exert control on species distribution and activities and vice versa (WHY, i.e. linkages with the environment)?

Biodiversity: The program was designed to capture a full seasonal sampling of ice and seawater habitats, including the dark season, with a wide range of established and innovative tools to achieve the most complete species inventory for ice and pelagic biota of the Central Arctic.

Ecosystem functioning: The flow of matter and energy in ice and seawater substantially changes with time, driven by the strong seasonality of environmental

variables (e.g., light and ice freeze-melt cycles) and organism life cycles. Therefore, it was essential to systematically determine organism abundances, biomass, and activity rates throughout the MOSAiC drift. The program aimed to quantify the seasonal fluctuations in algal and bacterial productivity, organismal physiologies (including metatranscriptomes) and life cycles, as well as grazing by micro- and mesozooplankton, diets of key species, and vertical particle fluxes.

Linkages with environment: The combined analysis of ecosystem characteristics with all available MOSAiC environmental data allows us to assess the importance of bottom-up (e.g., light, nutrients, sea ice characteristics) versus top-down (e.g., grazing, predation) controls on biological standing stocks and activities over a complete seasonal cycle. The program aimed to assess the contributions of ecosystem processes to the Arctic climate system, e.g., by driving gas fluxes across ice-ocean-atmosphere interfaces, or by affecting the heat budget of sea ice directly or through interactions with clouds.

These three major focal science areas were approached by considering both their interconnection as well as their relation to the overall MOSAiC science objectives. Therefore, a consistent, coordinated, and methodological framework linking individual measurements within the ECO team was developed. This included strong interdisciplinary partnership with the other MOSAiC teams, like co-located measurements of sea ice and water column properties to identify biologically-relevant linkages between the two habitats. The unique year-round access to the high Arctic environment was used to investigate poorly understood and undersampled habitats and seasons. For example, high heterotrophic biological activities and unique biodiversity patterns in winter were expected to precondition the biological response to the return of the light in spring. We furthermore expected that meta-genomic and -transcriptomic data can be used to identify unique physiological mechanisms that sustain survival of organisms and ecosystem services under polar seasonality. The program aimed to provide information relevant for understanding a wider Arctic system by determining the fluxes of climate-relevant compounds like CO_2.

2. APPROACH AND METHODS

The MOSAiC expedition (PS122) onboard the German research icebreaker RV *Polarstern* (Alfred-Wegener-Institut Helmholtz-Zentrum für Polar- und Meeresforschung, 2017) was organized into 5 cruise legs (Figure 1). The field campaign began in late September 2019, and north of the Laptev Sea (Krumpen et al., 2020; Nicolaus et al., 2022b) the first Central Observatory ice camp was established, which was used on cruise legs 1-3 until May 11, 2020 (Figure 3). Team ECO observations began on 15 October 2019, and the full regular weekly sampling by Team ECO started 31 October 2019, which involved measurements and sampling from the ship and ice floe. Leg 1 ended in mid-December and Leg 2 continued on until the end of February 2020. Leg 3 extended beyond its originally planned date due to logistical constraints caused by the global COVID-19 pandemic, and ended in mid-May 2020, when RV *Polarstern* had to leave the first Central Observatory.

359 Following a logistically necessary break, leg 4 re-established and occupied a new
360 Central Observatory (Figure 4) at a different location on the same ice floe from 20
361 June 2020 until the floe disintegrated in the Fram Strait on 31 July 2020. Continued
362 observations were made during leg 5, which involved establishing a new ice camp
363 (Figure 5) located on a new ice floe near the North Pole in the second half of August.
364 The MOSAiC ice drift study ended 20 September 2020, with ECO science operations
365 continuing in the marginal ice zone during the transit back to shore. More details on
366 the MOSAiC campaign, can be found in Nicolaus et al. (2022b), Rabe et al. (2022)
367 and Shupe et al. (2022).
368
369 **2.1 Water column work program**
370 Sampling and measurements in the water column occurred at frequencies from daily,
371 to weekly, with opportunistic, intensive observation sampling occurring a few times
372 over the duration of the expedition, which involved sampling at hourly time scales for
373 20-30 hr periods. Sampling frequency was partially based on feasibility and cost-
374 benefit evaluation. For most ECO properties, the primary sampling mode was weekly
375 sampling, matching the anticipated rates of change in ecological properties relative
376 to anticipated achievability of the sampling program by a small onboard team. The
377 daily sampling for chlorophyll *a* (Chl-a) and microbial community structure resolved
378 day-to-day changes in fundamental microbial properties, which would be missed with
379 only once-weekly sampling. Herein, major operations executed by Team ECO
380 organized by sampling frequency are briefly described, while detailed method
381 descriptions will be provided in later, targeted publications.
382
383 *2.1.1. Continuous measurements and daily sampling approaches*
384 A Membrane-Inlet Mass Spectrometer (MIMS) connected to the ship's flow-
385 through seawater system allowed the continuous measurement of dissolved O_2
386 and Ar concentrations to calculate O_2/Ar ratios and infer net community
387 production (NCP) (Tortell, 2005; Ulfsbo et al., 2014), Rokitta et al. unpublished
388 results). The depth of the seawater intake port was 11 m below sea level at the
389 keel of the ship. Continuous measurements of these properties were only
390 interrupted during 1) routine maintenance procedures by instrument operators, 2)
391 ship maintenance of flow-through systems, and 3) when discrete bottle sample
392 measurements were performed. Therefore, gaps in continuous data mostly
393 collected during March to October 2020 are approximately 1) once daily for 1-2
394 hrs, 2) 1-2 times monthly for 3-6 hrs, 3) 3-4 hrs weekly. Onboard, routine
395 calibration with reference gasses allowed for tracking of instrument drift over the
396 course of the expedition.
397   The AUTOmated FIltration for marine Microbes (AUTOFIM) instrument
398 (iSiTEC GmbH, Bremerhaven, Germany) automatically collected, filtered, and
399 preserved water samples for molecular genetic analyses (Metfies et al., 2016)
400 from December 2019 to October 2020. It is permanently installed on RV
401 *Polarstern* a few meters from the flow-through seawater intake system at 11 m at
402 the bow of the ship. AUTOFIM collected samples on a daily basis, and in some

403	instances at even higher temporal resolution to resolve spatial changes along the
404	drift path. Samples were analyzed for microbial community structure using 16S
405	and 18S rRNA amplicon sequence-based approaches.
406	The fishcam, an *in situ* video system (FishCam, MacArtney Germany GmbH,
407	Kiel, Germany), was deployed on average at 375 m water depth (range 369 - 376
408	m) from 23 October to 7 November 2019 and at 213 m depth (range 194 - 215 m)
409	from 12 December 2019 to 11 March 2020 through a hole in the ice,
410	approximately 500 m away from the ship (see Snoeijs-Leijonmalm et al. (2022)
411	for details). The system included two HD Internet Protocol cameras, one looking
412	sideward and one looking downward, two Luxus High-Power LED light sources of
413	6000 lm each, and a mini-CTD. The system was connected to a personal
414	computer onboard, running PortVis (Serial Port and Video Stream Visualizer)
415	software, version 2.1. Camera images were recorded in LED on:off cycles of
416	5:55, 15:15, or 55:5 min. Fish were also caught via long lines and fishing rods
417	deployed through the moon pool or holes in the ice (Snoeijs-Leijonmalm et al.,
418	2022).
419	Further, a number of discrete water samples were manually collected at a
420	daily or near-daily frequency over the duration of the expedition from a single tap
421	of the ship's flow-through seawater system, which was also used for the MIMS
422	measurements. This included separate samples for 1) Chl-a (except from mid-
423	December to end of February), 2) 16S and 18S rRNA amplicon-based microbial
424	community analyses (except from mid-December to end of February), and 3) ice
425	nucleating particles (INPs, full timeseries).
426	To investigate downward flux, a long-term ice-tethered time-series sediment
427	trap (McLane PARFLUX Mark 78H-21) with 21 sampling cups was deployed at
428	200 m water depth, and tethered to SYI, located ~1000 m away from the ship
429	(Figure 3). Sinking particles were automatically collected for two week intervals
430	(15 or 16 days) from March to November and every month (29-31 days) from
431	December to February. The sampling cups were filled with salt-saturated artificial
432	seawater and $HgCl_2$ prior to deployment. The sediment trap was operational from
433	26 October 2019 to 31 July 2020.
434	
435	*2.1.2. Discrete sampling*
436	The primary sampling approach for the weekly ECO time-series of water column
437	biological and chemical properties relied on the ship CTD rosette, a suite of
438	plankton nets, and a number of small animal- and particle-imaging instruments
439	with deployments over three consecutive days per calendar week. The CTD
440	sensor packages, calibration methods, and post-processing are described in
441	Rabe et al. (2022) and Tippenhauer et al. (2023a, 2023b). In brief, discrete
442	biological samples were collected from 12-liter OTD bottles attached to the
443	shipboard 24-bottle CTD rosette (PS-CTD). From November 2019 to May 2020,
444	additional water column sampling was conducted via a 5-liter 12-Niskin bottle
445	CTD rosette from Ocean City (OC-CTD; via a sheltered in-ice hole located 300
446	meters from RV *Polarstern*; see Figure 3*)*. In the period between mid-March and

447   mid-May, the PS-CTD was not operational due to the loss of the ice hole
448   alongside the ship (see Rabe et al., 2022), so all water column ECO samples
449   were collected at Ocean City. During this period, use of the OC-CTD led to a
450   lower vertical depth resolution as the total water volume collectable in one cast
451   was substantially less with the OC-CTD (60 L) versus the PS-CTD (288 L). All
452   sampling events are listed in Table S4. Sampling order from the individual rosette
453   bottles primarily followed WOCE procedures (Woods 1985), which prioritizes
454   sampling of tracers, gases, and nutrients in time before the sampling of other
455   properties. The sequence prioritized sampling of time-sensitive properties and
456   limited contamination between parameters. Co-location of many properties
457   across a smaller number of depth horizons was prioritized over higher vertical
458   resolution of a few properties (Figure 6). Additionally, upper 200 m water column
459   sampling was prioritized over full water column profiling to better resolve upper
460   ocean interactions with sea ice and the atmosphere. Sample types requiring large
461   volumes (e.g. POC/N, DNA and RNA) made it necessary to collect samples in
462   additional casts following a primary full water column cast used to collect small
463   volume ECO samples. Standard water depth horizons for biological properties
464   were 2 m, 10 m, Chl-a fluorescence maximum (if present based on CTD
465   fluorescence sensor profile) or 20 m, 50 m, 100 m, and the Atlantic Water core
466   depth. The depth of the Atlantic Water core, detected as the local temperature
467   maximum in each profile, varied significantly along the drift path, from
468   approximately 100 m close to Fram Strait up to 400 m in the Amundsen Basin
469   (Rabe et al., 2022; Schulz et al., 2023b). The depth-resolved sampling for Chl-a,
470   nutrients, and total DNA collected from the PS-CTD and OC-CTD rosettes over
471   the drift duration relative to a reference depth (400 m) and bottom depth highlight
472   the focus of sample collections in the upper water column (Figure 7).
473   Samples collected by team ECO during the routine CTD rosette-based water
474   column sampling included a wide range of standard variables such as inorganic
475   nutrients (nitrate+nitrite, nitrite, silicic acid, phosphate and ammonium) as well as
476   total dissolved nitrogen and total dissolved phosphorus, total dissolved inorganic
477   carbon (DIC) and total alkalinity (TA), dissolved organic carbon (DOC), colored
478   dissolved organic matter (CDOM), Chl-a, algal pigments, POC and PON
479   concentrations as well as their isotopic composition, biogenic silica (bSi), total
480   deoxyribonucleic acid (DNA) and ribonucleic acid (RNA) for sequencing,
481   taxonomic cell counts (via light microscopy), as well as cell abundance (via flow
482   cytometry). Samples for primary and bacterial production, dissolved oxygen,
483   DOM characterization after solid-phase extraction, and ^{14}C-DIC were collected at
484   a lower temporal frequency and with larger gaps due to instrumentation failures.
485   Additionally, several complementary samples were collected on a routine basis,
486   such as those for measurements of O_2/Ar ratios in discrete samples, INPs,
487   neutral sugars, and ^{15}N-nitrate isotopes. Processing of preserved water or filters
488   mainly occurred at the shore-based laboratories, with exceptions of onboard
489   measurements of nutrients (Nov 2019 to May 2020), dissolved oxygen (March to
490   Oct 2020), primary and bacterial production (Dec 2019 to May 2020), and a

subset of Chl-a samples (March to May 2020). Details on sample processing methods can be found in supplementary Table S2.

We aimed for all analyses for each variable to be done in the same laboratory and/or using the same instrument to decrease uncertainty due to laboratory or instrument calibration (see supplementary Table S2 for details). In cases where this was not possible (DIC/TA, DNA, RNA, POC/N), interlaboratory calibration samples were collected. In the case of nucleic acid samples, aliquots from the same extracted samples of the core time series were used for specific sequencing approaches in specialized labs (e.g. metabarcoding, genomics, sequencing of specific metazoan or functional primers). Details on the ECO multi-omics sampling program are given in Mock et al. (2022).

The seasonal life cycles and vertical distribution of zooplankton abundance and biomass were studied using imaging tools and plankton nets, deployed on the same or on two consecutive days during a calendar week. From November to March, a multinet midi (Hydrobios), three ring nets, the Underwater Vision Profiler (UVP) and the Light-frame On-sight Key Species Investigation system (LOKI) were deployed through a large hole in the ice alongside the RV *Polarstern* yielding an almost weekly resolution for many targeted parameters (Tables S4 and S5). The multinet was equipped with five nets of 150 µm mesh size to sample five discrete depth intervals between 2000 m and the ocean surface. Those samples were processed for zooplankton identification, abundance, and biomass at shore-based laboratories. The LOKI was deployed approximately weekly from 1000 m to the surface. In addition to high resolution images, the instrument obtained hydrographical parameters, e.g. depth, temperature, salinity, oxygen concentration and fluorescence. The UVP was mounted on the PS-CTD rosette and casts were conducted from various depths to the surface. Ring nets of 1 m^2 area (150- and 1000-µm mesh) and 0.28 m^2 area (53-µm mesh) were deployed to varying depths up to 2000 m, to collect zooplankton for analysis of taxonomy, energy content, biomarkers and gut DNA (Table S4). However, the hole next to the vessel could not be maintained in April and May due to strong ice dynamics. During that period, only a 150-µm mesh Nansen net and the 53-µm mesh ring net could be deployed at the ice hole at OC. The Nansen net was equipped with an opening/closing device and was deployed in a series of single casts to the same depth intervals as sampled by the Multinet down to a maximum depth of 800 m. Additional ring net tows were conducted over the same depth intervals as used for the Multinet to collect animals for biochemical and genetic analyses and physiological rate measurements. In addition, during all seasons, a net was attached to the under-ice Remotely Operated Vehicle (ROV) 'Beast' (Katlein et al., 2017) for sampling 2-3 depth horizons: the ice-ocean interface, 10 m, and 50 m under the ice.

To determine zooplankton abundance and biodiversity, usually complete samples from Multi-, Nansen-, and ROV net casts, as well as samples taken with the small ring net, were preserved with hexamethylenetetramine-buffered 4% formaldehyde, stored at room temperature and subsequently processed in

laboratories in Germany (AWI) and the US (University of Rhode Island). Live specimens for biochemical analyses and physiological rate measurements were sorted from ring net samples under a stereomicroscope onboard and determined to the lowest possible taxonomic level. Only when abundances were low, large organisms were also sorted from Multi- and ROV net samples allocated for taxonomic analyses to obtain sufficient individuals. Most of the live specimens (>10,000 individuals during the entire expedition) were deep-frozen, either individually or pooled in groups depending on size, for biochemical measurements (e.g., total lipid content, C/N ratio, energy content, lipid class composition, omega-3 fatty acids and level of animal sterols such as cholesterol and desmosterol, δ^{13}C and δ^{15}N values), as well as for molecular studies of gut contents (copepods, amphipods) and for biodiversity (gelatinous zooplankton). Key mesozooplankton species (e.g., *Calanus glacialis, C. hyperboreus, Metridia longa, Themisto spp.*) were photographed prior to freezing to digitally measure certain characteristics, e.g., prosome length (copepods) and oil sac volume (*Calanus* spp.). For experimental work, individuals of key species were incubated for at least 24 h to determine egg production, grazing and respiration rates, and thereafter, deep-frozen to measure organic carbon and nitrogen contents to calculate biomass specific rates (eee details in Case Study 1 below).

2.2. Sea ice coring and processing

The coordinated sea ice sampling by the MOSAiC teams ICE, ECO, and BGC was designed to study the seasonal changes of physical, biological, and geochemical properties of FYI and SYI in an interdisciplinary context (see also Angelopoulos et al., 2022; Nicolaus et al., 2022b; Evgenii Salganik et al., 2023a). During fall 2020, ice areas of undeformed FYI and SYI were identified that were safely accessible by snow machine, relatively homogeneous, and large enough to accommodate repeat visits, potentially for the entire drift. Most importantly, sites had to be located away from RV *Polarstern* to avoid and minimize the impacts of 1) artificial light pollution, 2) regular on-ice foot traffic, 3) fumes and particulate material from the ship's exhaust system and snow machines, and 4) 'technically clean water' discharges from the ship.

Tents were set up at each ice coring site to protect newly extracted ice cores from adverse environmental conditions during sectioning, which could quickly alter ice and its physical, biological, and chemical properties. Cores for biological properties were collected using a 9-cm diameter KOVACS Mark II coring system. All coring events are summarized in supplementary Table S6. Most cores were sectioned and parsed into sterile Whirlpak bags directly inside the tent under low and/or red-light conditions to minimize artifacts. In some instances, complete cores were bagged directly in the field and processed on the ship, but in-field sectioning was prioritized when conditions were amenable. Ice core properties were derived from individual core sections or pooled core sections (Figure 8) depending on individual property requirements. Core section pools provided larger melt volumes and sub-sampling for multiple properties from single horizons. Small-scale

horizontal variability was reduced by pooling core sections, creating a more homogeneous master sample from which to derive related properties.

Six to eight full-length ice cores designated for ecological and biological properties were sectioned using similar sectioning schemes and parsed into new, sterile Whirlpak bags in the field. Cores were sectioned from the bottom into two 5 cm sections, and then subsequently at 10 cm intervals from top and bottom, leaving a variable length middle section. Middle sections varied by several cms across 3-4 cores. Two pools (termed ECO1 and ECO2) using this procedure were generated and sub-sampled for a majority of biological properties from these two sets (Figure 8). In addition, the bottom 0-3 cm or 0-5 cm of sea ice from 3-4 cores were collected, sectioned, and pooled for individual sets of measurements of net primary productivity (NPP pool) and occasionally bacterial production (from NPP pool), as well as a pool for metatranscriptomes (RNA pool) in the field. Occasionally, full profiles of BP were measured from ECO1 pools.

A single core was collected for bulk salinity, oxygen isotopic composition, and inorganic nutrients. This core was sectioned in the field at 5 cm intervals from the top and bottom, leaving a variable-length middle section (Nicolaus et al., 2022b; Evgenii Salganik et al., 2023a). Individual cores were collected for DIC/TA and gypsum. These cores were bagged completely in the field and either sectioned and processed onboard, or stored frozen for future processing onshore.

Ice cores and sections were transported back to the ship in coolers, protecting cores from fluctuations in light and temperature. All ECO pool samples were melted after the addition of 0.2 μm filtered surface seawater (typically 50 ml per 1 cm of core section) to reduce the impact of osmotic stress and cell loss (Campbell et al., 2019; Chamberlain et al., 2022; Garrison and Buck, 1986). Ice core sections in bags were melted in the dark at room temperature (18-22°C) and checked every 4-6 hours. Upon completed melt, which took 12 to 40 hours, bags were transferred into dark, temperature-controlled laboratory containers, and parsed for sub-sampling of biological properties under red light to minimize artificial light stimulation of biological activities. Samples for Chl-a, algal pigments (HPLC analyses), particulate organic carbon and nitrogen (POC/N), biogenic silica (BSi), taxonomic counts (light microscopy) and cell abundances (flow cytometry), INPs, and neutral sugars were typically collected from ECO1 pool (Figure 8). DNA samples were filtered through 0.2 μm filters from ECO2 pool, and the filtrate was reserved for DOC and CDOM determinations. For each melted core section, melt volume factors were derived from added meltwater volume, which were used to derive to calculate melted ice volumes. Data are reported as per unit volume melted ice core as no correction for differences in density of ice and melt water were available.

Core sections for measurements of inorganic nutrients and nitrate isotopic composition were directly melted in the dark. Samples were pre-filtered through a 0.45 μm filter membrane and either analyzed directly onboard, or frozen for analysis onshore.

622   DIC/TA cores were sectioned onboard in a freezer laboratory (-15°C) at 10 cm
623   intervals from top and bottom, with a variable length middle section. Sections were
624   placed inside gas-tight bags and air was removed using a vacuum pump to avoid
625   CO_2 exchange. These core sections were directly melted in the dark at 4°C, without
626   addition of buffer or conservational solution. Melted samples were transferred into
627   250 ml borosilicate bottles, augmented with 60 µL of saturated mercuric chloride
628   ($HgCl_2$) solution, and sealed with a septum cap to prevent CO_2 exchange with the
629   atmosphere, then stored cool until post-cruise analyses in Japan (Nomura et al.,
630   2020).
631
632   2.3. *Event- and process-driven sampling*
633   In addition to the time-series sampling of water column and sea ice, additional
634   samples were collected either on an opportunistic or event- and process-driven
635   basis (see supplementary Table S7 for an overview on all sampling events). For
636   many of these sampling events, a smaller subset of parameters was sampled, with
637   Chl-a and nutrients being the most regularly sampled properties.
638   Water samples for biological properties were collected from leads from the
639   upper 1.5 m of water directly below newly forming ice or within the sea surface
640   using peristaltic or hand pumps, from October thru early March, and again from
641   early July till the end of the drift in September 2020. Newly-forming ice was
642   collected by sieves, saws, buckets, and/or ice corers throughout the drift period,
643   except during the continuous melt period between June and end of July 2020.
644   Ecological properties of the seasonally occurring melt ponds were sampled only
645   during August and September 2020. Similar to leads, both ice and water from
646   within and under melt ponds were sampled. Ice from leads and melt ponds was
647   processed without filtered seawater addition on most sampling instances, while
648   filtered seawater was added to ice collected between March and May 2020, similar
649   to the handling of time-series samples of sea ice. Sampling of various stages of ice
650   formation and consolidation was conducted in the marginal ice zone (MIZ) during
651   the transit back to shore at the end of the field campaign (September 2020). Here,
652   a small number of biological properties from sea ice, direct under-ice waters, and
653   the water column was collected from 3 stations. Ice types collected from these
654   transit stations were primarily from ice floe edges, and were not consolidated. The
655   distribution of biological properties in pressure ridges (deformed sea ice) was
656   studied using ice coring of keel blocks and collecting water from ridge keel voids
657   (seawater-filled voids between ice blocks in the ridge keel) and below ridges (see
658   case study 1 for details).
659   Water directly from the ice-water interface below level ice was collected
660   except for August to October 2020 for project-specific experimental work by
661   deploying a hand pump through a borehole in the ice. Similarly, under-ice water
662   from the upper 2 m of the water column was occasionally sampled via hand pumps
663   in connection to the time-series common coring activities.
664   In addition to these more opportunistic sampling events, intensive observation
665   periods (IOPs) were included to address research questions on timescales shorter

than the one-week interval of the time-series. For example, higher frequency temporal sampling (i.e., 4-10 time points in 20 - 30 hr periods) was conducted to observe potential diurnal dynamics as well as biological changes as a result of important events such as high wind periods, or the onset of freeze. In the beginning of December, a 24-hr IOP with zooplankton collections via both ROV nets and LOKI was conducted. In July, two 24 hr IOPs were conducted. The first one in the beginning of July consisted of 3 LOKI casts and six CTD rosette casts from the ship to cover diurnal patterns in the water column. A second IOP was conducted one week later during rapid melt to also investigate diurnal patterns in the direct under-ice habitat. In September 2020, two IOPs were conducted. In the beginning of September, a 36 hr intensive observation period in collaboration with team OCEAN was conducted to investigate the effects of a high wind event. Collections of under-ice waters occurred within a temporary on-ice laboratory, termed 'EcoLodge,' established during the summer period. From June to mid-August 2020, EcoLodge1 was situated approximately 110 m from the ship on level ice, i.e. closer than other major sites but with an under-ice environment that was comparable in terms of ice thickness to the FYI coring site, and with surface waters less affected by disturbance from the ship compared to the PS-CTD rosette system. Here, under-ice water with brackish salinity (10-15) was sampled using a peristaltic pump, and filtered directly for Chl-a, POC/N, and microbial community structure analyses. Samples for inorganic nutrients and cell abundance were also collected. During August and September, the re-established EcoLodge2 was located approximately 300 m from the ship on level ice and approximately 15 m from a small, dynamic lead. Here, ice thickness was 125-130 cm. EcoLodge2 served as a hub for under-ice water sampling via a peristaltic pump at 14 timepoints over 36 hrs. One week later a similar IOP at EcoLodge2 with 12 time points over 24 hrs was conducted to assess the impacts of the onset of freeze up.

2.4. Modifications to ship-based and on-ice routine operations for ecosystem sampling

A number of regular ship operations were considered as potential sources of contamination, for which we took precautions to limit their potential impact. For example, prior to MOSAiC, the ship would regularly release gray water continuously from an outlet located starboard side at 5 m depth. The location and constant release of gray water posed a potential risk to our sampling efforts as this location was within meters of the main PS-CTD sampling. While gray water is technically clean enough to drink, it could carry residual microbial, DOM and nutrient contamination. Also, there was a chance that the gray water, being less saline than ambient seawater, would float towards the surface and interact with the underside of the ice floe, potentially altering important characteristics of the ice and its development. Therefore, during MOSAiC, gray water was retained in the ship's hold for 2-3 days, had salt added back into the solution to increase its salinity, and pumped to 150 m depth from the ship's moon pool. Gray water pumping was conducted on days when no active water column sampling was conducted.

A monthly cleaning routine of the engine's boiler systems was one aspect of normal ship operations, which we had not been aware of in advance, that may have had an impact on our sampling efforts around the ship. Unlike gray water handling, this operation was not possible to adapt. While the dates of the monthly release and of measurements on and around those dates can be reviewed to identify any abnormalities, no direct measurements on possible contamination were done.

The ship also emitted continuous artificial light during the drift. Due to safety regulations, the use of light near the ship during our water column sampling could not be significantly reduced. When sampling of the PS-CTD rosette during times of natural darkness (i.e., the Polar night), we reduced the light contamination during sampling by combination of room shading and shaded containers for sample collections (Marangoni et al., 2022). Since the floe drifted in different directions and speeds compared to the water column below, the effects of light pollution on water column-based time series sampling of biogeochemical and many biological parameters can be expected to be minimal. However, e.g. physiological rates of sampled organisms as well as diel vertical migration pattern may have been impacted (Ludvigsen et al., 2018). Comparing migration patterns from different devices and locations (e.g., Acoustic Zooplankton Fish Profilers (AZFPs) located at different distances from the ship; Berge et al unpubl. results) may help to evaluate potential impacts. For sea ice, potential impacts of artificial light pollution on photosynthetic biomass and physiology are much larger, as small effects may accumulate over time. To account for this, the long-term sea ice time-series sites were established >1 km from the ship, where light pollution was not detectable. In the field, shaded tents were used for ice processing to reduce the effect of strong ambient light and temperature increases on ice samples during summertime. In the ship-board labs, samples were processed in temperature-controlled, red- and/or low-light conditions.

In addition to reducing artificial light pollution, we also aimed to reduce the introduction of nutrients and dissolved carbon to our sea ice samples through our melt process. For most ecological properties collected from sea ice, buffering the melt process with a known volume of saline solution can reduce the impact of osmotic stress and cell loss (Garrison and Buck, 1986). Therefore, we planned to make and add an artificial saline solution, consisting of distilled water and analytical grade sodium chloride, to our sea ice core sections. However, the onboard nutrient analyzer showed that the artificial saline solution contained about 1 µmol kg^{-1} nitrate+nitrite, which, at the start of the drift, was more than 10 times the ambient sea surface water nitrate+nitrite concentration. Therefore, despite our preparations, filtered surface seawater additions were used in the ice core melting process, which impacts some of our parameters such as DOC or INP.

2.5. Integrative approaches across the Team ECO work program
In the following sections, some of the approaches that were employed to gain a holistic understanding of seasonal variations in species composition and food web

dynamics are highlighted. Further, pathways are identified towards synthesizing different data sets to address overarching questions in how organisms, and physical properties and processes, control the flow of material and energy. In addition, the integrated multi-omics approaches are detailed in Mock et al. (2022).

2.5.1. Imaging

Imaging has become an essential tool in zooplankton studies in the last two decades (Giering et al., 2022; Lombard et al., 2019). The *in situ* cameras LOKI and UVP resolve plankton distributions at high vertical resolution (Kiko et al., 2017; Schulz et al., 2015). The main strength of the UVP is detecting marine snow, large-sized single-cell organisms (e.g., Rhizaria; Biard et al., 2016), and gelatinous zooplankton (Stemmann et al., 2008). The resolution of the images (1.5 megapixel, picture size depend on organisms size), however, is relatively low and often does not allow for species identification, especially of the dominant zooplankton group Copepoda. The LOKI concentrates the organisms with a net, leading to a flow-through chamber (Schulz et al., 2010). Jellyfish are often destroyed by the net, but LOKI captures Copepoda and other abundant taxa (e.g., Ostracoda, Chaetognatha) in high quality images, allowing the determination of copepod genera, species, and often developmental stages (Schmid et al., 2016). In addition to *in situ* imaging, preserved net samples collected during MOSAiC have been scanned using the laboratory on-desk system ZooScan and single object images have been extracted with the software application ZooProcess (Gorsky et al., 2010). To classify plankton organisms and share images among experts worldwide, all images taken by LOKI, UVP, and ZooScan have been uploaded to EcoTaxa. This is a web-based platform that is an established tool in classifying zooplankton organisms (Picheral et al., 2017) by applying simple machine learning techniques to predict taxonomic categories from image parameters. ZooProcess automatically provides size-related parameters of each object, and in combination with the taxonomic classification allows for estimating the zooplankton biomass from preserved net samples (Cornils et al., 2022) from the ice-ocean interface to the deep ocean (max. 2000 m).

To study the occurrence of squid and fish in the CAO (Snoeijs-Leijonmalm et al., 2022), a continuously recording deep-sea video system (FishCam, MacArtney Germany GmbH, Kiel, Germany) was deployed at 200-400 m water depth. Part of the videos (180 hrs) were studied in real-time mode (Snoeijs-Leijonmalm et al., 2022) while an automated procedure for identifying periods of interest (i.e., appearance of large organisms) in the extensive remainder of the video material is currently being developed. The combination of visual techniques, machine learning, and discrete sampling of animals and particulate matter can work together to address long-standing questions on the distributions and controls on these ecosystem components, where few such data are available.

2.5.2. Biomarkers and carbon transformations

Biomarkers are molecules (e.g., fatty acids, amino acids, sterols) or isotopic compositions of elements (e.g., carbon) that are somewhat source-specific to primary producers and are incorporated mostly unchanged into the tissue of their consumers. Tracing these biomarkers within the zooplankton and fish community is an essential tool in food web studies that address the relative importance of different sources of organic matter, the role of key Arctic primary producers, and the nutritional status of higher trophic levels (Kohlbach et al., 2022; Kunisch EH et al., 2021; Leu et al., 2020). Compared to previous studies, trophic marker analyses of the MOSAiC samples are improvements in two major aspects. First, a very broad range of trophic markers is being explored including fatty acids, sterols, highly-branched isoprenoids, bulk stable isotope compositions, fatty acid-specific stable isotope compositions, and essential amino acid specific stable isotope compositions (eAA-SIA) to balance the strengths and shortcomings of the individual approaches. Second, all the different trophic markers are measured from the same parent samples of homogenized animal tissue to allow a direct comparison of the results and to link the nutritional status of the animals to their food resources. Alongside the trophic marker approaches, animals were also collected for DNA sequencing of gut content. This approach provides a high taxonomic resolution of the ingested species and will further support the interpretation of the trophic marker data (Cleary, 2015).

One key question for studying Arctic marine food webs is to elucidate the role of ice algae as a source of organic matter. Trophic biomarkers determined across the food web including the particulate organic matter in surface waters and ice cores, as well as zooplankton, will help to identify seasonally varying food web interactions from primary producers to individual zooplankton species. These food web interactions will be linked to primary and bacterial production rates as well as vertical flux studies to enable more complete insights into the Arctic biological system.

2.5.3. Ecological modeling

A variety of bioinformatic and statistical modeling techniques aim at elucidating changes in composition and metabolic potential of Arctic marine microbial communities to improve our understanding of their influence on global biogeochemical cycles. The mechanistic understanding of ecological patterns is initially based on information from gene sequences combined with a descriptive approach of community members using co-occurrence networks that illustrate the occurrence of species at the same place and time (Popa et al., 2020). This graph approach, in which nodes are species and edges represent the correlation strength of their seasonality patterns, enables identification of i) central species (node hubs) and ii) species communities (network clusters) that are defined by several populations which are abundant in the same time period (Berry and Widder, 2014). The outcome of such studies allows us to investigate the seasonality of microbial community composition, activities, and functions. Further,

it enables the identification and definition of yet unknown ecological processes. These processes include the interaction of present species with each other and the environment. To understand this interaction in detail and especially to identify key parameters with strong impact on the Arctic ecology, it is necessary to combine all measured data into a modeling framework (Faust and Raes, 2012). For example, the co-occurrence information of photoautotrophic species with grazers isolated from the ice and water column combined with environmental parameters like water depth, temperature, daylight, etc., can be modeled using a Lotka-Volterra (LV) framework (Lotka, 1920; Volterra, 1927) with seasonal forcing approach (Sauve et al., 2020; Vandermeer, 1996). As a result, these models can be used to test several species interaction scenarios after varying the environmental parameters (Succurro and Ebenhöh, 2018). Furthermore, extending the LV by the dynamics of the available resources within the ecosystem (MacArthur consumer-resource models; Goldford et al., 2018; MacArthur, 1970) permits the development of a powerful, theoretical tool to explain the formation and occupation of ecological niches in dependence on external parameters with predictive capabilities for several future scenarios.

Microbial community structure and metabolic potential data are also being leveraged for biogeochemical predictions using machine learning. These techniques are well suited to complex, high dimensional, community structure data and can be used to extract patterns of succession and biogeochemical signatures from sequence information (Bowman, 2021). For example, the Random Forest (RF) regression model is effective at predicting biogeochemical signatures from amplicon sequence data, providing the potential for extending the data coverage of less frequently sampled key biogeochemical variables (Dutta et al., 2022). Additionally, potential microbial drivers for these processes can be identified by applying permutation to the RF models to assess the contributions of specific community members to model performance (DiMucci et al., 2018). Self-organizing maps (SOMs) are used to partition the microbial community into functionally distinct modes that can be applied as discrete variables in a variety of statistical (Bowman et al., 2017) and mechanistic (Kim et al., 2022) models. This discrete variable reflects key genetic traits of the microbial community, provides reasonable estimates of physiology, and allows for correlation between variability in taxonomic structure and function. Eco-physiological information can then be used to modify and better parameterize data-assimilative marine biogeochemical models for hypothesis testing and *in silico* experimentation – such as quantifying previously identified questions regarding microbial controls on ecological processes and assessing the sensitivity of carbon flow through the microbial food web to climate change scenarios.

3.   RESULTS

The MOSAiC Ecosystem work program generated > 50,000 unique samples and activity measurements characterizing organisms and processes from viruses to fish.

886 We sampled 195 CTD rosette casts, 44 multi-nets, and 21 FYI and 20 SYI common
887 ice coring events. We also collected samples from > 40 time points and sites during
888 events and IOPs covering a complete Arctic seasonal cycle. A majority of sampling
889 events were co-located in time and space or spanned long periods of continuous
890 measurement and/or sample collection (Figure 6). Vertical distributions of most
891 properties in the upper 400 m of the water column were resolved over the drift, but,
892 when possible, also full water column depth profiles of core properties at once-
893 weekly intervals were collected (Figures 7). The resolution of the year-long
894 observations to map essential ecosystem properties differed depending on
895 complexity of sampling and needed volumes, e.g. nutrient sampling could be
896 executed more frequently and with greater vertical resolution (Figures 7A, B) than
897 Chl-a (Figures 7C, D) and total DNA sampling (Figures 7E, F).
898
899   *3.1. Environmental controls over the drift period*
900 The MOSAiC expedition provided a wealth of environmental observations from ice,
901 ocean, and atmosphere. These data provide a critical context to interpret the
902 biological observations during the drift period. An evaluation of the meteorological
903 conditions during the MOSAiC drift indicates that unusually cold temperatures
904 relative to decades-long climatology occurred in November 2019 and March 2020
905 (Rinke et al., 2021). Additionally, Rinke et al. (2021) also identified that the 2019-
906 2020 drift year had more frequent storm events in spring, and that summer had a
907 longer sea ice melt season, from late May to early September, approximately a
908 month longer than the median from 1979 – 2019. Also, relative to climatology, the
909 July and August 2020 period was the all-time warmest.
910   Throughout winter, RV *Polarstern* drifted in northerly directions, with the
911 northernmost location at 88.6°N reached at the end of February 2020. Throughout
912 spring and summer, the floe drifted in southerly directions, with periods of faster
913 (mid-March to mid-April) and slower (mid-April to mid-July) drift speeds. The annual
914 changes in air and water temperature, surface ocean salinity, incoming PAR
915 (photosynthetically active radiation), and surface ocean nutrient concentrations along
916 the drift track are illustrated in Figure 9. These properties are relevant examples of
917 environmental changes over the annual cycle, which potentially influence ecosystem
918 processes. Air temperatures at 2 m (Figure 9B) varied between values as low as -
919 40°C in March and up to 6°C during the summer months (Cox et al., 2023; Shupe et
920 al., 2022), driving sea ice freeze-up and melt (Nicolaus et al., 2022b; Evgenii
921 Salganik et al., 2023a). Upper water column (10 m depth) temperatures (Figure 9C)
922 were much less variable, with average daily temperatures near the freezing point
923 during most of the year. Except for the transit periods, maximal temperatures of
924 about -1.3°C were reached at the end of July. Surface ocean salinity (Figure 9C)
925 reflected drift location (Rabe et al., 2022; Schulz et al., 2023b), with rather low levels
926 during drift in the TPD in winter 2019/20. In February and March, TPD influence was
927 gradually replaced by an increasing contribution of more saline Atlantic-influenced
928 waters. After crossing the Gakkel Ridge in late March, average daily surface salinity
929 remained high until reaching the ice edge in Fram Strait with stronger influence of

930 lower salinity waters from the polar waters of the East Greenland Current during July
931 2020 (Schulz et al., 2023b).
932   Solar incoming irradiance (Figure 9D), shown as PAR, at the surface of the
933 sea ice decreased quickly in fall and was below the detection limit from 8th of
934 October until March 13th, marking the period of the polar night. Surface PAR
935 increased as the solar elevation increased, and reached maximal values of >1300
936 µmol photons m^{-2} s^{-1} from May to July (note the data gap between mid-July and mid-
937 August). Thereafter, PAR decreased again, with daily maximum values below 200
938 µmol photons m^{-2} s^{-1} at the end of the drift.
939   Nutrient concentrations in surface waters (upper 30 m) varied with water
940 masses and through the seasons as the floe drifted (Figure 9E). As the floe drifted
941 northwards, silicic acid and phosphate concentrations increased from November to
942 January, from 1.5 to 4.7 µmol kg^{-1} and 0.19 to 0.52 µmol kg^{-1}, respectively. Nitrate
943 remained mostly constant until February at 1.05±0.37 µmol kg^{-1}. Silicic acid was
944 nearly constant until early February, but phosphate concentrations dropped to 0.35
945 µmol kg^{-1} after early January. Trends diverged further thereafter as the drifted further
946 southward, with nitrate and phosphate increasing to 4.7 and 0.42 µmol kg^{-1},
947 respectively, in May, but with silicic acid decreasing to 2.5 µmol kg^{-1}. These opposing
948 trends for the different nutrients likely reflect characteristics of the different water
949 masses as distinguished using the temperature and salinity observations, with
950 increasing influence of Atlantic waters containing relatively more nitrate and
951 phosphate, and less silicic acid. When sampling at the floe resumed in the second
952 half of June, maximum sea water nitrate, silicic acid, and phosphate concentrations
953 of 6.0, 7.5, and 0.66 µmol kg^{-1}, respectively, were measured. Towards the end of
954 August though, as the drift continued southwestward, nitrate levels quickly
955 decreased to <0.5 µmol kg^{-1}, but phosphate (~0.58 µmol kg^{-1}) and silicic acid (7.8
956 µmol kg^{-1}) remained comparably high. This is consistent with polar waters of the East
957 Greenland Current in Fram Strait, with more influence of silicic acid rich Pacific-
958 derived waters and/or the Transpolar Drift. Thereafter, nutrient concentrations were
959 variable between ~0.5 – 2 µmol kg^{-1} nitrate, 1-9 µmol kg^{-1} silicic acid, and 0.2-0.7
960 µmol kg^{-1} phosphate over the summer and fall, as RV *Polarstern* repositioned on a
961 new floe close to the North Pole.
962
963   *3.2. Observed organisms and biodiversity*
964 Despite the extreme seasonal variations in irradiance and other environmental
965 drivers (Figure 9), the same functional and taxonomic groups (flagellates,
966 dinoflagellates, and diatoms) were the major contributors to the sea ice protist
967 assemblages in the different seasons (Figure 10), although there were seasonal
968 changes in their relative and absolute abundances. Ongoing analyses based on
969 taxonomic counts via light microscopy, cell abundances via flow cytometry, 18S-
970 metabarcoding, and metagenomics (e.g., metagenome-assembled genomes of
971 protists) (Table S2) will elucidate seasonal trends in ice and water column protists in
972 unprecedented detail. Interestingly, the same groups and genera (e.g.,
973 *Gymnodinium* spp., *Pseudo-nitzschia* spp., unidentified flagellates) contributed

significantly to the protist communities in both habitats over the fully annual cycle despite strong variations in environmental conditions (Figure 9). Importantly, significant contributions of both in-ice microalgae (e.g., *Nitzschia frigida*) as well as under-ice-attached microalgae such as *Melosira arctica* to the protist assemblages were observed. The latter species was so abundant in certain under-ice habitats that it formed its own microhabitat, which team ECO sampled in more detail.

A diverse and abundant zooplankton community (Figure 11) was observed over the entire MOSAiC campaign. Ongoing analyses focus on the interplay between seasonal (Figure 9) as well as regional patterns to decipher their seasonally resolved biogeography. The different methods employed to assess fish (Table S2) show that their stocks in the Central Arctic Ocean were very low. Still, Atlantic cod was found unexpectedly as far north as 85.9°N, along with lanternfish, armhook squid, and the Arctic endemic polar cod *Boreogadus saida* (Snoeijs-Leijonmalm et al., 2022).

Consequences of different community structures for food web dynamics and biogeochemistry are being addressed at each trophic level by different methods along the drift track and over the annual cycle. Initial analyses indicate active fecal pellet production and sinking in both winter and summer season (Figure 12). Analyses of carbon, nitrogen, algal pigments, and material types from sinking particulate organic matter collected in short-term and long-term sediment traps will enable estimates of time-integrated fluxes of material over specific periods of the winter and summer seasons below level- and ridged sea ice, and from along the drift track at 200 m depth. Additionally, ongoing analyses of particle size spectra from the LISST and UVP will allow higher resolution estimates of POM fluxes. Profiles from the UVP also generated images of particles > 100 micron in size and based on machine learning techniques, these images can be cataloged into particle-specific types, further informing changes in particle size abundances and distributions along the drift.

3.3. Potential impacts of diverse and ephemeral habitats on ecosystem processes
Consistent with previous research, our initial observations suggest that the presence of meltwater layers represents a drastic change in the environmental and chemical nature of the upper ocean, and elicit changes in biological properties and activities (Smith et al., 2022). Stratification in the upper 1-2 m of the ocean creates a strong gradient and boundaries which most organisms are unable to cross, thus creating small microhabitats within each of these layers. These adjacent layers may support potentially disparate activity rates, standing stocks, and biogeochemical fluxes despite their close spatial relation. As such, meltwater layers may introduce habitat structuring which greatly impacts ecosystem functioning. Furthermore, meltwater layer formation affects the gas exchange process with the atmosphere, such that a meltwater layer at the surface may lead to the equilibrium of gases with the atmosphere, thereby reducing the gradient of concentration with the atmosphere and the flux (Smith et al., 2023; von Appen et al., 2021). The mixing of meltwater and the underlying seawater during summertime potentially produces water with low CO_2 concentration.

1018   Based on opportunistic sampling, we could observe ecosystem processes in
1019 various other sea ice types, resulting from different formation processes (Figure 13).
1020 Summer season sampling in leads (Figure 13 A, B) and water close to the bottom of
1021 the ice provided further insight into how ice dynamics and ephemeral phenomena
1022 may alter biological responses over time-scales missed by our regular weekly
1023 sampling. It indicated the formation of extremely high biomass layers on the
1024 boundary between meltwater and seawater, with distinct composition and
1025 biogeochemical characteristics (Smith et al., 2023).New ice formations, typically
1026 ranging from 1 to 10 cm in thickness, and from loosely-formed crystals to
1027 consolidated nilas ice, were sampled periodically throughout the drift, primarily from
1028 leads near or across the central floe (Figure 13 C, D), with preliminary data indicating
1029 higher organismal abundances and Chl-a concentrations than the surrounding
1030 seawater (data not shown). Our series of samples of newly formed ice at different
1031 time periods over the annual cycle will provide us with complementary data on how
1032 environmental conditions (Figure 9) influence biological and ecological processes
1033 during initial thermodynamic ice formation. Sea-ice ridges (Figure 13 G, H) were also
1034 sampled periodically for biological properties and vertical export of material during
1035 MOSAiC. This habitat featured seawater-filled voids with an accumulation and high
1036 activity of microbial biota (see 3.5.1. for details).
1037
1038   *3.4. Gaps in time-series measurements*
1039 Overall, the MOSAiC ecological field program captured a large number of co-located
1040 properties at a regular frequency. However, with differing competencies across each
1041 field team, and despite efforts to cross-train and build redundancy in skill sets, there
1042 are some gaps in the ecosystem time-series measurements. While risk assessments
1043 and prioritization schemes were devised, execution in the field was determined by
1044 what could be achieved by the field team, and different factors at different times
1045 contributed to variations in the continuity of specific data sets. Here, we outline the
1046 key gaps in measurements, so that future users of MOSAiC ECO data sets can
1047 easily identify when in the annual cycle certain measurements are not available.
1048 Activity rate measurements, such as primary and bacterial production, only began in
1049 January and late December 2019, respectively. Samples for water column DOM
1050 characterization after solid-phase extraction are only available from April, May,
1051 August and September 2020. ^{15}N-nitrate isotopes from sea ice were collected from
1052 December 2019 onwards. RNA samples from bottom portions of sea ice are only
1053 available from April 2020 onwards. There were no daily discrete sample collections
1054 for Chl-a and microbial community structure from December 2019 to end of February
1055 2020. Likewise, MIMS data from December 2019 to the beginning of March 2020 is
1056 of substantially lower reliability compared to the rest of the drift.
1057
1058   *3.5. Case Studies*
1059 In the following, two selected case studies are presented to illustrate the kinds of
1060 results the ECO team is working on to address specific scientific questions. These
1061 examples have been chosen because they demonstrate the interdisciplinary

connections within MOSAiC, specifically regarding the role the geophysical restructuring of ice had on habitat and with respect to how biological processes contributed to elemental transformations and influenced central Arctic biogeochemistry.

3.5.1. Pressure ridges, unique habitats for ice-associated biota?

Level, undeformed sea ice provides a wide range of niches for ice-related organisms, ranging from biota living in the brine channel systems within the ice to under-ice flora and fauna living at the ice-water interface (Lund-Hansen et al., 2020). These level sea-ice systems are studied in detail using the ICE and ECO time-series (see also Nicolaus et al., 2022b). However, deformed sea ice in pressure ridges adds substantial three-dimensional diversity in the available habitat space through macroporosity (voids filled with seawater between ice blocks, often referred to as rubble) in the ridge keels (Fig. 14). Ridge keels in the Arctic can reach substantial ice drafts exceeding 20 m keel depth (Wadhams and Toberg, 2012), making ridge coring or observations of voids within ridges exceptionally challenging. Sporadic observations from previous Arctic studies suggested unique biological hotspots associated with the water filled voids in unconsolidated keel rubble and ice block surfaces within the pressure ridges (Fernández-Méndez et al., 2018; Gradinger et al., 2010; Syvertsen, 1991). Truly understanding the ecological processes associated to pressure ridges was the core of one dedicated research project (*Safe HAVens for ice-associated flora and fauna in a seasonally ice-covered Arctic Ocean (HAVOC))*, that across several MOSAiC teams performed detailed and interdisciplinary observations of ridges (Figure 14) in the MOSAiC Central Observatories (CO1 and CO2), with the aim to study the year-round physical and biological characteristics of sea ice ridges.

Relocations of *Polarstern* and sea-ice deformation events in the CO caused disruptions in the time-series, resulting in four different pressure ridge sites being studied during December 2019 and August 2020, with most HAVOC data being collected between January and July 2020. Sampling included ice drilling, coring, and ridge ice and void water sampling to study the temporal evolution of physical characteristics of pressure ridges such as consolidation and melting (Lange et al., 2023; E. Salganik et al., 2023; Evgenii Salganik et al., 2023b). Further, the ridges were studied as habitats by examining the relationship between ridge structure and biological properties (e.g., algal and microbial diversity in ice and void water), under-ice hyperspectral imaging of algal biomass distribution along the pressure ridge keels (Figure 15), and vertical particle flux in the proximity of the ridges using sediment traps. The essential comparative measurements of level first-year and second-year sea ice properties were provided by the ICE and ECO time-series data.

Ongoing interdisciplinary discussions within the HAVOC team already showcased significant science gains.

- Ridge consolidation: Freeze and melt cycles within ridge rubble are more complex than for level sea ice and significantly impact biological habitat diversity and availability. For example, refreezing of snow-slush transported to

ridge keel during dynamic event in early spring and surface meltwater in summer led to rapid ridge consolidation with implications on the structure and functioning of the microbial community and habitat loss for larger fauna in ridge keels (Salganik et al., 2023ab, Lange et al., 2023).

- Hyperspectral imaging of the bottom of level and ridged sea ice indicates higher fractions of ice surfaces inhabited by algae in the ridged ice (Figure 16). For this purpose, a new Relative ice algal Biomass Index (RBI) was developed (Lange et al., submitted).

- Ice surfaces and water-filled voids within ridges contained distinct microalgal and bacterial communities in contrast to level sea ice and seawater.

- Changes in ice structure due to ridge formation, consolidation, and melting have consequences on biological processes reaching beyond the physical location of ridges, as frozen organic material can be released during ridge formation in winter, and melt water can accumulate under level ice next to ridges during summer, both affecting food availability and habitat for under-ice fauna and flora, respectively.

- A new sediment trap deployment methodology under the ridge revealed unique ice-associated particle dynamics and vertical flux measurements,

Upcoming analyses will focus on comprehensive characterizations of ridge properties (e.g., using time-series data) and will be compared to those from level ice and under-ice seawater samples. This will help to assess how ridge biodiversity and ecosystem functioning are driven by this specific physical habitat (i.e. find answers to the who, how and why?). In addition to the knowledge gain, the field experience with sampling ridges provides an additional legacy product by HAVOC and MOSAiC through methodological recommendations for future ridge studies.

3.3.2. Effects of seasonally changing mesozooplankton grazing on carbon and nitrogen cycling in the central Arctic

Mesozooplankton are important transformers of organic carbon (C) and nitrogen (N), converting phytoplankton and microzooplankton into larger-sized biomass (Figure 17). Mesozooplankton feeding activity and fecal pellet production regulates the retention of organic C and N in the upper ocean mixed layer versus their transfer to deeper waters. The Arctic mesozooplankton community is often dominated by copepods of the genus *Calanus*, including two high-Arctic species (*C. hyperboreus* and *C. glacialis*) as well as the advected North Atlantic indicator species *C. finmarchicus* (Ershova et al., 2021). These species' life cycles differ in their adaptations to Arctic seasonality. Until MOSAiC, there had been no year-round direct measurements of *Calanus*-related food web dynamics in the Central Arctic. This is a complex and challenging task, as evaluating the importance of mesozooplankton-mediated transformations and fluxes requires quantification both of standing stocks and of rate processes as well as understanding of zooplankton diet in relation to food abundance. It was achievable within the MOSAiC framework only through the tight collaboration of several science teams providing time series data of ocean and sea

ice physical properties, food availability (microalgae and microzooplankton abundances and standing stocks), as well as quantification of mesozooplankton standing stocks and distributions. These time series data provide the necessary context for a research project (Collaborative Research: The role of planktonic lower trophic levels in carbon and nitrogen transformations in the Central Arctic, a MOSAiC proposal) focused on direct measurements of the transformations of C and N by the zooplankton using rate process measurements. The key overarching questions are:

- How closely aligned are the life histories and productivity cycles of the dominant secondary producers to the ice algal and/or phytoplankton blooms?
- What are the transformations that occur (e.g., respiration, feeding, growth/reproduction, fecal pellet export) and how do these vary throughout the year?
- How do food webs change seasonally? What is the importance of ice vs. water column production to spring zooplankton productivity and how important is the microbial food web during summer to growth and overwintering survival of mesozooplankton?

To answer these questions, project members participated in the MOSAiC cruise from December 2019 to October 2020, with supportive measurements provided by Team ECO before that period. The experimental studies included measurements of respiration, egg production timing and rates, egg hatching success of two dominant copepods (*C. glacialis* and *C. hyperboreus*), and grazing rates on both phytoplankton and microzooplankton of dominant copepods (*C. glacialis, C. hyperboreus, Metridia longa*). These experiments were augmented by DNA gut content analyses. In spring and early summer, when the ice floe had drifted across the Gakkel Ridge into the more Atlantic-influenced Nansen Basin, the Atlantic indicator species *C. finmarchicus* also was included. Individual copepods were photographed for identification and used for determination of carbon and nitrogen content, and trophic marker characteristics.

The final detailed analyses of the data sets will relate the experimental rate measurements to their distribution as estimated from nets and the LOKI, prey type and food concentrations will be augmented by gut DNA contents. The outcomes of will provide critical data to all three ECO science questions ('who', 'how', and 'why'), help determine the C and N flow through the planktonic ecosystem (Figure 17) during different seasons over the course of the drift (Figure 9), and provide critical information for integrative ecosystem modeling during the ECO synthesis phase.

4.   STATUS, LINKAGES, PERSPECTIVES, AND SCIENTIFIC IMPACTS

4.1. Current status and major achievements

MOSAiC ECO sample and data analyses are still ongoing, and new and exciting data and scientific findings will continue to emerge over the next decade. Nevertheless, some major achievements can already be identified, some of which

will lead to a step-change in understanding of the 'whos, hows, and whys' of the high Arctic ecosystem:

- The largest number of samples to assess biodiversity ever collected at such a high spatiotemporal resolution in the central Arctic Ocean will allow for a comprehensive ecosystem description from viruses to fish and squid for all seasons along the drift.
- Unprecedentedly high winter standing stocks and activity levels of organisms in the largely unstudied high Arctic polar night were observed.
- The biological property measurements in a diverse range of seasonally-occurring habitats were conducted, including in-depth characterizations of biological hotspots (e.g., pressure ridges, meltwater layers).
- Rate measurements for key biological processes (e.g., primary and bacterial production, zooplankton grazing and respiration rates) throughout all seasons provide a crucial foundation for the parameterization of biogeochemical models over complete annual cycles.
- The largest sequencing effort for polar ecosystems will provide a benchmark for biodiversity change (Mock et al., 2022).
- Cross-cutting analysis have revealed that Central Arctic biological processes can affect the atmospheric composition during the melt season (Yue et al., 2023) and have the potential to impact cloud processes (Creamean et al., 2022).
- MOSAiC ECO supported a large and diverse suite of projects covering either a particular season or environment, or a full year, which will enable us to obtain a wealth of knowledge on specific aspects of species biology and ecology, and a better understanding of seasonal changes in these aspects.

The co-located, in-depth characterization of environmental conditions driven by the interdisciplinary character of MOSAiC allows to link biological observations to abiotic driving factors (e.g., for fast transition periods that are hard to predict in terms of timing), and in turn to determine when biological interactions are likely the main driving force of ecosystem dynamics (Behrenfeld, 2010). As one example, nutrients, representing one major controlling factor of Arctic productivity (Randelhoff et al., 2020; Tremblay et al., 2015), indicate strong spatial differences across water masses along the drift (Schulz et al., 2023b) that dominate variability due to potential signals of seasonal uptake and limitation dynamics. The presence of surface ocean nitrate concentrations around 2 µM at the end of summer and into fall at >84 °N warrant close inspection concerning the dynamics supplying nutrients to the sunlit layers, potentially indicating iron limitation of primary production in Nansen Basin (Rijkenberg et al., 2018). This could lead to a paradigm shift in our understanding of Arctic primary production (Ardyna and Arrigo, 2020; Tremblay et al., 2015; Wassmann and Reigstad, 2011). The large imprint that water masses had on important environmental drivers such as nutrient concentrations illustrate that many statements about the Arctic cannot be generalized but need to be region-specific.

1235   The interdisciplinary approach of MOSAiC will also allow us to better
1236   parameterize and map cross-disciplinary linkages that may not be obvious a-priori.
1237   For example, sea ice algae might change the energy absorption of ice and ocean
1238   (Manizza et al., 2013), thereby affecting Arctic heat budgets along the atmosphere-
1239   ice-ocean continuum (Shupe et al., 2022). New tools such as hyperspectral imagers
1240   deployed on remotely operated vehicles (see case study 1) may enable
1241   comprehensive mapping of ice algae potentially facilitating improved quantitative
1242   evaluation of biological effects on ice transmission and heat budgets.
1243   Comprehensive studies of a number of periodically-occurring habitats found
1244   them to be biological hotspots, including meltwater-influenced systems and pressure
1245   ridges. Unique habitat-specific processes may provide major additions to fluxes of
1246   energy and matter; thus, their quantification is needed for a complete view on high
1247   Arctic biogeochemistry and ecology. Our data will allow us to evaluate the relative
1248   role of these short-lived hotspot habitats compared to the perennial habitats, such as
1249   level sea ice. Several of these habitats develop during the summer season (e.g.,
1250   melt ponds, meltwater layers, unconsolidated water-filled voids in pressure ridges),
1251   but later in the year may have residual structuring of habitats, which affect
1252   organismal life strategies during different periods of the annual cycle. While these
1253   features primarily form during the summertime, their altered states can persist into
1254   later seasons and even the following year. For example, remnants or "fingerprints" of
1255   these hotspots may be identifiable, such as refrozen melt ponds or refrozen
1256   (consolidated) voids in ridges, and characterized during the winter season as
1257   overwintering habitats for a range of Arctic organisms.
1258
1259   *4.2. Challenges and Lessons Learned*
1260   MOSAiC observations and samples were conducted year-round, often in challenging
1261   conditions. This required frequently adapting standard ship and on-ice operations
1262   and team operations as well as adjusting the science objectives. Given the major
1263   focus of MOSAiC on interactions between atmosphere, sea ice, and ocean, we
1264   intentionally limited our work program to focus on the ecological and biogeochemical
1265   components that are relevant for the sea ice and upper ocean, excluding the deepest
1266   water layers and the benthos. Additionally, in an effort to focus on measurements
1267   that would elucidate biological feedbacks in the Arctic climate system, we did not
1268   include observations of megafauna, such as sea birds and mammals, although they
1269   provide important ecosystem services and are highly impacted by climate change
1270   (Hamilton et al., 2022).
1271   Some unique challenges we addressed in the preparation phase were related
1272   to potential impacts of the anticipated long-term drift on the scientific data collection.
1273   Key adaptations were made in conjunction with other science teams and the ship´s
1274   crew (see section 2.4 for details). Additionally, during the preparation phase, we took
1275   steps to train and prepare field personnel to execute a variety of tasks and protocols
1276   encompassing a broader range of activities than they would have been responsible
1277   for within an expedition of narrower scope than MOSAiC. Building competencies and
1278   redundancies in the skill sets of field personnel was important to realizing the diverse

1279   work program. However, it was not always possible, and in some instances gaps in
1280   our time-series measurements exist because it was not feasible for the field team to
1281   accomplish all the tasks (see Section 3.4). Additional modifications were necessary
1282   onboard based on expected irregular disturbances (e.g., storms, ice break-up) as
1283   well as unexpected events (e.g., the COVID-19 outbreak). In the future, improved
1284   prioritization of sample collections, development of more semi-automated sampling
1285   and processing devices, and increased training on unfamiliar data logging routines
1286   will strengthen execution of complex work programs. Our experience with MOSAiC
1287   ECO work will also provide us with the opportunity to better determine which suites
1288   of properties are most needed for addressing future questions and objectives related
1289   to high Arctic ecosystem changes.
1290   Our data analyses will need to disentangle temporal versus spatial aspects to
1291   observed changes in biological properties and ecological processes over the course
1292   of the drift. This can be nicely illustrated by the development of nitrate concentrations
1293   over the course of the expedition (Figure 9E). Even though nitrate is considered one
1294   of the two major limiting factors for Arctic primary production (Tremblay et al., 2015),
1295   its concentrations increased over the main microalgal growing season, i.e., from
1296   March to July. While this seems counterintuitive at first, it can be explained by the
1297   drift of the ice floe into areas with increasingly larger influence by nitrate-rich Atlantic
1298   water masses (Rabe et al., 2022; Schulz et al., 2023b). Such water mass effects
1299   also influence other measured parameters such as DOM characteristics (Gonçalves-
1300   Araujo et al., 2016, Kong et al., under review), and potentially the presence or
1301   absence of certain organismal groups and species (Kaiser et al., 2022). Also, the
1302   faster-than-expected drift speed of the main MOSAiC floe resulted in earlier arrival
1303   into Atlantic inflow-influenced waters and proximity to the ice edge, resulting in
1304   significant deformation and instability of the first Central Observatory. Therefore,
1305   after the logistical departure in May 2020, the ice camp had to be relocated to a
1306   different part of the original ice floe and a second Central Observatory was
1307   established. While these aspects are part of the nature of a drift campaign, their
1308   influence on how one can interpret our observations is central to our understanding
1309   of ecosystem processes during the MOSAiC field year.
1310

1311   *4.3. Ecosystem research in the context of Arctic System Science*
1312 MOSAiC was designed to improve our understanding of the governing principles of
1313 the Arctic climate system and thus can be used in an earth system science
1314 approach. This is particularly urgent as the Arctic is warming four times faster than
1315 the global average (Rantanen et al., 2022). Developing baseline knowledge on the
1316 'who', 'how', and 'why' of the high Arctic was the foundational principle of the
1317 ecosystem science program, and the data already demonstrate multiple connections
1318 within the ecosystem compartments and to the whole Arctic system including the
1319 presence of INPs of marine biological origin (Creamean et al., 2022). The Arctic
1320 Ocean can be both a source and sink for greenhouse gases, like CO_2 and methane.
1321 Annual cycles of fluxes of such substances are currently being investigated in
1322 relation to bacterial biodiversity, algal activity, and respiration. For instance, it is

1323 expected that a combination of the broad scope of information from several MOSAiC
1324 science teams will help resolve the "ocean methane paradox" explaining periodically
1325 enhanced CH_4 concentrations in ocean surface waters (Rees et al., 2022). Great
1326 uncertainty exists regarding the future role of the Arctic Ocean as a source or sink for
1327 CO_2, where melting of sea ice combined with increased productivity could regionally
1328 lead to an intensified sink (Rees et al., 2022), while other Arctic areas might
1329 experience a reduction of carbon fixation and export due to increased sea ice melt-
1330 induced stratification (von Appen et al., 2021). Other processes which can potentially
1331 lead to CO_2 outgassing by the Arctic Ocean include decreased solubility driven by
1332 warmer temperatures, equilibration with the atmosphere (Cai et al., 2010; Else et al.,
1333 2013), or wind-driven mixing of surface waters with more carbon-rich subsurface
1334 layers (Lannuzel et al., 2020). MOSAiC ECO data will fill important regional and pan-
1335 Arctic knowledge gaps in our understanding and may help to determine those
1336 mechanisms that will drive the effects of climate change on the Arctic carbon cycle.
1337   A set of different ecosystem and fully coupled Arctic Ocean models will be
1338 essential tools for integrating information across the ecosystem and the entire Arctic
1339 system using MOSAiC data, targeting not only specific questions like carbon cycling
1340 in the Arctic or production of climate relevant greenhouse gases, but also
1341 transferring these process-focused knowledge gains into products to understand
1342 climate change on larger regional and temporal scales. The unprecedented increase
1343 in knowledge on biodiversity and gene expressions in relation to environmental
1344 variables (Mock et al., 2022) will allow for the application of models to elucidate
1345 metabolic and energetic fluxes within the Arctic microbial consortia (Succurro and
1346 Ebenhöh, 2018). This combined application of different model types (e.g. see will be
1347 an important tool to differentiate the intertwined role of spatial and temporal
1348 variability in MOSAiC data sets.
1349
1350 **5.   OUTLOOK**
1351 The knowledge created by the ecological research during MOSAiC will provide a
1352 lasting legacy for future studies focusing on the Arctic System. For the first time,
1353 biodiversity and ecosystem functioning were studied on multiple trophic levels over a
1354 full seasonal cycle using traditional and novel approaches.
1355   The legacy of MOSAiC goes beyond publications, developing novel sampling
1356 approaches and the openly accessible data archives. Indeed, the open and growing
1357 network of researchers across many nations and disciplines can be expected to
1358 have a lasting effect on Arctic marine research, particularly considering the high
1359 number of early career scientists that are already involved. New spin-off projects
1360 initiated through MOSAiC include projects on microbial processing and
1361 biogeochemical modeling, remote sensing of under-ice blooms, sea ice-ecosystem
1362 modeling, and a yearround ecosystem study in an Arctic fjord. The gained
1363 knowledge will help to evaluate the importance of the Arctic for climate regulation.
1364 Although incomplete, several publications have demonstrated the broad range of
1365 currently known ecosystem services provided by the Arctic marine system to
1366 humans including regulation of greenhouse gases and biodiversity (Malinauskaite et

1367 al., 2019). MOSAiC-based knowledge will also support political decision-making
1368 processes through, e.g., Arctic Council initiatives on the management of Arctic
1369 marine ecosystems (e.g. PAME). Although MOSAiC ECO covers a very broad range
1370 of ecological topics and will fill many knowledge gaps, many research questions
1371 remain unanswered or are now newly defined. The free, findable, accessible,
1372 interoperable, and reusable MOSAiC data will be a major milestone of success,
1373 providing together with the gained knowledge, the backbone for interdisciplinary
1374 marine Arctic research for decades to come.
1375   The broad range of realized measurements and samples from MOSAiC ECO
1376 will make it possible to move from the observed answers of the 'who' and 'how' to
1377 developing process-based mechanistic understanding of the 'why', also by means of
1378 modeling approaches (see below). Mechanistic understanding in turn will allow
1379 moving beyond the specific locations and conditions during our observational period.
1380 The observation of high levels of biomass presence and organismal activity during
1381 the months-long cold and dark polar night, for example, provides the foundations for
1382 new investigations regarding overwintering mechanisms, strategies, and
1383 physiological adaptations. The combination of rate measurements, observations on
1384 different life stages, physiological and food web experimental work, as well as
1385 information originating from metagenomics and metatranscriptomics will allow an
1386 improved understanding the current overwintering mechanisms. Also, it will provide
1387 improve scenarios regarding the potential impacts of a future warmer Arctic with a
1388 reduced and changed ice cover, for example on effects on winter survival, annual
1389 productivity, and biogeochemical cycles. Here, synergies between the ECO team
1390 and the BGC science with its focus on trace and greenhouse gases as well as
1391 cycling of sulfur, nitrogen and carbon will be essential. Entrainment of the detected
1392 processes and rates into ecosystem and biogeochemical models will also greatly
1393 improve the validity of such future scenario estimations. While a one-year field-
1394 period cannot observe climate change trends directly, MOSAiC science is a step-
1395 change in Arctic ecosystem understanding that will provide a baseline upon which
1396 future changes can be identified, while also providing the potential for improved
1397 projections of future changes based on the advanced process-based interdisciplinary
1398 understanding.
1399
1400

1401 Data accessibility statement
1402 Drift track data for each MOSAiC leg is available via Pangaea (Haas, 2020; Kanzow,
1403 2020; Rex, 2021a, 2021b, 2020).
1404 Combined surface ocean temperature and salinity from different sensors as
1405 described in (Schulz et al., 2023b) is available via the Arctic Data Center (Schulz et
1406 al., 2023a),
1407 Air temperatures at 2 m over the MOSAiC floe are available at the Arctic Data Center
1408 (Cox, 2023).
1409 Incoming PAR data was derived from radiation station measurements published at
1410 PANGAEA (Nicolaus et al., 2023b, 2023a, 2022a).

1411 Data publication of nutrient data is under way. Data is available upon request from
1412 Sinhué Torres-Valdes (sinhue.torres-valdes@awi.de). Other metadata shown is
1413 either available in the supplementary information or will be published together with
1414 the data once quality controlled, and are available from the authors upon request.
1415

Author contributions
1416
1417 Developed the concept and design: AAF and RRG with input from co-authors
1418 Conducted the field sampling: AAF, CJMH, CJA, YB, JPB, JB, DB, RGC, GC, EJC,
1419 JMC, ESD, SLE, AAF, JG, CEG, NH, AI, BAL, KM, OM, DN, LMO, SR, SS, ES, KS,
1420 KMS, PSL, JS, AS, STV, AT, AU, ALW
1421 Drafted and revised the article: AAF, CJMH and RRG with contributions from
1422 co-authors
1423 Approved the submitted version for publication: all co-authors
1424

References

Alfred-Wegener-Institut Helmholtz-Zentrum für Polar- und Meeresforschung, 2017. Polar Research and Supply Vessel POLARSTERN Operated by the Alfred-Wegener-Institute. J. Large-Scale Res. Facil. 3, A119. https://doi.org/10.17815/jlsrf-3-163

Angelopoulos, M., Damm, E., Simões Pereira, P., Abrahamsson, K., Bauch, D., Bowman, J., Castellani, G., Creamean, J., Divine, D.V., Dumitrascu, A., 2022. Deciphering the properties of different arctic ice types during the growth phase of MOSAiC: Implications for future studies on gas pathways. Front. Earth Sci. 10, 864523.

Ardyna, M., Arrigo, K.R., 2020. Phytoplankton dynamics in a changing Arctic Ocean. Nat. Clim. Change. https://doi.org/10.1038/s41558-020-0905-y

Ardyna, M., Mundy, C.J., Mills, M.M., Oziel, L., Grondin, P.-L., Lacour, L., Verin, G., van Dijken, G., Ras, J., Alou-Font, E., Babin, M., Gosselin, M., Tremblay, J.-É., Raimbault, P., Assmy, P., Nicolaus, M., Claustre, H., Arrigo, K.R., 2020. Environmental drivers of under-ice phytoplankton bloom dynamics in the Arctic Ocean. Elem. Sci. Anthr. 8. https://doi.org/10.1525/elementa.430

Ashjian, C.J., Campbell, R.G., Welch, H.E., Butler, M., Van Keuren, D., 2003. Annual cycle in abundance, distribution, and size in relation to hydrography of important copepod species in the western Arctic Ocean. Deep Sea Res. Part Oceanogr. Res. Pap. 50, 1235–1261. https://doi.org/10.1016/S0967-0637(03)00129-8

Assmy, P., Fernández-Méndez, M., Duarte, P., Meyer, A., Randelhoff, A., Mundy, C.J., Olsen, L.M., Kauko, H.M., Bailey, A., Chierici, M., Cohen, L., Doulgeris, A.P., Ehn, J.K., Fransson, A., Gerland, S., Hop, H., Hudson, S.R., Hughes, N., Itkin, P., Johnsen, G., King, J.A., Koch, B.P., Koenig, Z., Kwasniewski, S., Laney, S.R., Nicolaus, M., Pavlov, A.K., Polashenski, C.M., Provost, C., Rösel, A., Sandbu, M., Spreen, G., Smedsrud, L.H., Sundfjord, A., Taskjelle, T., Tatarek, A., Wiktor, J., Wagner, P.M., Wold, A., Steen, H., Granskog, M.A., 2017. Leads in Arctic pack ice enable early phytoplankton blooms below snow-covered sea ice. Sci. Rep. 7, 40850. https://doi.org/10.1038/srep40850

Babin, M., Arrigo, K., Bélanger, S., Forget, M.-H., 2015. Ocean Colour Remote Sensing in Polar Seas.

Balmonte, J.P., Teske, A., Arnosti, C., 2018. Structure and function of high Arctic pelagic, particle-associated and benthic bacterial communities. Environ. Microbiol. 20, 2941–2954. https://doi.org/10.1111/1462-2920.14304

Barber, D.G., Hop, H., Mundy, C.J., Else, B., Dmitrenko, I.A., Tremblay, J.-E., Ehn, J.K., Assmy, P., Daase, M., Candlish, L.M., Rysgaard, S., 2015. Selected physical, biological and biogeochemical implications of a rapidly changing Arctic Marginal Ice Zone. Overarching Perspect. Contemp. Future Ecosyst. Arct. Ocean 139, 122–150. https://doi.org/10.1016/j.pocean.2015.09.003

Behrenfeld, M.J., 2010. Abandoning Sverdrup's Critical Depth Hypothesis on phytoplankton blooms. Ecology 91, 977–989.

Berge, J., Daase, M., Renaud, P.E., Ambrose, W.G., Darnis, G., Last, K.S., Leu, E., Cohen, J.H., Johnsen, G., Moline, M.A., Cottier, F., Varpe, Ø., Shunatova, N.,

Bałazy, P., Morata, N., Massabuau, J.-C., Falk-Petersen, S., Kosobokova, K., Hoppe, C.J.M., Węsławski, J.M., Kukliński, P., Legeżyńska, J., Nikishina, D., Cusa, M., Kędra, M., Włodarska-Kowalczuk, M., Vogedes, D., Camus, L., Tran, D., Michaud, E., Gabrielsen, T.M., Granovitch, A., Gonchar, A., Krapp, R., Callesen, T.A., 2015. Unexpected Levels of Biological Activity during the Polar Night Offer New Perspectives on a Warming Arctic. Curr. Biol. 25, 2555–2561. https://doi.org/10.1016/j.cub.2015.08.024

Berry, D., Widder, S., 2014. Deciphering microbial interactions and detecting keystone species with co-occurrence networks. Front. Microbiol. 5, 219.

Biard, T., Stemmann, L., Picheral, M., Mayot, N., Vandromme, P., Hauss, H., Gorsky, G., Guidi, L., Kiko, R., Not, F., 2016. In situ imaging reveals the biomass of giant protists in the global ocean. Nature 532, 504–507.

Bluhm, B.A., Gebruk, A.V., Gradinger, R., Hopcroft, R.R., Huettmann, F., Kosobokova, K.N., Sirenko, B.I., Weslawski, J.M., 2011. Arctic Marine Biodiversity. Oceanography 24, 232–248.

Bluhm, B.A., Hop, H., Vihtakari, M., Gradinger, R., Iken, K., Melnikov, I.A., Søreide, J.E., 2018. Sea ice meiofauna distribution on local to pan-Arctic scales. Ecol. Evol. 8, 2350–2364. https://doi.org/10.1002/ece3.3797

Bluhm, B.A., Kosobokova, K.N., Carmack, E.C., 2015. A tale of two basins: An integrated physical and biological perspective of the deep Arctic Ocean. Overarching Perspect. Contemp. Future Ecosyst. Arct. Ocean 139, 89–121. https://doi.org/10.1016/j.pocean.2015.07.011

Boetius, A., Anesio, A.M., Deming, J.W., Mikucki, J.A., Rapp, J.Z., 2015. Microbial ecology of the cryosphere: sea ice and glacial habitats. Nat. Rev. Microbiol. 13, 677–690. https://doi.org/10.1038/nrmicro3522

Bowman, J.S., 2021. Making sense of a scent-sensing metaphor for microbes and environmental predictions. Msystems 6, 10–1128.

Bowman, J.S., Amaral-Zettler, L.A., J Rich, J., M Luria, C., Ducklow, H.W., 2017. Bacterial community segmentation facilitates the prediction of ecosystem function along the coast of the western Antarctic Peninsula. ISME J. 11, 1460–1471. https://doi.org/10.1038/ismej.2016.204

Cai, W.-J., Chen, L., Chen, B., Gao, Z., Lee, S.H., Chen, J., Pierrot, D., Sullivan, K., Wang, Y., Hu, X., Huang, W.-J., Zhang, Y., Xu, S., Murata, A., Grebmeier, J.M., Jones, E.P., Zhang, H., 2010. Decrease in the CO_2 Uptake Capacity in an Ice-Free Arctic Ocean Basin. Science 329, 556–559. https://doi.org/10.1126/science.1189338

Campbell, K., Lange, B.A., Landy, J.C., Katlein, C., Nicolaus, M., Anhaus, P., Matero, I., Gradinger, R., Charette, J., Duerksen, S., Tremblay, P., Rysgaard, S., Tranter, M., Haas, C., Michel, C., 2022. Net heterotrophy in High Arctic first-year and multi-year spring sea ice. Elem. Sci. Anthr. 10, 00040. https://doi.org/10.1525/elementa.2021.00040

Campbell, K., Mundy, C.J., Juhl, A.R., Dalman, L.A., Michel, C., Galley, R.J., Else, B.E., Geilfus, N.X., Rysgaard, S., 2019. Melt Procedure Affects the Photosynthetic Response of Sea Ice Algae. Front. Earth Sci. 7.

Carlyle, C.G., Roth, J.D., Yurkowski, D.J., Kohlbach, D., Young, B.G., Brown, T.A., Riget, F.F., Dietz, R., Ferguson, S.H., 2022. Spatial variation in carbon source use and trophic position of ringed seals across a latitudinal gradient of sea ice. Ecol. Indic. 145, 109746. https://doi.org/10.1016/j.ecolind.2022.109746

1594 Chamberlain, E.J., Balmonte, J.P., Torstensson, A., Fong, A.A., Snoeijs-Leijonmalm,
1595 P., Bowman, J.S., 2022. Impacts of sea ice melting procedures on measurements of
1596 microbial community structure. Elem. Sci. Anthr. 10, 00017.
1597 https://doi.org/10.1525/elementa.2022.00017

1598 Cleary, A.C., 2015. Distributions and interactions in three groups of polar marine
1599 plankton. University of Rhode Island.

1600 Clement Kinney, J., W. Maslowski, R. Osinski, M. Jin, M. Frants, N. Jeffery, Y. J. Lee
1601 (2020) Hidden production: On the importance of pelagic phytoplankton blooms
1602 beneath Arctic sea ice, J. Geophys. Res. Oceans, 125(9), e2020JC016211,
1603 https://doi.org/10.1029/2020JC016211

1604 Clement Kinney, J., M. Frants, W. Maslowski, R. Osinski, N. Jeffery, M. Jin, Y. J. Lee
1605 (2023) Evaluation of Under Sea-ice Phytoplankton Blooms in the Fully-Coupled,
1606 High-Resolution Regional Arctic System Model, J. Geophys. Res. Oceans, 128,
1607 e2022JC019000, https://doi.org/10.1029/2022JC019000

1608 Cornils, A., Thomisch, K., Hase, J., Hildebrandt, N., Auel, H., Niehoff, B., 2022.
1609 Testing the usefulness of optical data for zooplankton long-term monitoring:
1610 Taxonomic composition, abundance, biomass, and size spectra from ZooScan
1611 image analysis. Limnol. Oceanogr. Methods 20, 428–450.
1612 https://doi.org/10.1002/lom3.10495

1613 Cox, C., 2023. Atmospheric Surface Flux Station #40 measurements (Level 3 Final),
1614 Multidisciplinary Drifting Observatory for the Study of Arctic Climate (MOSAiC),
1615 central Arctic, October 2019 - September 2020. NSF Arctic Data Center.

1616 Cox, C.J., Gallagher, M.R., Shupe, M.D., Persson, P.O.G., Solomon, A., Fairall,
1617 C.W., Ayers, T., Blomquist, B., Brooks, I.M., Costa, D., 2023. Continuous
1618 observations of the surface energy budget and meteorology over the Arctic sea ice
1619 during MOSAiC. Sci. Data 10, 519.

1620 Creamean, J.M., Barry, K., Hill, T.C., Hume, C., DeMott, P.J., Shupe, M.D., Dahlke,
1621 S., Willmes, S., Schmale, J., Beck, I., 2022. Annual cycle observations of aerosols
1622 capable of ice formation in central Arctic clouds. Nat. Commun. 13, 3537.

1623 DiMucci, D., Kon, M., Segrè, D., 2018. Machine learning reveals missing edges and
1624 putative interaction mechanisms in microbial ecosystem networks. Msystems 3, 10–
1625 1128.

1626 Dutta, A., Goldman, T., Keating, J., Burke, E., Williamson, N., Dirmeier, R., Bowman,
1627 J.S., 2022. Machine learning predicts biogeochemistry from microbial community
1628 structure in a complex model system. Microbiol. Spectr. 10, e01909-21.

1629 Ehrlich, J., Schaafsma, F.L., Bluhm, B.A., Peeken, I., Castellani, G., Brandt, A.,
1630 Flores, H., 2020. Sympagic Fauna in and Under Arctic Pack Ice in the Annual Sea-
1631 Ice System of the New Arctic. Front. Mar. Sci. 7.

1632 Else, B., Papakyriakou, T., Asplin, M., Barber, D., Galley, R., Miller, L., Mucci, A.,
1633 2013. Annual cycle of air-sea CO_2 exchange in an Arctic polynya region. Glob.
1634 Biogeochem. Cycles 27, 388–398.

1635 Ershova, E.A., Kosobokova, K.N., Banas, N.S., Ellingsen, I., Niehoff, B., Hildebrandt,
1636 N., Hirche, H.-J., 2021. Sea ice decline drives biogeographical shifts of key Calanus
1637 species in the central Arctic Ocean. Glob. Change Biol. 27, 2128–2143.
1638 https://doi.org/10.1111/gcb.15562

1639 Falkowski, P.G., Barber, R.T., Smetacek, V., 1998. Biogeochemical Controls and
1640 Feedbacks on Ocean Primary Production. Science 281, 200–206.

https://doi.org/10.1126/science.281.5374.200

Faust, K., Raes, J., 2012. Microbial interactions: from networks to models. Nat. Rev. Microbiol. 10, 538–550.

Fernández-Méndez, M., Olsen, L.M., Kauko, H.M., Meyer, A., Rösel, A., Merkouriadi, I., Mundy, C.J., Ehn, J.K., Johansson, A.M., Wagner, P.M., Ervik, Å., Sorrell, B.K., Duarte, P., Wold, A., Hop, H., Assmy, P., 2018. Algal Hot Spots in a Changing Arctic Ocean: Sea-Ice Ridges and the Snow-Ice Interface. Front. Mar. Sci. 5.

Fouilland, E., Gosselin, M., Rivkin, R.B., Vasseur, C., Mostajir, B., 2007. Nitrogen uptake by heterotrophic bacteria and phytoplankton in Arctic surface waters. J. Plankton Res. 29, 369–376. https://doi.org/10.1093/plankt/fbm022

Fransson, A., Chierici, M., Miller, L.A., Carnat, G., Shadwick, E., Thomas, H., Pineault, S., Papakyriakou, T.N., 2013. Impact of sea-ice processes on the carbonate system and ocean acidification at the ice-water interface of the Amundsen Gulf, Arctic Ocean. J. Geophys. Res. Oceans 118, 7001–7023. https://doi.org/10.1002/2013JC009164

Fransson, A., Chierici, M., Skjelvan, I., Olsen, A., Assmy, P., Peterson, A.K., Spreen, G., Ward, B., 2017. Effects of sea-ice and biogeochemical processes and storms on under-ice water fCO_2 during the winter-spring transition in the high A rctic O cean: Implications for sea-air CO_2 fluxes. J. Geophys. Res. Oceans 122, 5566–5587.

Fransson, A., Chierici, M., Yager, P.L., Smith Jr., W.O., 2011. Antarctic sea ice carbon dioxide system and controls. J. Geophys. Res. Oceans 116. https://doi.org/10.1029/2010JC006844

Garrison, D.L., Buck, K.R., 1986. Organism losses during ice melting: A serious bias in sea ice community studies. Polar Biol. 6, 237–239. https://doi.org/10.1007/BF00443401

Giering, S.L., Culverhouse, P.F., Johns, D.G., McQuatters-Gollop, A., Pitois, S.G., 2022. Are plankton nets a thing of the past? An assessment of in situ imaging of zooplankton for large-scale ecosystem assessment and policy decision-making. Front. Mar. Sci. 9, 986206.

Goldford, J.E., Lu, N., Bajić, D., Estrela, S., Tikhonov, M., Sanchez-Gorostiaga, A., Segrè, D., Mehta, P., Sanchez, A., 2018. Emergent simplicity in microbial community assembly. Science 361, 469–474.

Gonçalves-Araujo, R., Granskog, M.A., Bracher, A., Azetsu-Scott, K., Dodd, P.A., Stedmon, C.A., 2016. Using fluorescent dissolved organic matter to trace and distinguish the origin of Arctic surface waters. Sci. Rep. 6, 33978.

Gorsky, G., Ohman, M.D., Picheral, M., Gasparini, S., Stemmann, L., Romagnan, J.-B., Cawood, A., Pesant, S., García-Comas, C., Prejger, F., 2010. Digital zooplankton image analysis using the ZooScan integrated system. J. Plankton Res. 32, 285–303. https://doi.org/10.1093/plankt/fbp124

Gosselin, M., Levasseur, M., Wheeler, P.A., Horner, R.A., Booth, B.C., 1997. New measurements of phytoplankton and ice algal production in the Arctic Ocean. Deep Sea Res. Part II Top. Stud. Oceanogr. 44, 1623–1644. https://doi.org/10.1016/S0967-0645(97)00054-4

Gradinger, R., Bluhm, B., Iken, K., 2010. Arctic sea-ice ridges—Safe heavens for sea-ice fauna during periods of extreme ice melt? Obs. Explor. Arct. Can. Basin Chukchi Sea Hidden Ocean RUSALCA Exped. 57, 86–95. https://doi.org/10.1016/j.dsr2.2009.08.008

Granskog, M.A., Fer, I., Rinke, A., Steen, H., 2018. Atmosphere-Ice-Ocean-Ecosystem Processes in a Thinner Arctic Sea Ice Regime: The Norwegian Young Sea ICE (N-ICE2015) Expedition. J. Geophys. Res. Oceans 123, 1586–1594. https://doi.org/10.1002/2017JC013328

Haas, C., 2020. Links to master tracks in different resolutions of POLARSTERN cruise PS122/2, Arctic Ocean - Arctic Ocean, 2019-12-13 - 2020-02-24 (Version 2). Alfred Wegener Inst. Helmholtz Cent. Polar Mar. Res. Bremerhaven https://doi.org/10.1594/PANGAEA.924674

Hamilton, B.M., Jantunen, L., Bergmann, M., Vorkamp, K., Aherne, J., Magnusson, K., Herzke, D., Granberg, M., Hallanger, I.G., Gomiero, A., 2022. Microplastics in the atmosphere and cryosphere in the circumpolar North: a case for multicompartment monitoring. Arct. Sci. 8, 1116–1126.

Hobbs, L., Banas, N.S., Cottier, F.R., Berge, J., Daase, M., 2020. Eat or Sleep: Availability of Winter Prey Explains Mid-Winter and Spring Activity in an Arctic *Calanus* Population. Front. Mar. Sci. 7.

Hop, H., Vihtakari, M., Bluhm, B.A., Assmy, P., Poulin, M., Gradinger, R., Peeken, I., von Quillfeldt, C., Olsen, L.M., Zhitina, L., Melnikov, I.A., 2020. Changes in Sea-Ice Protist Diversity With Declining Sea Ice in the Arctic Ocean From the 1980s to 2010s. Front. Mar. Sci. 7, 243. https://doi.org/10.3389/fmars.2020.00243

Hop, H., Wold, A., Meyer, A., Bailey, A., Hatlebakk, M., Kwasniewski, S., Leopold, P., Kuklinski, P., Søreide, J.E., 2021. Winter-Spring Development of the Zooplankton Community Below Sea Ice in the Arctic Ocean. Front. Mar. Sci. 8.

Hoppe, C.J.M., 2022. Always ready? Primary production of Arctic phytoplankton at the end of the polar night. Limnol. Oceanogr. Lett. 7, 167–174. https://doi.org/10.1002/lol2.10222

Ibarbalz, F.M., Henry, N., Mahé, F., Ardyna, M., Zingone, A., Scalco, E., Lovejoy, C., Lombard, F., Jaillon, O., Iudicone, D., Malviya, S., Tara Oceans Coordinators, Sullivan, M.B., Chaffron, S., Karsenti, E., Babin, M., Boss, E., Wincker, P., Zinger, L., de Vargas, C., Bowler, C., Karp-Boss, L., 2023. Pan-Arctic plankton community structure and its global connectivity. Elem. Sci. Anthr. 11, 00060. https://doi.org/10.1525/elementa.2022.00060

Ingvaldsen, R.B., Assmann, K.M., Primicerio, R., Fossheim, M., Polyakov, I.V., Dolgov, A.V., 2021. Physical manifestations and ecological implications of Arctic Atlantification. Nat. Rev. Earth Environ. 2, 874–889.

Intergovernmental Panel on Climate Change (IPCC) (Ed.), 2023. Frontmatter, in: Climate Change 2021 – The Physical Science Basis: Working Group I Contribution to the Sixth Assessment Report of the Intergovernmental Panel on Climate Change. Cambridge University Press, Cambridge, pp. i–ii.

Johnsen, G., Leu, E., Gradinger, R., 2020. Marine Micro- and Macroalgae in the Polar Night, in: Berge, J., Johnsen, G., Cohen, J.H. (Eds.), POLAR NIGHT Marine Ecology: Life and Light in the Dead of Night. Springer International Publishing, Cham, pp. 67–112. https://doi.org/10.1007/978-3-030-33208-2_4

Kaiser, P., Hagen, W., Bode-Dalby, M., Auel, H., 2022. Tolerant but facing increased competition: Arctic zooplankton versus Atlantic invaders in a warming ocean. Front. Mar. Sci. 9, 908638.

Kanzow, T., 2020. Links to master tracks in different resolutions of POLARSTERN cruise PS122/3, Arctic Ocean - Longyearbyen, 2020-02-24 - 2020-06-04 (Version 2).

Alfred Wegener Inst. Helmholtz Cent. Polar Mar. Res. Bremerhaven
https://doi.org/10.1594/PANGAEA.924681

Katlein, C., Schiller, M., Belter, H.J., Coppolaro, V., Wenslandt, D., Nicolaus, M., 2017. A New Remotely Operated Sensor Platform for Interdisciplinary Observations under Sea Ice. Front. Mar. Sci. 4.

Kauko, H.M., Taskjelle, T., Assmy, P., Pavlov, A.K., Mundy, C.J., Duarte, P., Fernández-Méndez, M., Olsen, L.M., Hudson, S.R., Johnsen, G., Elliott, A., Wang, F., Granskog, M.A., 2017. Windows in Arctic sea ice: Light transmission and ice algae in a refrozen lead. J. Geophys. Res. Biogeosciences 122, 1486–1505. https://doi.org/10.1002/2016JG003626

Kiko, R., Biastoch, A., Brandt, P., Cravatte, S., Hauss, H., Hummels, R., Kriest, I., Marin, F., McDonnell, A.M., Oschlies, A., 2017. Biological and physical influences on marine snowfall at the equator. Nat. Geosci. 10, 852–858.

Kim, H.H., Bowman, J.S., Luo, Y.-W., Ducklow, H.W., Schofield, O.M., Steinberg, D.K., Doney, S.C., 2022. Modeling polar marine ecosystem functions guided by bacterial physiological and taxonomic traits. Biogeosciences 19, 117–136. https://doi.org/10.5194/bg-19-117-2022

Kohlbach, D., Graeve, M., A. Lange, B., David, C., Peeken, I., Flores, H., 2016. The importance of ice algae-produced carbon in the central Arctic Ocean ecosystem: Food web relationships revealed by lipid and stable isotope analyses. Limnol. Oceanogr. 61, 2027–2044. https://doi.org/10.1002/lno.10351

Kohlbach, D., Smik, L., Belt, S.T., Hop, H., Wold, A., Graeve, M., Assmy, P., 2022. A multi-trophic marker approach reveals high feeding plasticity in Barents Sea under-ice fauna. Prog. Oceanogr. 208, 102895.

Kosobokova, K., Hirche, H.-J., 2000. Zooplankton distribution across the Lomonosov Ridge, Arctic Ocean: species inventory, biomass and vertical structure. Deep Sea Res. Part Oceanogr. Res. Pap. 47, 2029–2060.

Krembs, C., Eicken, H., Deming, J.W., 2011. Exopolymer alteration of physical properties of sea ice and implications for ice habitability and biogeochemistry in a warmer Arctic. Proc. Natl. Acad. Sci. 108, 3653–3658.

Krumpen, T., Birrien, F., Kauker, F., Rackow, T., von Albedyll, L., Angelopoulos, M., Belter, H.J., Bessonov, V., Damm, E., Dethloff, K., Haapala, J., Haas, C., Harris, C., Hendricks, S., Hoelemann, J., Hoppmann, M., Kaleschke, L., Karcher, M., Kolabutin, N., Lei, R., Lenz, J., Morgenstern, A., Nicolaus, M., Nixdorf, U., Petrovsky, T., Rabe, B., Rabenstein, L., Rex, M., Ricker, R., Rohde, J., Shimanchuk, E., Singha, S., Smolyanitsky, V., Sokolov, V., Stanton, T., Timofeeva, A., Tsamados, M., Watkins, D., 2020. The MOSAiC ice floe: sediment-laden survivor from the Siberian shelf. The Cryosphere 14, 2173–2187. https://doi.org/10.5194/tc-14-2173-2020

Kunisch EH, Graeve M, Gradinger R, Haug T, Kovacs KM, Lydersen C, Varpe Ø, Bluhm BA, 2021. Ice-algal carbon supports harp and ringed seal diets in the European Arctic: evidence from fatty acid and stable isotope markers. Mar. Ecol. Prog. Ser. 675, 181–197.

Kvernvik, A.C., Hoppe, C.J.M., Lawrenz, E., Prášil, O., Greenacre, M., Wiktor, J.M., Leu, E., 2018. Fast reactivation of photosynthesis in arctic phytoplankton during the polar night. J. Phycol. 54, 461–470. https://doi.org/doi:10.1111/jpy.12750

Lange, B.A., Salganik, E., Macfarlane, A., Schneebeli, M., Høyland, K., Gardner, J., Müller, O., Divine, D.V., Kohlbach, D., Katlein, C., Granskog, M.A., 2023. Snowmelt

1782 contribution to Arctic first-year ice ridge mass balance and rapid consolidation during
1783 summer melt. Elem. Sci. Anthr. 11, 00037.
1784 https://doi.org/10.1525/elementa.2022.00037

1785 Lannuzel, D., Tedesco, L., van Leeuwe, M., Campbell, K., Flores, H., Delille, B.,
1786 Miller, L., Stefels, J., Assmy, P., Bowman, J., Brown, K., Castellani, G., Chierici, M.,
1787 Crabeck, O., Damm, E., Else, B., Fransson, A., Fripiat, F., Geilfus, N.-X., Jacques,
1788 C., Jones, E., Kaartokallio, H., Kotovitch, M., Meiners, K., Moreau, S., Nomura, D.,
1789 Peeken, I., Rintala, J.-M., Steiner, N., Tison, J.-L., Vancoppenolle, M., Van der
1790 Linden, F., Vichi, M., Wongpan, P., 2020. The future of Arctic sea-ice
1791 biogeochemistry and ice-associated ecosystems. Nat. Clim. Change 10, 983–992.
1792 https://doi.org/10.1038/s41558-020-00940-4

1793 Laurion, I., Demers, S., Vézina, A. F., 1995. The microbial food web associated with
1794 the ice algal assemblage: biomass and bacterivory of nanoflagellate protozoans in
1795 Resolute Passage (High Canadian Arctic). Mar. Ecol. Prog. Ser. 120, 77–87.

1796 Leu, E., Brown, T.A., Graeve, M., Wiktor, J., Hoppe, C.J.M., Chierici, M., Fransson,
1797 A., Verbiest, S., Kvernvik, A.C., Greenacre, M.J., 2020. Spatial and Temporal
1798 Variability of Ice Algal Trophic Markers—With Recommendations about Their
1799 Application. J. Mar. Sci. Eng. 8. https://doi.org/10.3390/jmse8090676

1800 Leu, E., Mundy, C.J., Assmy, P., Campbell, K., Gabrielsen, T.M., Gosselin, M., Juul-
1801 Pedersen, T., Gradinger, R., 2015. Arctic spring awakening – Steering principles
1802 behind the phenology of vernal ice algal blooms. Prog. Oceanogr. 139, 151–170.
1803 https://doi.org/10.1016/j.pocean.2015.07.012

1804 Lombard, F., Boss, E., Waite, A.M., Vogt, M., Uitz, J., Stemmann, L., Sosik, H.M.,
1805 Schulz, J., Romagnan, J.-B., Picheral, M., 2019. Globally consistent quantitative
1806 observations of planktonic ecosystems. Front. Mar. Sci. 6, 196.

1807 Lotka, A.J., 1920. Analytical note on certain rhythmic relations in organic systems.
1808 Proc. Natl. Acad. Sci. 6, 410–415.

1809 Ludvigsen, M., Berge, J., Geoffroy, M., Cohen, J.H., De La Torre, P.R., Nornes,
1810 S.M., Singh, H., Sørensen, A.J., Daase, M., Johnsen, G., 2018. Use of an
1811 autonomous surface vehicle reveals small-scale diel vertical migrations of
1812 zooplankton and susceptibility to light pollution under low solar irradiance. Sci. Adv.
1813 4, eaap9887.

1814 Lund-Hansen, L.C., Hawes, I., Hancke, K., Salmansen, N., Nielsen, J.R., Balslev, L.,
1815 Sorrell, B.K., 2020. Effects of increased irradiance on biomass, photobiology,
1816 nutritional quality, and pigment composition of Arctic sea ice algae. Mar. Ecol. Prog.
1817 Ser. 648, 95–110.

1818 MacArthur, R., 1970. Species packing and competitive equilibrium for many species.
1819 Theor. Popul. Biol. 1, 1–11.

1820 Malinauskaite, L., Cook, D., Davíðsdóttir, B., Ögmundardóttir, H., Roman, J., 2019.
1821 Ecosystem services in the Arctic: a thematic review. Ecosyst. Serv. 36, 100898.

1822 Manizza, M., Follows, M.J., Dutkiewicz, S., Menemenlis, D., Hill, C.N., Key, R.M.,
1823 2013. Changes in the Arctic Ocean CO_2 sink (1996–2007): A regional
1824 model analysis. Glob. Biogeochem. Cycles 2012GB004491.
1825 https://doi.org/10.1002/2012gb004491

1826 Marangoni, L.F., Davies, T., Smyth, T., Rodríguez, A., Hamann, M., Duarte, C.,
1827 Pendoley, K., Berge, J., Maggi, E., Levy, O., 2022. Impacts of artificial light at night
1828 in marine ecosystems—A review. Glob. Change Biol. 28, 5346–5367.

1829 Melnikov, I., 1980. Ecosystem of the Arctic drift ice. Biol. Cent. Arct. Basin Mosc.
1830 Nauka 61–97.

1831 Metfies, K., Schroeder, F., Hessel, J., Wollschläger, J., Micheller, S., Wolf, C., Kilias,
1832 E., Sprong, P., Neuhaus, S., Frickenhaus, S., Petersen, W., 2016. High-resolution
1833 monitoring of marine protists based on an observation strategy integrating
1834 automated on-board filtration and molecular analyses. Ocean Sci 12, 1237–1247.
1835 https://doi.org/10.5194/os-12-1237-2016

1836 Miller, L.A., Carnat, G., Else, B.G., Sutherland, N., Papakyriakou, T.N., 2011.
1837 Carbonate system evolution at the Arctic Ocean surface during autumn freeze-up. J.
1838 Geophys. Res. Oceans 116.

1839 Mo, A., Kim, D., Yang, E.J., Jung, J., Ko, Y.H., Kang, S.-H., Cho, K.-H., Park, K.,
1840 Kim, T.-W., 2022. Factors affecting the subsurface aragonite undersaturation layer in
1841 the Pacific Arctic region. Mar. Pollut. Bull. 183, 114060.

1842 Mock, T., Boulton, W., Balmonte, J.-P., Barry, Kevin, Bertilsson, S., Bowman, J.,
1843 Buck, M., Bratbak, G., Chamberlain, E.J., Cunliffe, M., Creamean, J., Ebenhöh, O.,
1844 Eggers, S.L., Fong, A.A., Gardner, J., Gradinger, R., Granskog, M.A., Havermans,
1845 C., Hill, T., Hoppe, C.J.M., Korte, K., Larsen, A., Müller, O., Nicolaus, A., Oldenburg,
1846 E., Popa, O., Rogge, S., Schäfer, H., Shoemaker, K., Snoeijs-Leijonmalm, P.,
1847 Torstensson, A., Valentin, K., Vader, A., Barry, Kerrie, Chen, I.-M.A., Clum, A.,
1848 Copeland, A., Daum, C., Eloe-Fadrosh, E., Foster, Brian, Foster, Bryce, Grigoriev,
1849 I.V., Huntemann, M., Ivanova, N., Kuo, A., Kyrpides, N.C., Mukherjee, S.,
1850 Palaniappan, K., Reddy, T.B.K., Salamov, A., Roux, S., Varghese, N., Woyke, T.,
1851 Wu, D., Leggett, R.M., Moulton, V., Metfies, K., 2022. Multiomics in the central Arctic
1852 Ocean for benchmarking biodiversity change. PLOS Biol. 20, e3001835.
1853 https://doi.org/10.1371/journal.pbio.3001835

1854 Nicolaus, M., Anhaus, P., Hoppmann, M., Tao, R., Katlein, C., 2023a. Spectral
1855 radiation fluxes, albedo and transmittance from autonomous measurement from
1856 Radiation Station 2020R12, deployed during MOSAiC 2019/20.
1857 https://doi.org/10.1594/PANGAEA.948712

1858 Nicolaus, M., Belter, H.J., Rohde, J., Hoppmann, M., Tao, R., Katlein, C., 2023b.
1859 Spectral radiation fluxes, albedo and transmittance from autonomous measurement
1860 from Radiation Station 2019R8, deployed during MOSAiC 2019/20.
1861 https://doi.org/10.1594/PANGAEA.948876

1862 Nicolaus, M., Hoppmann, M., Tao, R., Katlein, C., 2022a. Spectral radiation fluxes,
1863 albedo and transmittance from autonomous measurement from Radiation Station
1864 2020R22, deployed during MOSAiC 2019/20, Alfred Wegener Institute, Helmholtz
1865 Centre for Polar and Marine Research, Bremerhaven. PANGAEA.
1866 https://doi.org/10.1594/PANGAEA.942602

1867 Nicolaus, M., Perovich, D.K., Spreen, G., Granskog, M.A., von Albedyll, L.,
1868 Angelopoulos, M., Anhaus, P., Arndt, S., Belter, H.J., Bessonov, V., Birnbaum, G.,
1869 Brauchle, J., Calmer, R., Cardellach, E., Cheng, B., Clemens-Sewall, D., Dadic, R.,
1870 Damm, E., de Boer, G., Demir, O., Dethloff, K., Divine, D.V., Fong, A.A., Fons, S.,
1871 Frey, M.M., Fuchs, N., Gabarró, C., Gerland, S., Goessling, H.F., Gradinger, R.,
1872 Haapala, J., Haas, C., Hamilton, J., Hannula, H.-R., Hendricks, S., Herber, A.,
1873 Heuzé, C., Hoppmann, M., Høyland, K.V., Huntemann, M., Hutchings, J.K., Hwang,
1874 B., Itkin, P., Jacobi, H.-W., Jaggi, M., Jutila, A., Kaleschke, L., Katlein, C., Kolabutin,
1875 N., Krampe, D., Kristensen, S.S., Krumpen, T., Kurtz, N., Lampert, A., Lange, B.A.,
1876 Lei, R., Light, B., Linhardt, F., Liston, G.E., Loose, B., Macfarlane, A.R., Mahmud,

M., Matero, I.O., Maus, S., Morgenstern, A., Naderpour, R., Nandan, V., Niubom, A., Oggier, M., Oppelt, N., Pätzold, F., Perron, C., Petrovsky, T., Pirazzini, R., Polashenski, C., Rabe, B., Raphael, I.A., Regnery, J., Rex, M., Ricker, R., Riemann-Campe, K., Rinke, A., Rohde, J., Salganik, E., Scharien, R.K., Schiller, M., Schneebeli, M., Semmling, M., Shimanchuk, E., Shupe, M.D., Smith, M.M., Smolyanitsky, V., Sokolov, V., Stanton, T., Stroeve, J., Thielke, L., Timofeeva, A., Tonboe, R.T., Tavri, A., Tsamados, M., Wagner, D.N., Watkins, D., Webster, M., Wendisch, M., 2022b. Overview of the MOSAiC expedition: Snow and sea ice. Elem. Sci. Anthr. 10, 000046. https://doi.org/10.1525/elementa.2021.000046

Nomura, D., Granskog, M.A., Fransson, A., Chierici, M., Silyakova, A., Ohshima, K.I., Cohen, L., Delille, B., Hudson, S.R., Dieckmann, G.S., 2018. CO_2 flux over young and snow-covered Arctic pack ice in winter and spring. Biogeosciences 15, 3331–3343.

Nomura, D., Wongpan, P., Toyota, T., Tanikawa, T., Kawaguchi, Y., Ono, T., Ishino, T., Tozawa, M., Tamura, T.P., Yabe, I.S., 2020. Saroma-ko Lagoon Observations for sea ice Physico-chemistry and Ecosystems 2019 (SLOPE2019). Bull. Glaciol. Res. 38, 1–12.

Olsen, L.M., Laney, S.R., Duarte, P., Kauko, H.M., Fernández-Méndez, M., Mundy, C.J., Rösel, A., Meyer, A., Itkin, P., Cohen, L., Peeken, I., Tatarek, A., Różańska-Pluta, M., Wiktor, J., Taskjelle, T., Pavlov, A.K., Hudson, S.R., Granskog, M.A., Hop, H., Assmy, P., 2017. The seeding of ice algal blooms in Arctic pack ice: The multiyear ice seed repository hypothesis. J. Geophys. Res. Biogeosciences 122, 1529–1548. https://doi.org/10.1002/2016JG003668

Patrohay, E., Gradinger, R., Marquardt, M., Bluhm, B.A., 2022. First trait-based characterization of Arctic ice meiofauna taxa. Polar Biol. 45, 1673–1688. https://doi.org/10.1007/s00300-022-03099-0

Picheral, M., Colin, S., Irisson, J.-O., 2017. EcoTaxa, a tool for the taxonomic classification of images.

Polyakov, I.V., Alkire, M.B., Bluhm, B.A., Brown, K.A., Carmack, E.C., Chierici, M., Danielson, S.L., Ellingsen, I., Ershova, E.A., Gårdfeldt, K., Ingvaldsen, R.B., Pnyushkov, A.V., Slagstad, D., Wassmann, P., 2020. Borealization of the Arctic Ocean in Response to Anomalous Advection From Sub-Arctic Seas. Front. Mar. Sci. 7.

Popa, O., Oldenburg, E., Ebenhöh, O., 2020. From sequence to information. Philos. Trans. R. Soc. B 375, 20190448.

Poulin, M., Daugbjerg, N., Gradinger, R., Ilyash, L., Ratkova, T., von Quillfeldt, C., 2011. The pan-Arctic biodiversity of marine pelagic and sea-ice unicellular eukaryotes: a first-attempt assessment. Mar. Biodivers. 41, 13–28. https://doi.org/10.1007/s12526-010-0058-8

Qi, D., Ouyang, Z., Chen, L., Wu, Y., Lei, R., Chen, B., Feely, R.A., Anderson, L.G., Zhong, W., Lin, H., Polukhin, A., Zhang, Yixing, Zhang, Yongli, Bi, H., Lin, X., Luo, Y., Zhuang, Y., He, J., Chen, J., Cai, W.-J., 2022. Climate change drives rapid decadal acidification in the Arctic Ocean from 1994 to 2020. Science 377, 1544–1550. https://doi.org/10.1126/science.abo0383

Rabe, B., Heuzé, C., Regnery, J., Aksenov, Y., Allerholt, J., Athanase, M., Bai, Y., Basque, C., Bauch, D., Baumann, T.M., Chen, D., Cole, S.T., Craw, L., Davies, A., Damm, E., Dethloff, K., Divine, D.V., Doglioni, F., Ebert, F., Fang, Y.-C., Fer, I., Fong, A.A., Gradinger, R., Granskog, M.A., Graupner, R., Haas, C., He, H., He, Y.,

1925   Hoppmann, M., Janout, M., Kadko, D., Kanzow, T., Karam, S., Kawaguchi, Y.,
1926   Koenig, Z., Kong, B., Krishfield, R.A., Krumpen, T., Kuhlmey, D., Kuznetsov, I., Lan,
1927   M., Laukert, G., Lei, R., Li, T., Torres-Valdés, S., Lin, Lina, Lin, Long, Liu, H., Liu, N.,
1928   Loose, B., Ma, X., McKay, R., Mallet, M., Mallett, R.D.C., Maslowski, W., Mertens,
1929   C., Mohrholz, V., Muilwijk, M., Nicolaus, M., O'Brien, J.K., Perovich, D., Ren, J., Rex,
1930   M., Ribeiro, N., Rinke, A., Schaffer, J., Schuffenhauer, I., Schulz, K., Shupe, M.D.,
1931   Shaw, W., Sokolov, V., Sommerfeld, A., Spreen, G., Stanton, T., Stephens, M., Su,
1932   J., Sukhikh, N., Sundfjord, A., Thomisch, K., Tippenhauer, S., Toole, J.M.,
1933   Vredenborg, M., Walter, M., Wang, H., Wang, L., Wang, Y., Wendisch, M., Zhao, J.,
1934   Zhou, M., Zhu, J., 2022. Overview of the MOSAiC expedition: Physical
1935   oceanography. Elem. Sci. Anthr. 10, 00062.
1936   https://doi.org/10.1525/elementa.2021.00062

1937   Randelhoff, A., Holding, J., Janout, M., Sejr, M.K., Babin, M., Tremblay, J.-É., Alkire,
1938   M.B., 2020. Pan-Arctic Ocean Primary Production Constrained by Turbulent Nitrate
1939   Fluxes. Front. Mar. Sci. 7.

1940   Rantanen, M., Karpechko, A.Yu., Lipponen, A., Nordling, K., Hyvärinen, O.,
1941   Ruosteenoja, K., Vihma, T., Laaksonen, A., 2022. The Arctic has warmed nearly four
1942   times faster than the globe since 1979. Commun. Earth Environ. 3, 168.
1943   https://doi.org/10.1038/s43247-022-00498-3

1944   Rees, A.P., Bange, H.W., Arévalo-Martínez, D.L., Artioli, Y., Ashby, D.M., Brown, I.,
1945   Campen, H.I., Clark, D.R., Kitidis, V., Lessin, G., 2022. Nitrous oxide and methane in
1946   a changing Arctic Ocean. Ambio 51, 398–410.

1947   Rex, M., 2021a. Master tracks in different resolutions of POLARSTERN cruise
1948   PS122/4, Longyearbyen - Arctic Ocean, 2020-06-04 - 2020-08-12. Alfred Wegener
1949   Inst. Helmholtz Cent. Polar Mar. Res. Bremerhaven.
1950   https://doi.org/10.1594/PANGAEA.926829

1951   Rex, M., 2021b. Master tracks in different resolutions of POLARSTERN cruise
1952   PS122/5, Arctic Ocean - Bremerhaven, 2020-08-12 - 2020-10-12. Alfred Wegener
1953   Inst. Helmholtz Cent. Polar Mar. Res. Bremerhaven.
1954   https://doi.org/10.1594/PANGAEA.926910

1955   Rex, M., 2020. Links to master tracks in different resolutions of POLARSTERN
1956   cruise PS122/1, Tromsø - Arctic Ocean, 2019-09-20 - 2019-12-13 (Version 2). Alfred
1957   Wegener Inst. Helmholtz Cent. Polar Mar. Res. Bremerhaven.
1958   https://doi.org/10.1594/PANGAEA.924668

1959   Rijkenberg, M.J.A., Slagter, H.A., Rutgers van der Loeff, M., van Ooijen, J.,
1960   Gerringa, L.J.A., 2018. Dissolved Fe in the Deep and Upper Arctic Ocean With a
1961   Focus on Fe Limitation in the Nansen Basin. Front. Mar. Sci. 5.

1962   Rinke, A., Cassano, J.J., Cassano, E.N., Jaiser, R., Handorf, D., 2021.
1963   Meteorological conditions during the MOSAiC expedition: Normal or anomalous?
1964   Elem. Sci. Anthr. 9, 00023. https://doi.org/10.1525/elementa.2021.00023

1965   Royo-Llonch, M., Sánchez, P., Ruiz-González, C., Salazar, G., Pedrós-Alió, C.,
1966   Sebastián, M., Labadie, K., Paoli, L., M. Ibarbalz, F., Zinger, L., Churcheward, B.,
1967   Babin, M., Bork, P., Boss, E., Cochrane, G., de Vargas, C., Gorsky, G., Grimsley, N.,
1968   Guidi, L., Hingamp, P., Iudicone, D., Jaillon, O., Kandels, S., Not, F., Ogata, H.,
1969   Pesant, S., Poulton, N., Raes, J., Sardet, C., Speich, S., Setmmann, L., Sullivan,
1970   M.B., Chaffron, S., Eveillard, D., Karsenti, E., Sunagawa, S., Wincker, P., Karp-Boss,
1971   L., Bowler, C., Acinas, S.G., Tara Oceans Coordinators, 2021. Compendium of 530
1972   metagenome-assembled bacterial and archaeal genomes from the polar Arctic

1973 Ocean. Nat. Microbiol. 6, 1561–1574. https://doi.org/10.1038/s41564-021-00979-9

1974 Rudels, B., Carmack, E., 2022. Arctic Ocean water mass structure and circulation.
1975 Oceanography 35, 52–65.

1976 Rybakova, E., Kremenetskaia, A., Vedenin, A., Boetius, A., Gebruk, A., 2019. Deep-
1977 sea megabenthos communities of the Eurasian Central Arctic are influenced by ice-
1978 cover and sea-ice algal falls. PLoS One 14, e0211009.

1979 Rysgaard, S., Glud, R., Sejr, M., Bendtsen, J., Christensen, P., 2007. Inorganic
1980 carbon transport during sea ice growth and decay: A carbon pump in polar seas. J.
1981 Geophys. Res. Oceans 112.

1982 Rysgaard, S., Glud, R.N., Lennert, K., Cooper, M., Halden, N., Leakey, R.,
1983 Hawthorne, F., Barber, D., 2012. Ikaite crystals in melting sea ice–implications for
1984 pCO_2 and pH levels in Arctic surface waters. The Cryosphere 6, 901–908.

1985 Salganik, Evgenii, Katlein, C., Lange, B.A., Matero, I., Lei, R., Fong, A.A., Fons,
1986 S.W., Divine, D., Oggier, M., Castellani, G., Bozzato, D., Chamberlain, E.J., Hoppe,
1987 C.J.M., Müller, O., Gardner, J., Rinke, A., Pereira, P.S., Ulfsbo, A., Marsay, C.,
1988 Webster, M.A., Maus, S., Høyland, K.V., Granskog, M.A., 2023a. Temporal evolution
1989 of under-ice meltwater layers and false bottoms and their impact on summer Arctic
1990 sea ice mass balance. Elem. Sci. Anthr. 11, 00035.
1991 https://doi.org/10.1525/elementa.2022.00035

1992 Salganik, Evgenii, Lange, B.A., Itkin, P., Divine, D., Katlein, C., Nicolaus, M.,
1993 Hoppmann, M., Neckel, N., Ricker, R., Høyland, K.V., 2023b. Different mechanisms
1994 of Arctic first-year sea-ice ridge consolidation observed during the MOSAiC
1995 expedition. Elem. Sci. Anthr. 11.

1996 Salganik, E., Lange, B.A., Katlein, C., Matero, I., Anhaus, P., Muilwijk, M., Høyland,
1997 K.V., Granskog, M.A., 2023. Observations of preferential summer melt of Arctic sea-
1998 ice ridge keels from repeated multibeam sonar surveys. The Cryosphere 17, 4873–
1999 4887. https://doi.org/10.5194/tc-17-4873-2023

2000 Sauve, A.M., Taylor, R.A., Barraquand, F., 2020. The effect of seasonal strength and
2001 abruptness on predator–prey dynamics. J. Theor. Biol. 491, 110175.

2002 Schmid, M.S., Aubry, C., Grigor, J., Fortier, L., 2016. The LOKI underwater imaging
2003 system and an automatic identification model for the detection of zooplankton taxa in
2004 the Arctic Ocean. Methods Oceanogr. 15, 129–160.

2005 Schulz, J., Barz, K., Ayon, P., Luedtke, A., Zielinski, O., Mengedoht, D., Hirche, H.-
2006 J., 2010. Imaging of plankton specimens with the lightframe on-sight keyspecies
2007 investigation (LOKI) system. J. Eur. Opt. Soc.-Rapid Publ. 5.

2008 Schulz, J., Möller, K.O., Bracher, A., Hieronymi, M., Cisewski, B., Zielinski, O., Voss,
2009 D., Gutzeit, E., Dolereit, T., Niedzwiedz, G., 2015. Aquatische optische Technologien
2010 in Deutschland. Mar. Sci. Rep.-Meereswissenschaftliche Berichte 97, 1–83.

2011 Schulz, K., Koenig, Z., Muilwijk, M., 2023a. The Eurasian Arctic Ocean along the
2012 MOSAiC drift (2019-2020): Core hydrographic parameters.
2013 https://doi.org/10.18739/A21J9790B

2014 Schulz, K., Koenig, Z., Muilwijk, M., Bauch, D., Hoppe, C.J., Droste, E., Hoppmann,
2015 M., Chamberlain, E.J., Laukert, G., Stanton, T., 2023b. The Eurasian Arctic Ocean
2016 along the MOSAiC drift (2019-2020): An interdisciplinary perspective on properties
2017 and processes. https://doi.org/10.31223/X5TT2W

2018 Sherr, E.B., Sherr, B.F., Wheeler, P.A., Thompson, K., 2003. Temporal and spatial
2019 variation in stocks of autotrophic and heterotrophic microbes in the upper water

2020   column of the central Arctic Ocean. Deep Sea Res. Part Oceanogr. Res. Pap. 50,
2021   557–571. https://doi.org/10.1016/S0967-0637(03)00031-1

2022   Shupe, M.D., Rex, M., Blomquist, B., Persson, P.O.G., Schmale, J., Uttal, T.,
2023   Althausen, D., Angot, H., Archer, S., Bariteau, L., Beck, I., Bilberry, J., Bucci, S.,
2024   Buck, C., Boyer, M., Brasseur, Z., Brooks, I.M., Calmer, R., Cassano, J., Castro, V.,
2025   Chu, D., Costa, D., Cox, C.J., Creamean, J., Crewell, S., Dahlke, S., Damm, E., de
2026   Boer, G., Deckelmann, H., Dethloff, K., Dütsch, M., Ebell, K., Ehrlich, A., Ellis, J.,
2027   Engelmann, R., Fong, A.A., Frey, M.M., Gallagher, M.R., Ganzeveld, L., Gradinger,
2028   R., Graeser, J., Greenamyer, V., Griesche, H., Griffiths, S., Hamilton, J., Heinemann,
2029   G., Helmig, D., Herber, A., Heuzé, C., Hofer, J., Houchens, T., Howard, D., Inoue, J.,
2030   Jacobi, H.-W., Jaiser, R., Jokinen, T., Jourdan, O., Jozef, G., King, W.,
2031   Kirchgaessner, A., Klingebiel, M., Krassovski, M., Krumpen, T., Lampert, A.,
2032   Landing, W., Laurila, T., Lawrence, D., Lonardi, M., Loose, B., Lüpkes, C., Maahn,
2033   M., Macke, A., Maslowski, W., Marsay, C., Maturilli, M., Mech, M., Morris, S., Moser,
2034   M., Nicolaus, M., Ortega, P., Osborn, J., Pätzold, F., Perovich, D.K., Petäjä, T., Pilz,
2035   C., Pirazzini, R., Posman, K., Powers, H., Pratt, K.A., Preußer, A., Quéléver, L.,
2036   Radenz, M., Rabe, B., Rinke, A., Sachs, T., Schulz, A., Siebert, H., Silva, T.,
2037   Solomon, A., Sommerfeld, A., Spreen, G., Stephens, M., Stohl, A., Svensson, G.,
2038   Uin, J., Viegas, J., Voigt, C., von der Gathen, P., Wehner, B., Welker, J.M.,
2039   Wendisch, M., Werner, M., Xie, Z., Yue, F., 2022. Overview of the MOSAiC
2040   expedition: Atmosphere. Elem. Sci. Anthr. 10, 00060.
2041   https://doi.org/10.1525/elementa.2021.00060

2042   Shupe, M.D., Rex, M., Dethloff, K., Damm, E., Fong, A.A., Gradinger, R., Heuzé, C.,
2043   Loose, B., Makarov, A., Maslowski, W., Nicolaus, M., Perovich, D., Rabe, B., Rinke,
2044   A., Sokolov, V., Sommerfeld, A., 2020. Arctic Report Card 2020: The MOSAiC
2045   Expedition: A Year Drifting with the Arctic Sea Ice. Arctic Report Card.
2046   https://doi.org/10.25923/9g3v-xh92

2047   Smith, M.M., Angot, H., Chamberlain, E.J., Droste, E.S., Karam, S., Muilwijk, M.,
2048   Webb, A.L., Archer, S.D., Beck, I., Blomquist, B.W., Bowman, J., Boyer, M., Bozzato,
2049   D., Chierici, M., Creamean, J., D'Angelo, A., Delille, B., Fer, I., Fong, A.A., Fransson,
2050   A., Fuchs, N., Gardner, J., Granskog, M.A., Hoppe, C.J.M., Hoppema, M.,
2051   Hoppmann, M., Mock, T., Muller, S., Müller, O., Nicolaus, M., Nomura, D., Petäjä, T.,
2052   Salganik, E., Schmale, J., Schmidt, K., Schulz, K.M., Shupe, M.D., Stefels, J.,
2053   Thielke, L., Tippenhauer, S., Ulfsbo, A., van Leeuwe, M., Webster, M., Yoshimura,
2054   M., Zhan, L., 2023. Thin and transient meltwater layers and false bottoms in the
2055   Arctic sea ice pack—Recent insights on these historically overlooked features. Elem.
2056   Sci. Anthr. 11, 00025. https://doi.org/10.1525/elementa.2023.00025

2057   Smith, M.M., von Albedyll, L., Raphael, I.A., Lange, B.A., Matero, I., Salganik, E.,
2058   Webster, M.A., Granskog, M.A., Fong, A., Lei, R., 2022. Quantifying false bottoms
2059   and under-ice meltwater layers beneath Arctic summer sea ice with fine-scale
2060   observations. Elem Sci Anth 10, 000116.

2061   Snoeijs-Leijonmalm Pauline, Flores Hauke, Sakinan Serdar, Hildebrandt Nicole,
2062   Svenson Anders, Castellani Giulia, Vane Kim, Mark Felix C., Heuzé Céline,
2063   Tippenhauer Sandra, Niehoff Barbara, Hjelm Joakim, Hentati Sundberg Jonas,
2064   Schaafsma Fokje L., Engelmann Ronny, 2022. Unexpected fish and squid in the
2065   central Arctic deep scattering layer. Sci. Adv. 8, eabj7536.
2066   https://doi.org/10.1126/sciadv.abj7536

2067   Søreide, J.E., Leu, E., Berge, J., Graeve, M., Falk-Petersen, S., 2010. Timing of
2068   blooms, algal food quality and *Calanus glacialis* reproduction and growth in a

2069   changing Arctic. Glob. Change Biol. 16, 3154–3163. https://doi.org/10.1111/j.1365-
2070   2486.2010.02175.x

2071   Stemmann, L., Youngbluth, M., Robert, K., Hosia, A., Picheral, M., Paterson, H.,
2072   Ibanez, F., Guidi, L., Lombard, F., Gorsky, G., 2008. Global zoogeography of fragile
2073   macrozooplankton in the upper 100–1000 m inferred from the underwater video
2074   profiler. ICES J. Mar. Sci. 65, 433–442.

2075   Succurro, A., Ebenhöh, O., 2018. Review and perspective on mathematical modeling
2076   of microbial ecosystems. Biochem. Soc. Trans. 46, 403–412.

2077   Syvertsen, E.E., 1991. Ice algae in the Barents Sea: types of assemblages, origin,
2078   fate and role in the ice-edge phytoplankton bloom. Polar Res. 10, 277–288.

2079   Taskjelle, T., Granskog, M.A., Pavlov, A.K., Hudson, S.R., Hamre, B., 2017. Effects
2080   of an Arctic under-ice bloom on solar radiant heating of the water column. J.
2081   Geophys. Res. Oceans 122, 126–138. https://doi.org/10.1002/2016JC012187

2082   Tedesco, L., Vichi, M., Scoccimarro, E., 2019. Sea-ice algal phenology in a warmer
2083   Arctic. Sci. Adv. 5, eaav4830. https://doi.org/10.1126/sciadv.aav4830

2084   Tippenhauer, S., Vredenborg, M., Heuzé, C., Ulfsbo, A., Rabe, B., Granskog, M.A.,
2085   Allerholt, J., Balmonte, J.P., Campbell, R.G., Castellani, G., Chamberlain, E.,
2086   Creamean, J., D'Angelo, A., Dietrich, U., Droste, E.S., Eggers, L., Fang, Y.-C., Fong,
2087   A.A., Gardner, J., Graupner, R., Grosse, J., He, H., Hildebrandt, N., Hoppe, C.J.M.,
2088   Hoppmann, M., Kanzow, T., Karam, S., Koenig, Z., Kong, B., Kuhlmey, D.,
2089   Kuznetsov, I., Lan, M., Liu, H., Mallet, M., Mohrholz, V., Muilwijk, M., Müller, O.,
2090   Olsen, L.M., Rember, R., Ren, J., Sakinan, S., Schaffer, J., Schmidt, K.,
2091   Schuffenhauer, I., Schulz, K., Shoemaker, K., Spahic, S., Sukhikh, N., Svenson, A.,
2092   Torres-Valdés, S., Torstensson, A., Wischnewski, L., Zhuang, Y., 2023a. Physical
2093   oceanography water bottle samples based on ship CTD during POLARSTERN
2094   cruise PS122. https://doi.org/10.1594/PANGAEA.959965

2095   Tippenhauer, S., Vredenborg, M., Heuzé, C., Ulfsbo, A., Rabe, B., Granskog, M.A.,
2096   Allerholt, J., Balmonte, J.P., Campbell, R.G., Castellani, G., Chamberlain, E.,
2097   Creamean, J., D'Angelo, A., Dietrich, U., Droste, E.S., Eggers, L., Fang, Y.-C., Fong,
2098   A.A., Gardner, J., Graupner, R., Grosse, J., He, H., Hildebrandt, N., Hoppe, C.J.M.,
2099   Hoppmann, M., Kanzow, T., Karam, S., Koenig, Z., Kong, B., Kuhlmey, D.,
2100   Kuznetsov, I., Lan, M., Liu, H., Mallet, M., Mohrholz, V., Muilwijk, M., Müller, O.,
2101   Olsen, L.M., Rember, R., Ren, J., Sakinan, S., Schaffer, J., Schmidt, K.,
2102   Schuffenhauer, I., Schulz, K., Shoemaker, K., Spahic, S., Sukhikh, N., Svenson, A.,
2103   Torres-Valdés, S., Torstensson, A., Wischnewski, L., Zhuang, Y., 2023b. Physical
2104   oceanography water bottle samples based on Ocean City CTD during
2105   POLARSTERN cruise PS122. https://doi.org/10.1594/PANGAEA.959966

2106   Tortell, P.D., 2005. Dissolved gas measurements in oceanic waters made by
2107   membrane inlet mass spectrometry. Limnol. Oceanogr. Methods 3, 24–37.

2108   Tremblay, J.-É., Anderson, L.G., Matrai, P., Coupel, P., Bélanger, S., Michel, C.,
2109   Reigstad, M., 2015. Global and regional drivers of nutrient supply, primary
2110   production and CO_2 drawdown in the changing Arctic Ocean. Prog. Oceanogr. 139,
2111   171–196. https://doi.org/10.1016/j.pocean.2015.08.009

2112   Ulfsbo, A., Cassar, N., Korhonen, M., van Heuven, S., Hoppema, M., Kattner, G.,
2113   Anderson, L.G., 2014. Late summer net community production in the central Arctic
2114   Ocean using multiple approaches. Glob. Biogeochem. Cycles 2014GB004833.
2115   https://doi.org/10.1002/2014gb004833

2116   Vandermeer, J., 1996. Seasonal isochronic forcing of Lotka Volterra equations. Prog.

2117   Theor. Phys. 96, 13–28.

2118   Volterra, V., 1927. Variazioni e fluttuazioni del numero d'individui in specie animali
2119   conviventi. Societá anonima tipografica" Leonardo da Vinci".

2120   von Appen, W.-J., Waite, A.M., Bergmann, M., Bienhold, C., Boebel, O., Bracher, A.,
2121   Cisewski, B., Hagemann, J., Hoppema, M., Iversen, M.H., 2021. Sea-ice derived
2122   meltwater stratification slows the biological carbon pump: results from continuous
2123   observations. Nat. Commun. 12, 7309.

2124   Wadhams, P., Toberg, N., 2012. Changing characteristics of arctic pressure ridges.
2125   Polar Sci. 6, 71–77.

2126   Wang, S.W., Budge, S.M., Iken, K., Gradinger, R.R., Springer, A.M., Wooller, M.J.,
2127   2015. Importance of sympagic production to Bering Sea zooplankton as revealed
2128   from fatty acid-carbon stable isotope analyses. Mar. Ecol. Prog. Ser. 518, 31–50.

2129   Wassmann, P., Reigstad, M., 2011. Future Arctic Ocean seasonal ice zones and
2130   implications for pelagic-benthic coupling. Oceanography 24, 220–231.
2131   https://doi.org/10.5670/ oceanog.2011.74.

2132   Wiedmann, I., Ershova, E., Bluhm, B.A., Nöthig, E.-M., Gradinger, R.R.,
2133   Kosobokova, K., Boetius, A., 2020. What Feeds the Benthos in the Arctic Basins?
2134   Assembling a Carbon Budget for the Deep Arctic Ocean. Front. Mar. Sci. 7.

2135   Wietz, M., Bienhold, C., Metfies, K., Torres-Valdés, S., von Appen, W.-J., Salter, I.,
2136   Boetius, A., 2021. The polar night shift: seasonal dynamics and drivers of Arctic
2137   Ocean microbiomes revealed by autonomous sampling. ISME Commun. 1, 76.
2138   https://doi.org/10.1038/s43705-021-00074-4

2139   Yue, F., Angot, H., Blomquist, B., Schmale, J., Hoppe, C.J., Lei, R., Shupe, M.D.,
2140   Zhan, L., Ren, J., Liu, H., 2023. The Marginal Ice Zone as a dominant source region
2141   of atmospheric mercury during central Arctic summertime. Nat. Commun. 14, 4887.

2142   Zeebe, R.E., Eicken, H., Robinson, D.H., Wolf-Gladrow, D., Dieckmann, G.S., 1996.
2143   Modeling the heating and melting of sea ice through light absorption by microalgae.
2144   J. Geophys. Res. Oceans 101, 1163–1181.

Tables

Table 1. MOSAiC ecosystem core measurements. Catalog of biological and

biogeochemical properties and processes measured during the MOSAiC expedition.

Additional geochemical properties (i.e. gases) were measured by the MOSAiC

Biogeochemistry Team. Details can be found in the supplementary Table S2.

ECO variable	Sampled environments	Method
Nutrients (nitrate+nitrite, ammonium, phosphate, silicic acid, dissolved organic nitrogen, dissolved organic phosphorus)	Water column, ice, special habitats	Colourimetric continuous flow; AA3 (SEAL)
Dissolved oxygen (DO)	water column	Winkler titration
Carbonate chemistry: total alkalinity (TA) and dissolved inorganic carbon DIC)	water column, special habitats	VINDTA
Carbonate chemistry: TA, DIC	ice, special habitats	Coulometry/ VINDTA
Dissolved organic carbon (DOC) and nitrogen (DON), concentrations	water column, ice, special habitats	TOC-VCPN, high temperature catalytic combustion
Dissolved organic matter characterization and chemometrics	water column, special habitats	Ultrahigh resolution mass spectrometry
Particulate organic carbon and nitrogen (POC and PON); stable isotopic composition and concentrations	water column, ice, special habitats, short- and longterm sediment traps	%C, %N, δ^{13}C, δ^{15}N; EA-IRMS (Flash 2000-Delta V Plus, Thermo Scientific)
POC and PON, concentrations	water column, ice, special habitats, short- and longterm sediment traps	Euro EA 3000, HEKAtech
Biogenic silica (bSi)	water column, ice,	Photometrically after NaOH digestion
Oceanic particle size spectra and distributions	Water column	Optical - Underwater Vision Profiler (UVP)
Chlorophyll *a* (Chl-a)	water column, ice, special habitats	Fluorometric analyses of extractd samples
Pigment biomarkers	water column, ice, special habitats	High Performance Liquid Chromatography (HPLC)
Enumeration and diversity of prokaryotes, eukaryotic microbes and viruses	water column, ice, special habitats	Attune NxT (ThermoFisher) and Facs Calibur (Becton Dickson) flow cytometers (FCM)
Diversity and abundance of protists	water column, ice, special habitats, sediment traps	Inverse light microscopy
Diversity of prokaryotes and eukaryotic microbes	water column, ice, special habitats, underway	16S/18S rRNA amplicon sequencing (Illumina)

	water column, ice, special habitats	Illumina
Metagenomes	water column, ice, special habitats	Illumina
Metatranscriptomes	water column, ice, special habitats	Illumina
Primary productivity (NPP)	water column, ice, special habitats, underway	^{14}C-based incubations
Net community production (NCP)	surface water	MIMS O_2/Ar
Bacterial productivity (BP)	water column, ice, special habitats, underway	3H-leucine incubations
PSII fluorescence-based photophysiology	water column, special habitats	FRRF; FastOcean with FastAct /Fastact2 (Chelsea Tech)
Mesozooplankton: abundance/distribution	water column	Microscopy, Zooscan
Small mesozooplanton: abundance/distribution	water column	Microscopy, Zooscan
Macrozooplankton: abundance/distribution	water column	Microscopy, Zooscan
Macrozooplankton: biomarkers	water column	diverse
Macrozooplankton: carbon & nitrogen	water column	Elemental analyser
Surface mesozooplankton: biomarkers	water column	diverse
Surface mesozooplankton: carbon & nitrogen	water column	Elemental analyser
Surface mesozooplankton: individual respiration	water column	optodes
Deep mesozooplankton: biomarkers	water column	diverse
Deep mesozooplankton: carbon & nitrogen	water column	Elemental analyser
Deep mesozooplankton: individual respiration	water column	optodes
Mesozooplankton: high vertical resolution distribution	water column	Microscopy, Zooscan
Under-ice fauna: abundance/distribution	ice	Microscopy
Grazing rates (microzooplankton & copepods)	water column	experiments
Egg production (copepods)	water column	experiments
Gut contents & DNA (fish, copepods, amphipods)	water column	Microscopy, scales, DNA
Energy content macrofauna	water column	oxygen calorimeter

2152

2153
2154
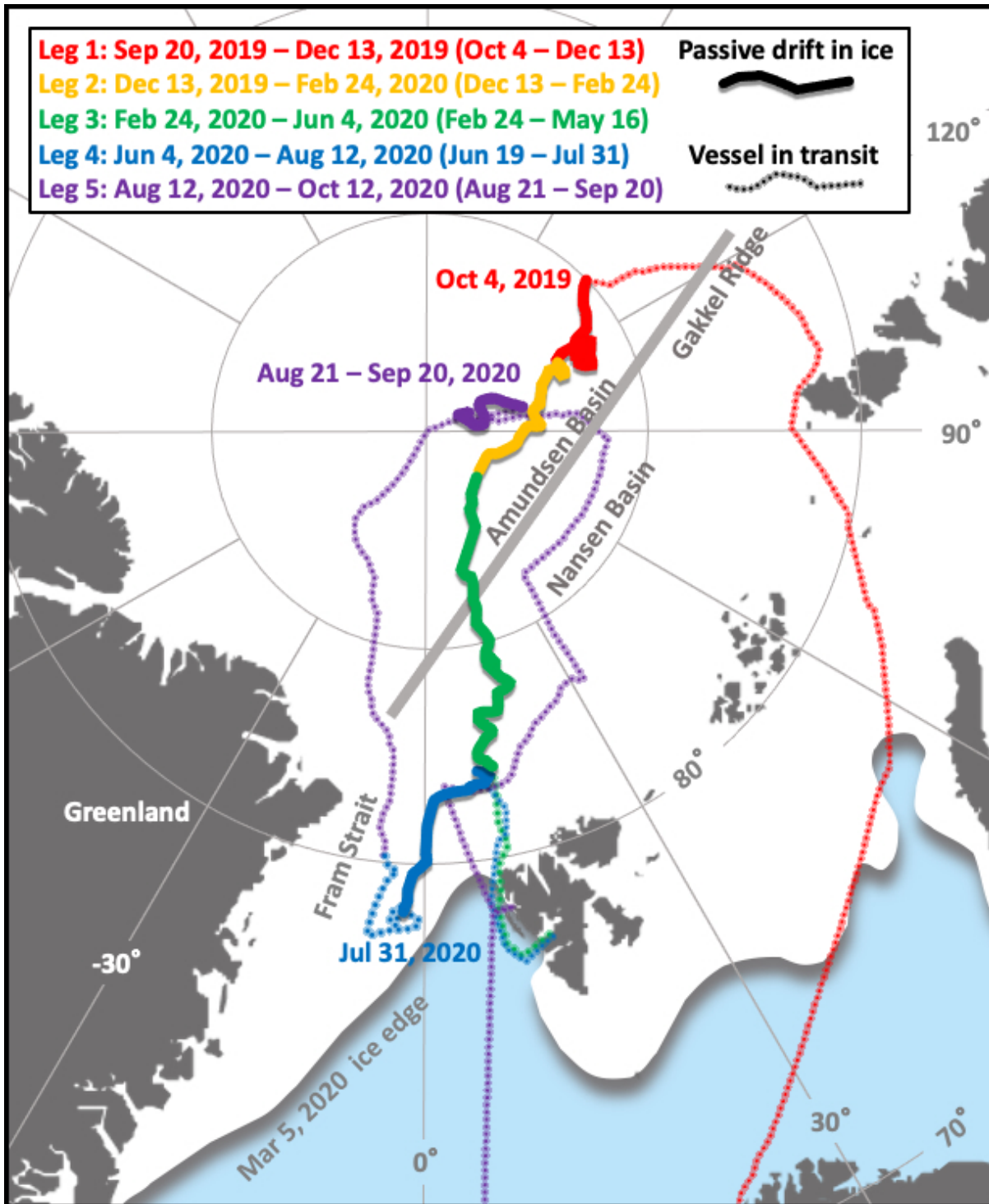
Figure 1. MOSAiC expedition track. Passive periods of drift are shown in solid-colored lines, with each color-coded line delineating one of the MOSAiC legs. Dates are periods of each leg and dates shown in parentheses identify passive drift periods per leg. Dotted lines depict transit tracks of the ship initially and for repositioning after legs 3 and 4. The solid grey line approximates the location of the Gakkel Ridge between the Amundsen and Nansen Basins. The approximate sea ice edge at the

2162 annual maximum (Mar 5, 2020) and minimum (Sept 15, 2020) is also shown.
2163 Modified after (Shupe et al., 2020).
2164
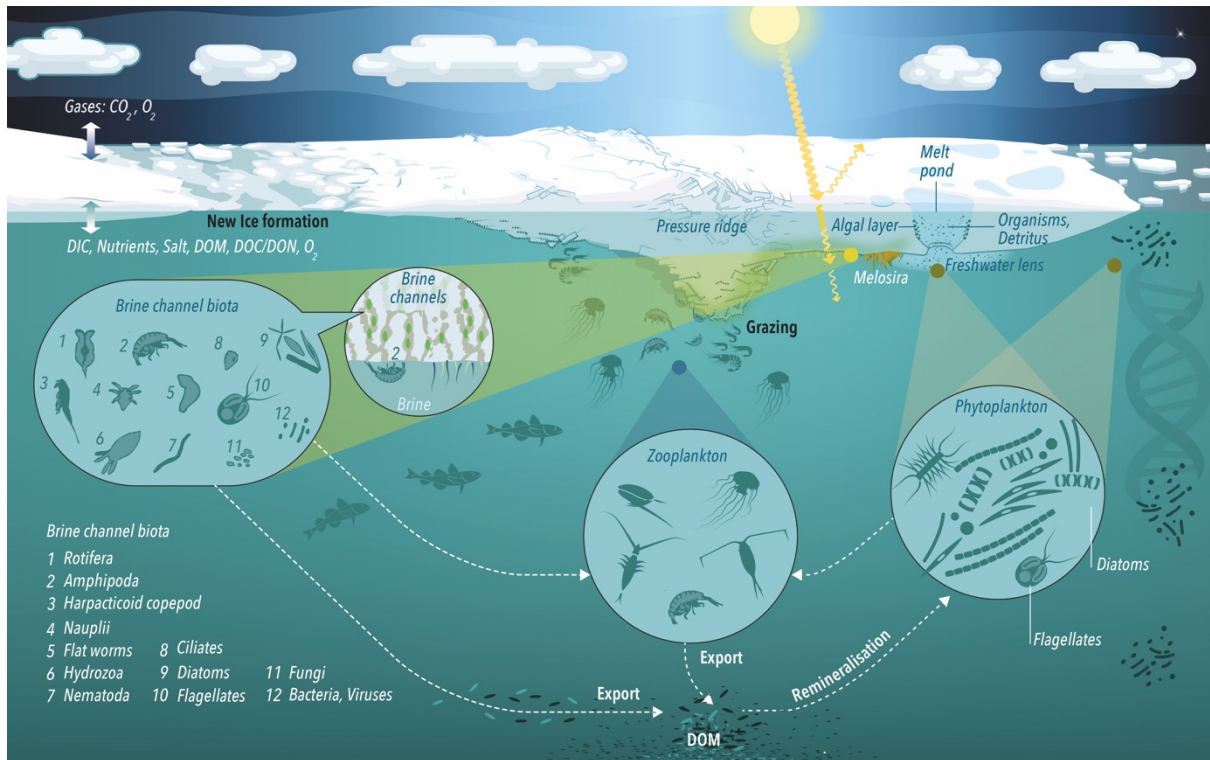
2165
2166 **Figure 2. Ecosystem compartments and processes of the Central Arctic.**
2167 Illustrated are the primary components and processes investigated by the ECO team
2168 during the MOSAiC (Multidisciplinary drifting Observatory for the Study of Arctic
2169 Climate) expedition.
2170
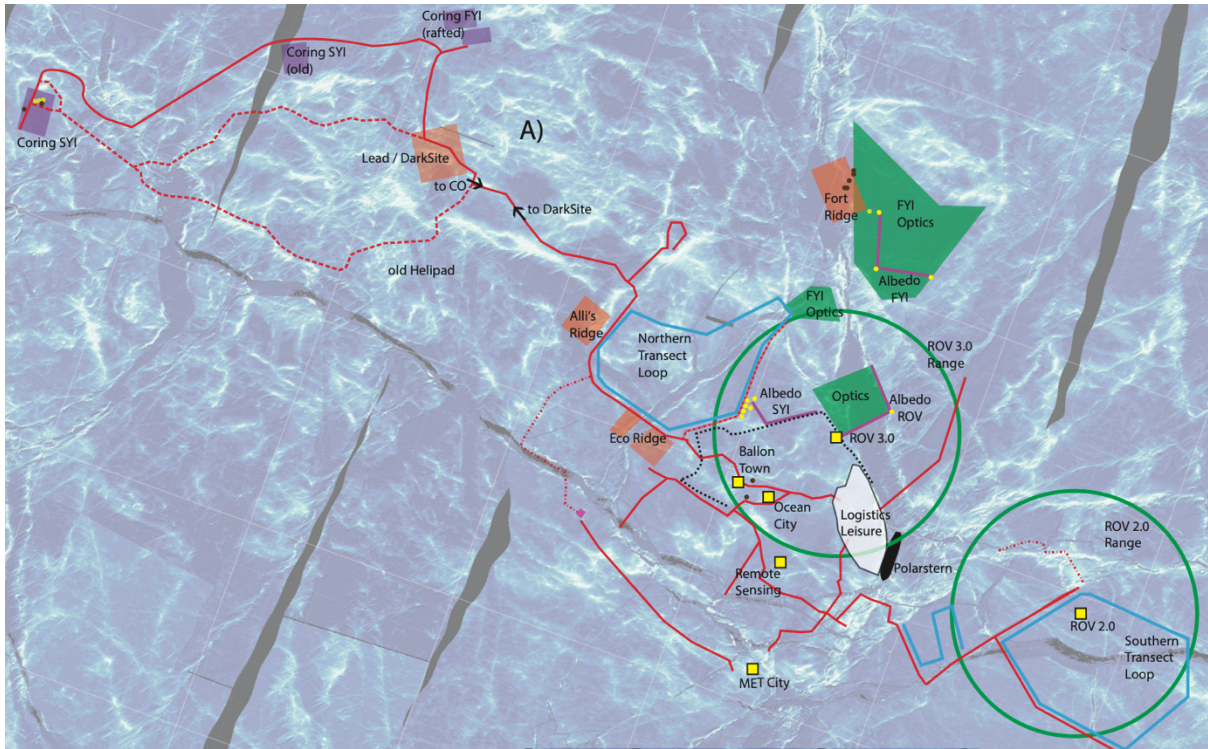
Figure 3. Main sampling locations and measurement sites of the first MOSAiC Central Observatory

in April 2020. Map background shows the airborne laser scanner (ALS) image from April 23, 2020 with grey areas indicating no data. White, brighter areas depict sea ice of greater elevation (i.e. ridge sails). Some site locations were approximate due to active ice dynamics. Sites labeled "old" were previously active sampling locations, but were no longer accessible and maintained after the winter. The primary water column sampling locations during October 2019 and May 2020 were conducted at RV *Polarstern* (black) and Ocean City (yellow square). Common ice coring sites are shown in purple and approximately 1 km from RV *Polarstern*. The map had been simplified to show main sampling and measurement positions for the ecosystem work program. Additional MOSAiC measurement sites from teams ATMO, ICE, and OCEAN can be viewed in the respective MOSAiC Overviews by Nicolaus et al. (2022b), Rabe et al. (2022) and Shupe et al. (2022).
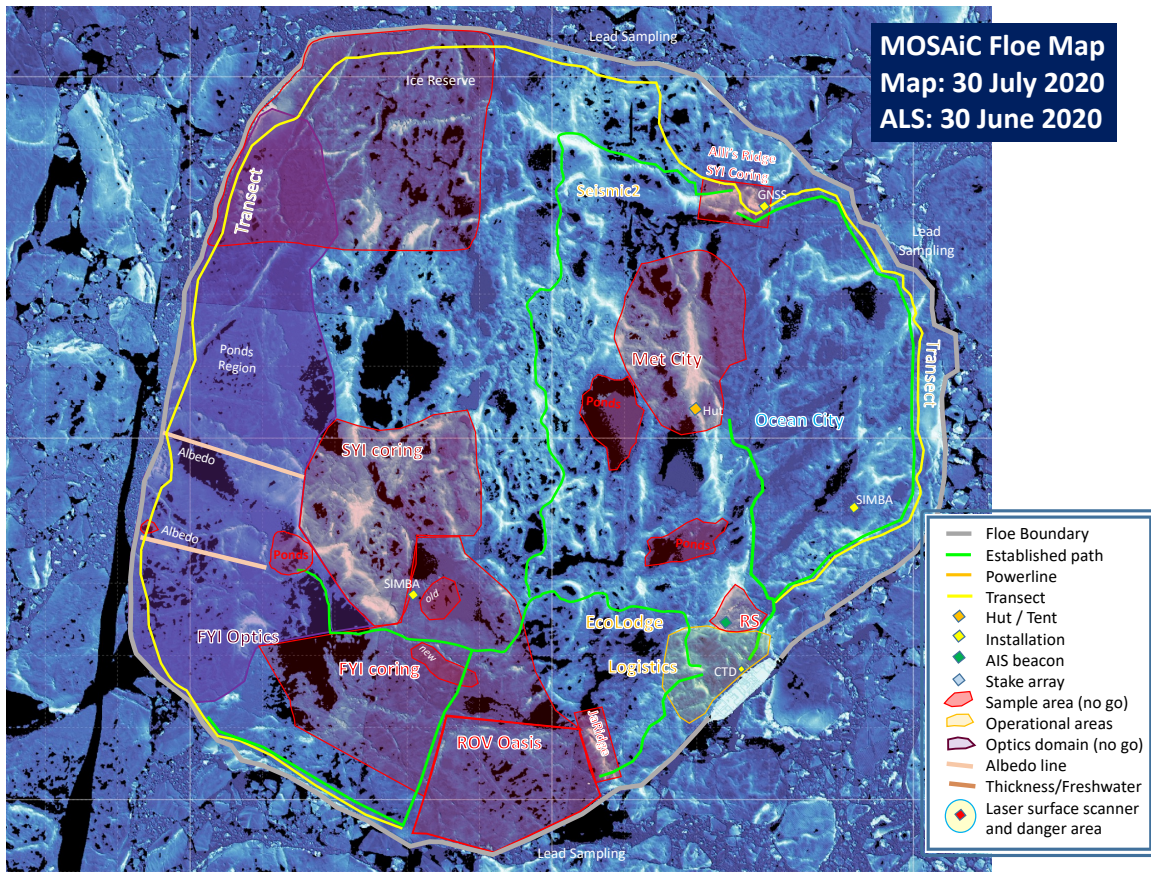
Figure 4. Main sampling locations and measurement sites of the second MOSAiC Central Observatory during summer 2020. Primary water column sampling was from RV *Polarstern* (light blue, lower righthand side). Ocean City did not have a CTD-rosette system. FYI coring site was an original portion of the FYI site established in Oct 2019. SYI coring site adjacent to FYI shown here was a reserve SYI site identified earlier, but was not actively sampled. Original SYI coring site is not depicted in this map as that part of the ice floe detached from the main floe. SYI coring in June and July 2020 occurred near Alli's ridge. ECO Lodge was established beyond the perimeter of the logistics area. The map had been simplified to show main sampling and measurement positions for the ecosystem work program. Additional MOSAiC measurement sites from teams ATMO, ICE, and OCEAN can be viewed in the respective MOSAiC Overviews by Nicolaus et al. (2022b), Rabe et al. (2022) and Shupe et al. (2022).

Figure 5. Main sampling locations and measurement sites of the third MOSAiC Central Observatory during late summer 2020. The background of the map is an aerial photo of the ice floe (photo credit S. Graupner). Primary water column sampling was from RV *Polarstern* (light blue, lower righthand side). Ocean City did not have a CTD-rosette system. Ice cores (not new ice formations) in August and September 2020 were sampled from a single site (yellow area). New ice formation and waters from the upper ocean (1-2m) were sampled at RS, OC, ROV, and Luna leads. ECO Lodge (red square) was established adjacent to Ocean City lead, approximately 300 m from the ship. The map had been simplified to show main sampling and measurement positions for the ecosystem work program. Additional MOSAiC measurement sites from teams ATMO, ICE, and OCEAN can be viewed in the respective MOSAiC Overviews by Nicolaus et al. (2022b), Rabe et al. (2022) and Shupe et al. (2022).
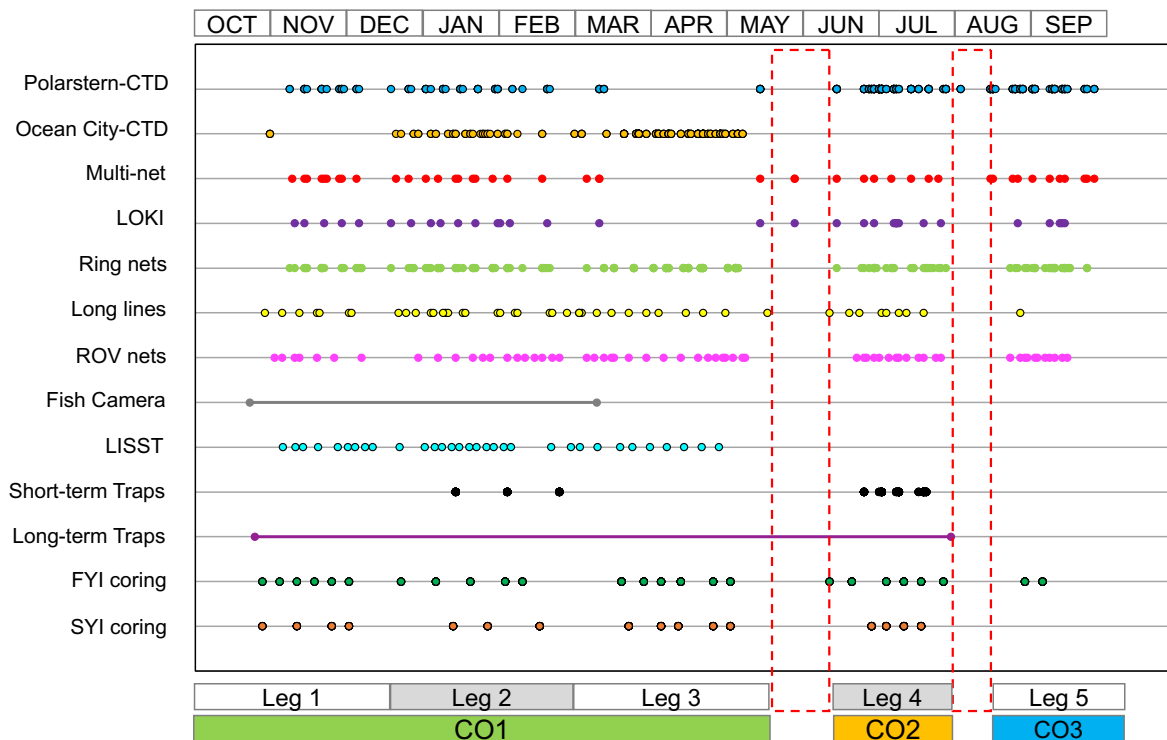
Figure 6. Ecosystem observations and measurements during the field phase of MOSAiC. Each row shows the dates of a sampling event for a specific type of gear (e.g. Polarstern-CTD) or sampling activity (e.g. FYI coring). Solid lines indicate instrumentation deployed through the ice for a continuous period. A number of parameters are collected from an individual sampling event, such as deployment of the Polarstern-CTD rosette system. Alternating white and grey horizontal bars at the bottom of the chart indicate the MOSAiC leg. Colored horizontal bars indicate from which Central Observatory (CO) samples were collected. Dashed red line boxes identify the periods when RV Polarstern was transiting to/from an ice floe. LOKI = Light-frame On-sight Key species Investigation system (zooplankton camera system). ROV nets = Plankton nets towed by a Remotely Operated Vehicle. LISST = Laser In-Situ Scattering and Transmissometer (particle counter). FYI = First Year Ice. SYI = Second Year Ice.
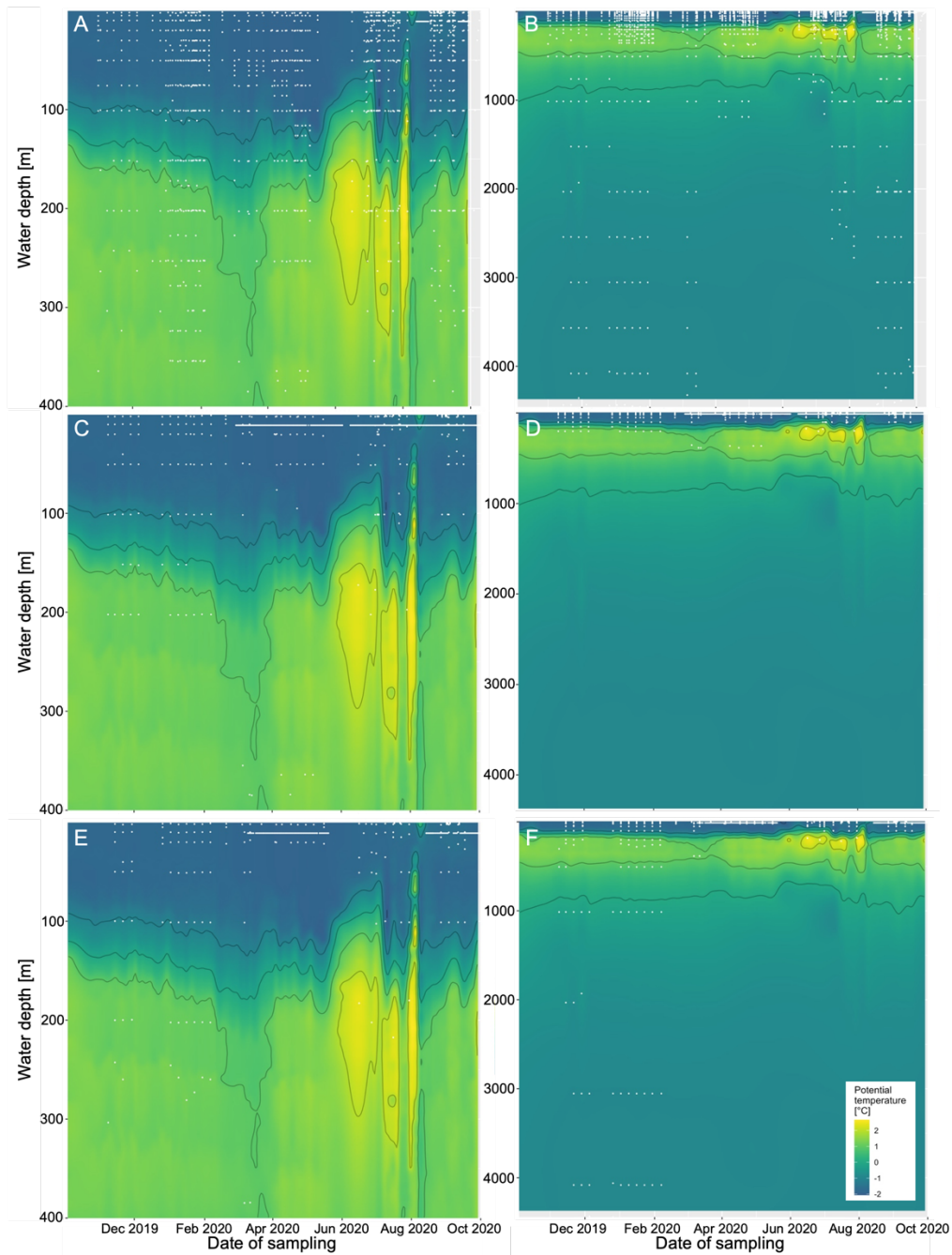
Figure 7. Distribution of CTD-rosette-based water column samples for nutrients, Chl-a, and total DNA in depth and time. Discrete samples (while circles) for the upper 400 m (A, C, and E) and for full depth (0-4000 m; B, D, and F) are overlain on temperature contours with isotherms shown by thin, solid lines. Temperature data shown here are from temperature sensors mounted to the CTD-rosette system. During mid-March to May 2020, the Polarstern-CTD was not operational due to the closure of the ice hole alongside the ship; water column sampling was limited to the upper 1000 m using the OC-CTD-rosette system. A) Nutrient samples collected in the upper 400 m; B) Nutrient samples collected over the full water column depth; C) Chl-a samples collected in the upper 400 m; D) Chl-a samples collected over the full water column depth; E) Total DNA samples collected

in the upper 400 m; F) Total DNA samples collected over the full water column

depth.

2245
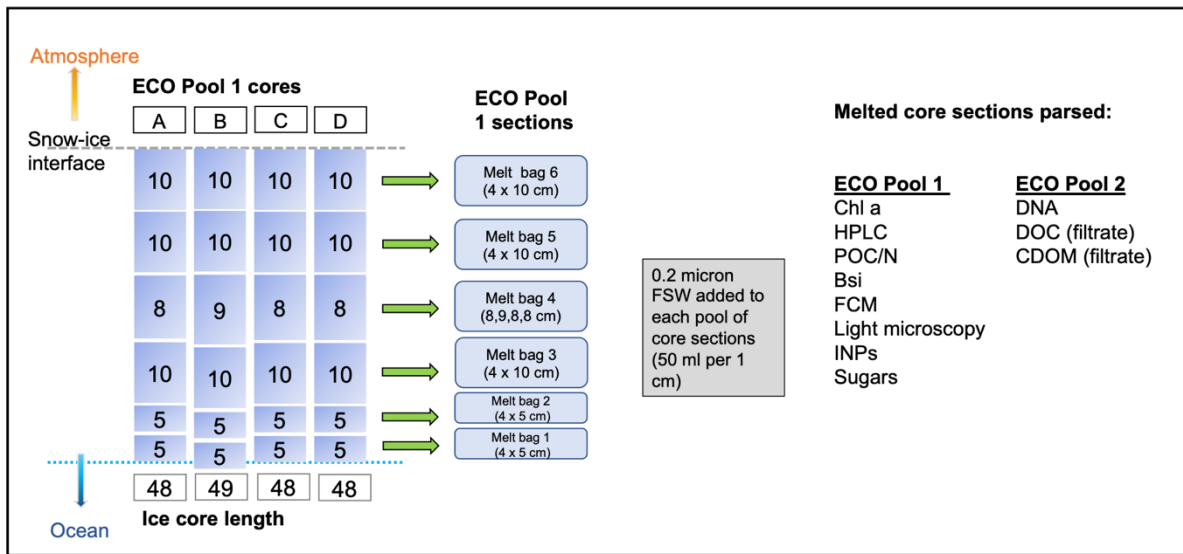
2246

2247 Figure 8. Ecological sea ice core pooling and processing. Full length cores were

2248 sectioned in the field and placed in prelabeled melt bags. Filtered seawater (FSW)

2249 was added onboard to each melt bag, and after complete melt, pooled sample were

2250 parsed for different properties. When possible, 2 ECO pools were generated.

2251 Properties collected from each pool are shown, see Table 1 for abbreviation

2252 explanations. Additional samples were collected from SALO18 and DIC/TA cores as

2253 well as additional bottom sections.

2254
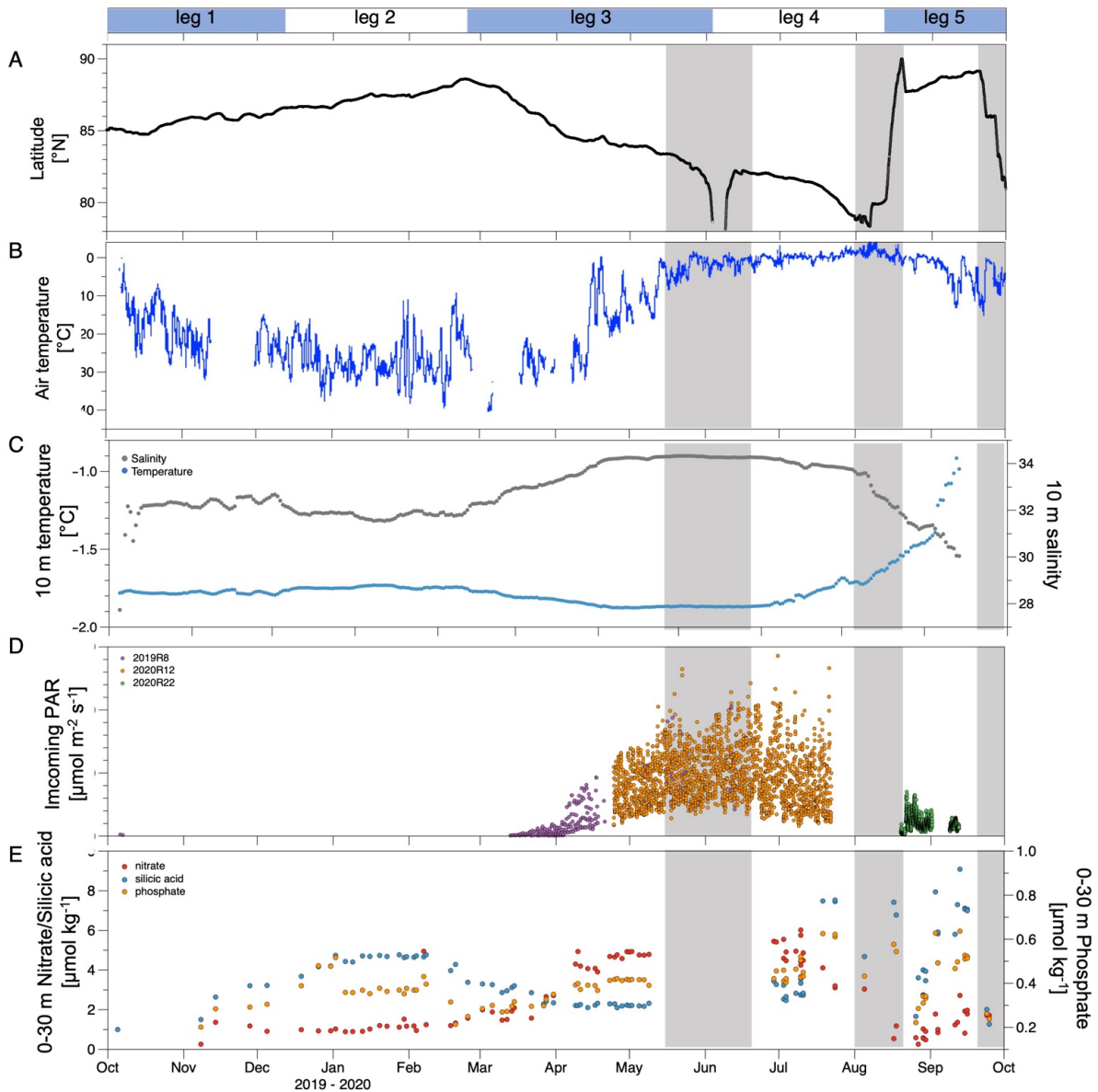
Figure 9. Environmental conditions over the annual cycle. A) latitude (°N), B) air and C) surface ocean temperature (blue) and salinity (grey) at 10 ±3 m depth, D) incoming PAR (photosynthetically active radiation, 400-700 nm, measured as photon flux density), and E) surface ocean nutrients (nitrate+nitrite, silicic acid, and phosphate) from the upper 30 m water depths. Grey shaded areas indicate transit periods. Here, latitude and nutrients are from the location of RV *Polarstern*, while PAR, water temperature, and surface air temperature are representative of CO conditions.
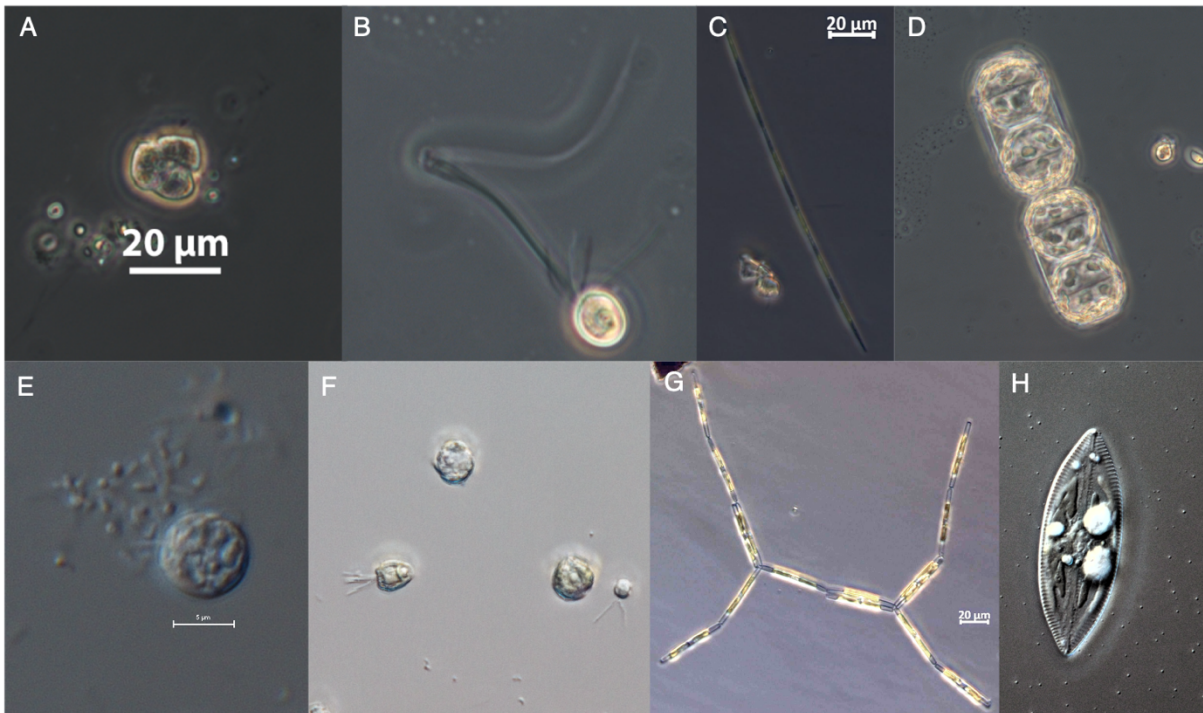
Figure 10. Dominant pelagic (water column) and sympagic (ice-associated) protists during the MOSAiC cruise. A) dinoflagellate belonging to Gymnodiniaceae, B) unidentified flagellate, C) *Pseudo-nitzschia* sp. and D) *Melosira arctica* from water column samples; E) and F) unidentified flagellates, G) *Nitzschia frigida* and H) *Navicula* sp. from bottom sea ice samples.
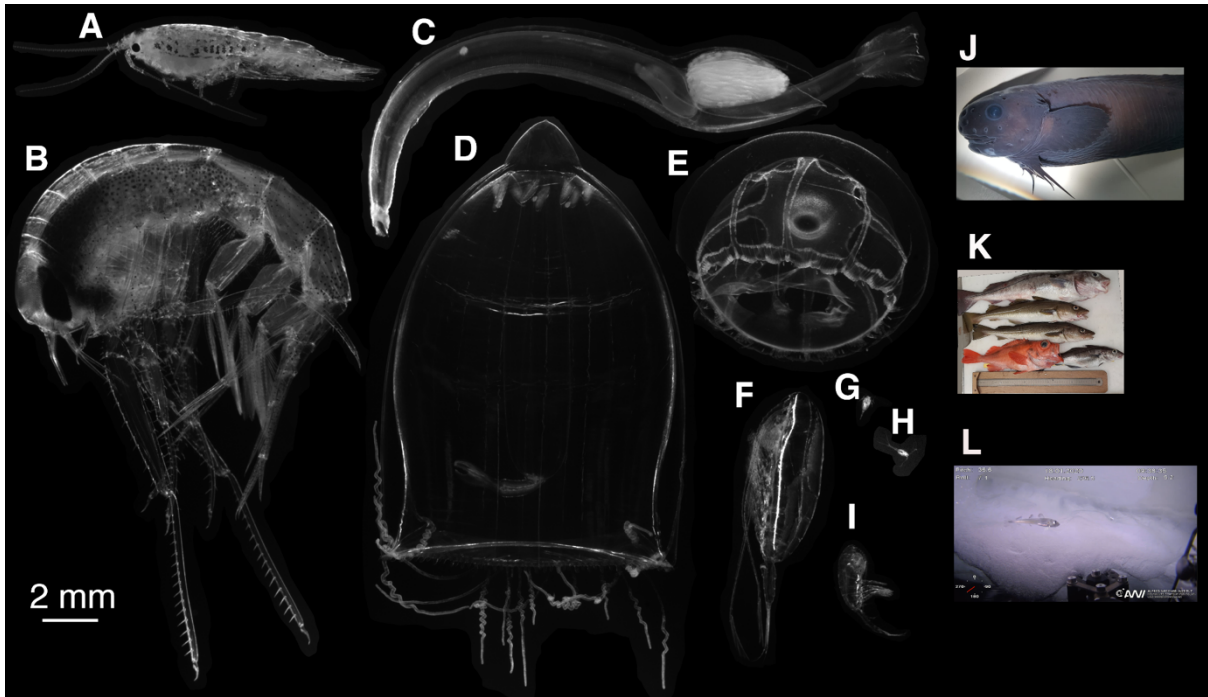
Figure 11. Zooplankton and fish species caught during the MOSAiC cruise. A) *Apherusa glacialis*, B) *Themisto libellula*, C) *Eukrohnia hamata*, D) *Aglantha digitale*, E) *Botrynema ellinorae*, F) *Calanus hyperboreus*, G) *Microcalanus sp.,* H) *Oithona similis*, I) *Metridia longa*, J) *Paraliparis bathybius*, K) from top to bottom: Haddock (*Melanogrammus aeglefinus)*, 2 x Atlantic cod (*Gadus morhua*), Beaked redfish (*Sebastes mentella*), Haddock (*Melanogrammus aeglefinus)*; L) *Boreogadus saida*. The specimens A - I were obtained with the LOKI (Lightframe on-sight key species investigation), further sampling methods were J) zooplankton ring net, K) longlines, and L) ROVnet camera.
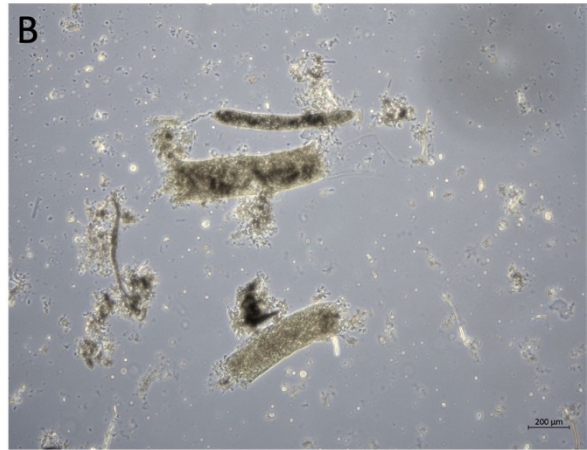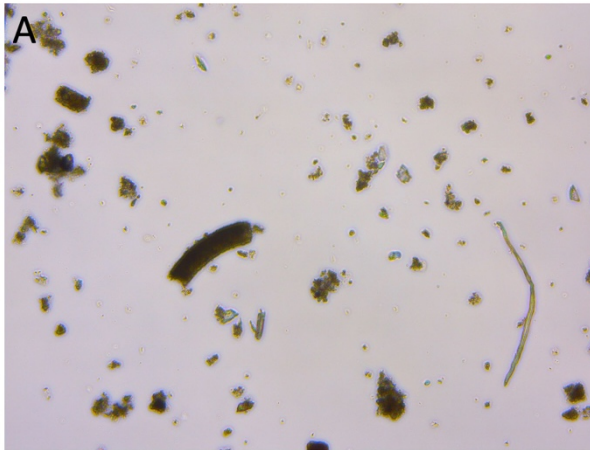
2280

Figure 12. Sediment trap material from winter vs summer. Overview images of sediment trap material from A) January 14, and B) July 21, 2020.

2283
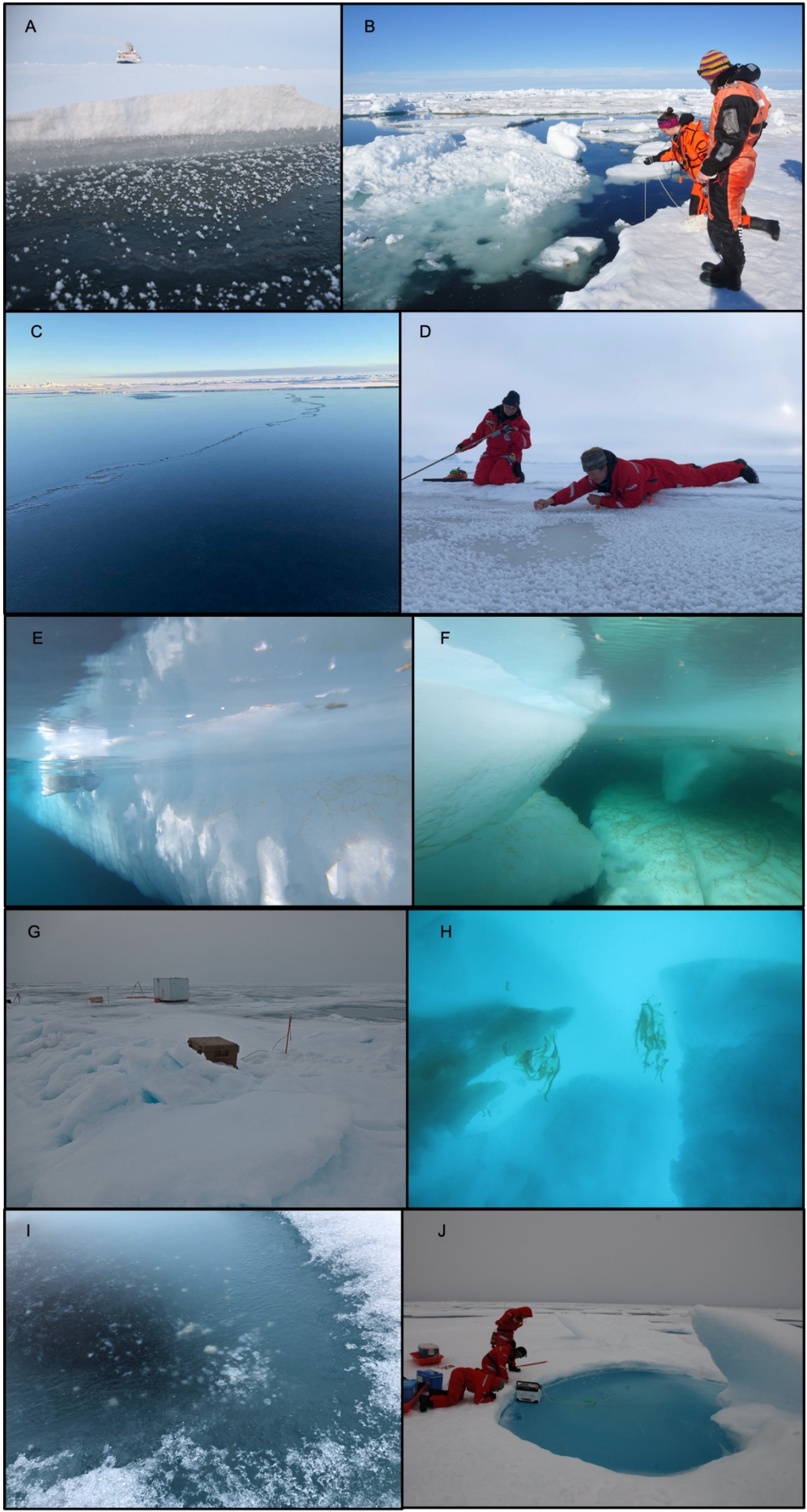
2284 **Figure 13. A variety of different seawater and sea ice habitats sampled over the**
2285 **drift year.** A) Frost flowers developing on a refrozen lead on March 11, 2020; B)
2286 Sampling an open lead on 22, 2020; C) New ice formation on a lead located near
2287 ECO Lodge 2 on September 07, 2020; D) Sampling new ice and direct under-ice
2288 waters from a lead located near ECO Lodge 2 on September 12, 2020; E)
2289 Underwater photos of ice blocks within an open lead from July 01, 2020 and F) from
2290 the same location on 29, 2020, showing the development of thin, stratified fresh and
2291 brackish layers within leads. G) Jaridge Observatory from the surface with piled up
2292 ice blocks on June 26, 2020; H) Underwater photo of ice blocks in Jaridge
2293 Observatory with strands of Melosira; I) Refrozen surface of a melt pond showing
2294 large aggregate material through the ice surface from Aug 21, 2020; and J) Melt
2295 pond sampling from August 31, 2020.
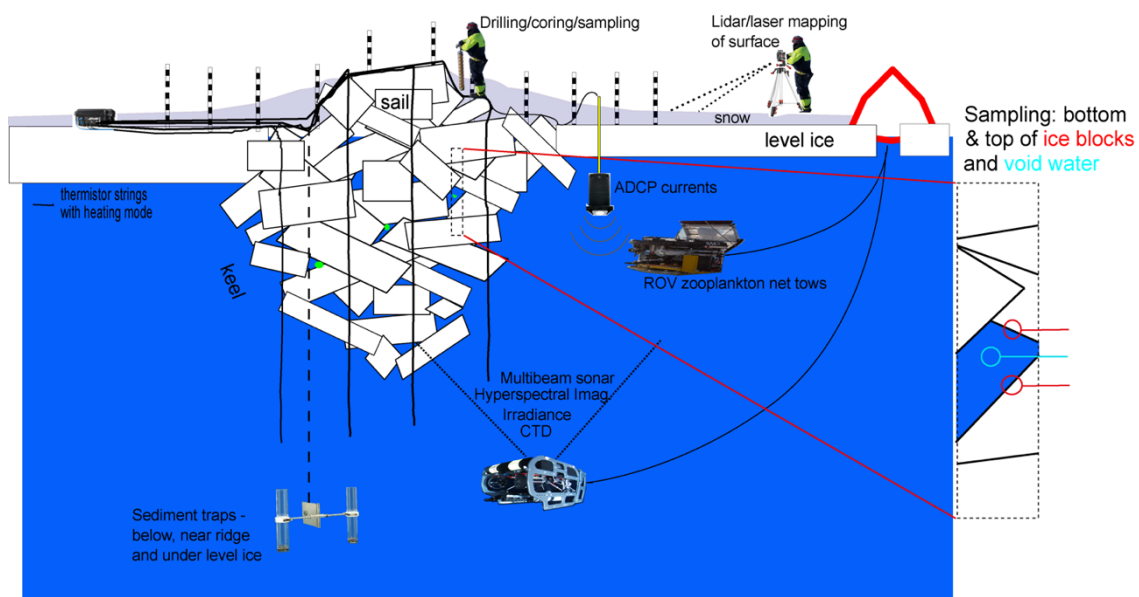
Figure 14. Components of the multidisciplinary ridge sampling strategy during MOSAiC. Schematic representation of the sampling strategy of sea ice ridges developed by the HAVOC project., including autonomous systems (e.g. thermistor strings), coring and drilling, sampling of ice and void water in the ridge keel, as well as ROV- and sediment trap-based measurements, with the former including zooplankton net tows and various sensor-based measurements (including hyperspectral imager mapping of the ice underside, see Figure 16).
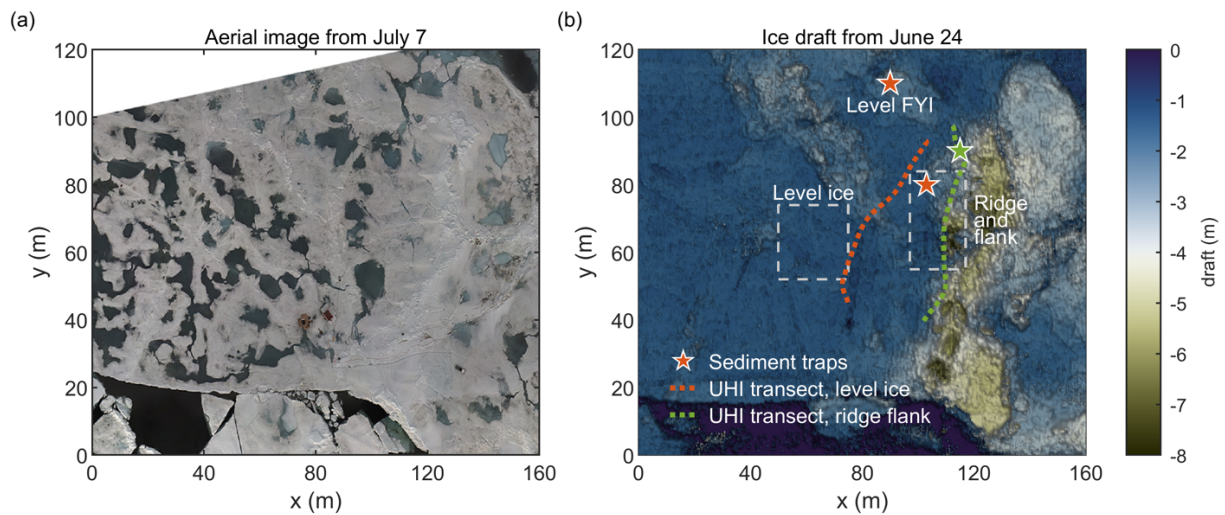
Figure 15. The Jaridge ridge sampling areas during summer 2020. A) Shows an aerial image of the study area with ponded level ice and the Jaridge ridge sampling site. Shading in B) indicates ice draft from the ROV multibeam sonar with keel depths of the pressure ridge exceeding 7 m, and red stars indicate locations of deployed sediment traps, and the blue star the location of underwater hyperspectral imager (UHI) data collection shown in Figure 16.

a) RGB composite b) RBI index c) SVM suitable habitat

~ 1 m

~ 1 m
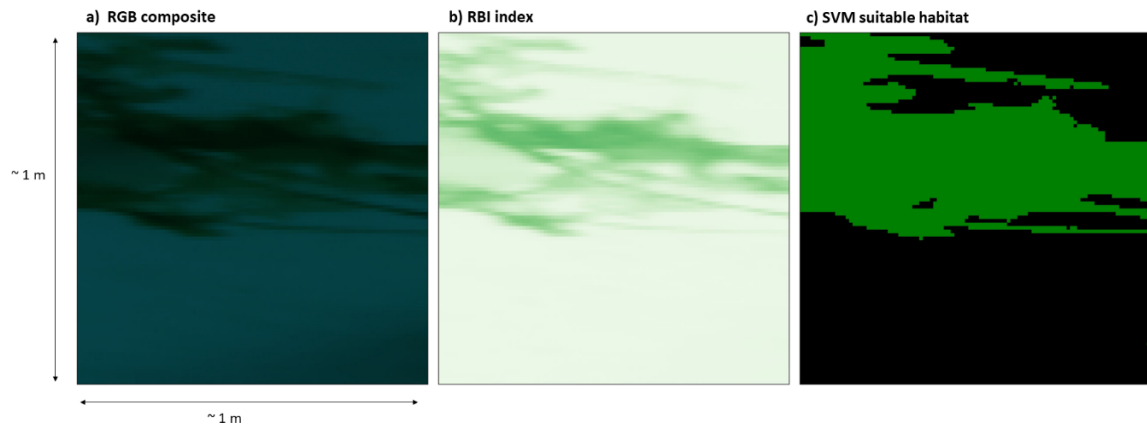
2311
2312 **Figure 16. Determination of ice algal habitable space in pressure ridges and**
2313 **level sea ice using underwater hyperspectral image (UHI) information**. A) An
2314 example of composite RGB (red, green, and blue) image of one area along the ridge
2315 flank transect (blue star in Figure 15b) compared to model results to estimate B)
2316 relative algal quantity estimated via the Relative ice algal Biomass Index (RBI), and
2317 C) inhabited area based on support vector machine (SVM) machine learning
2318 approaches of sea ice using the signature of the spectral light transmitted through
2319 the ridge (Lange et al., submitted).
2320

2321
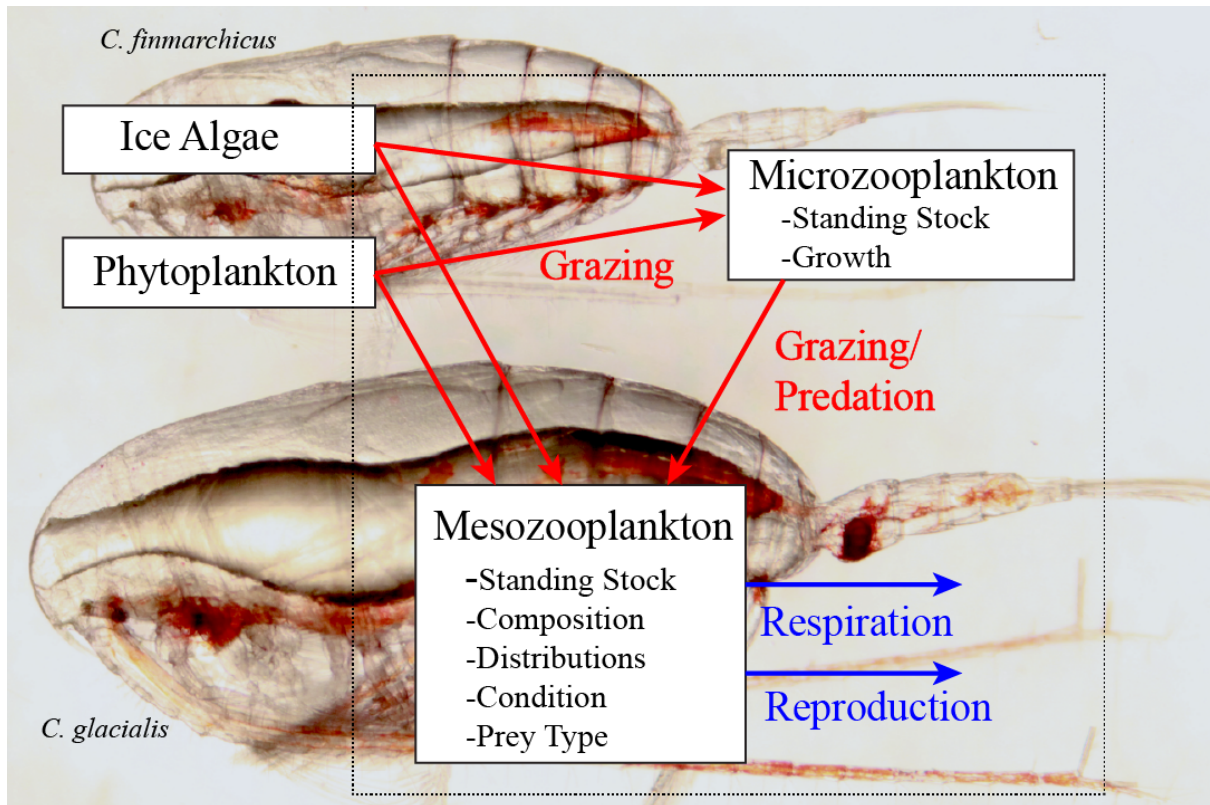
2322
2323 **Figure 17. Transformations of energy, carbon and nitrogen by**
2324 **mesozooplankton in the upper water column and near the sea ice-ocean**
2325 **boundary.** Arrows indicate transformation rates and component linkages that were
2326 quantified; red arrows show incorporation of carbon/nitrogen while blue arrows show
2327 export of carbon/nitrogen from the organisms. Characteristics of each ecosystem
2328 component that were measured indicated inside boxes.

Supplementary Information

Table S1. Project-specific contributions to the ECO work program. Information on Project Title, PI, involved institutions, funding agencies, and science foci.

Table S2. List of ECO sampling events based on rosette casts and optical particle profiling. Event Operation IDs, date and time, location and bottom depth for PS-CTD rosette, OC-CTD rosette and LISST casts as well as UVP profiles.

Table S3. Overview on sample processing and applied methods. Detailed overview of sampled parameters, applied methods, responsible PIs, coverage, and estimated number of samples. The table represents an extended version of Table 1 from the main document.

Table S4. Overview of quantitively analyzed zooplankton sampling events and collected samples. Samples were collected via LOKI (up to 20 frames sec-1), UVP, multinet (MN), ring nets (RN), Nansen net (NCN) and a net mounted on an ROV (ROVN), from Nov. 2019 to Oct. 2020. For each month, the number of samples is given; depth strata MN: 2000-1000-500-200-50-0 m; depth strata NCN: 1000-200 m & 200 - 0 m.

Table S5. List of ECO sampling events for zooplankton and fish sampling. Event Operation IDs, date and time, location (of *RV Polarstern*), and bottom depth for all zooplankton and fish sampling events for multinets (NM), Light-frame On-sight Key species Investigation system (LOKI), Ring nets, Nansen Nets, long lines, remotely operated vehicle nets (BEAST), finish rods and Gill nets.

Table S6. List of ECO sampling events for first and second year ice. Event Operation IDs, date and time, location and bottom depth for all common time-series ice coring activities at the first and second year ice (FYI and SYI) coring sites.

Table S7. List of ECO sampling events for event driven sampling and intense observation periods (IOPs). Event Operation IDs, date and time, location and bottom depth for event-driven sampling of direct under ice water, leads, melt ponds, new ice formation as well as high frequency IOP sampling.